



This is to certify that the
dissertation entitled

CONVENIENT SYNTHESIS OF CAPROLACTAM FROM
LYSINE: ALTERNATIVE OF CURRENT BENZENE-BASED
CAPROLACTAM PRODUCTION

presented by

Jinsong Yang

has been accepted towards fulfillment
of the requirements for the

Ph. D. degree in Chemistry

Major Professor's Signature

07 / 10 / 2007

Date

**CONVENIENT SYNTHESIS OF CAPROLACTAM FROM LYSINE:
ALTERNATIVE OF CURRENT BENZENE-BASED CAPROLACTAM
PRODUCTION.**

By

Jinsong Yang

A DISSERTATION

Submitted to
Michigan State University
in partial fulfillment of the requirements
for the degree of

DOCTOR OF PHILOSOPHY

Department of Chemistry

2007

ABSTRACT

CONVENIENT SYNTHESIS OF CAPROLACTAM FROM LYSINE:ALTERNATIVE OF CURRENT BENZENE-BASED CAPROLACTAM PRODUCTION.

By

Jinsong Yang

As the monomer of the widely used nylon 6, ϵ -caprolactam is currently manufactured from petroleum-derived feedstocks, which are characterized by depleting supplies and increasing prices. In the long run, society tends to look for catalytic routes to commodity chemicals starting from renewable sources as substitutes for our current reliance on petroleum. An alternative route toward ϵ -caprolactam has been developed starting from the renewable, D-glucose-derived L-lysine. Cyclization of L-lysine in various alcohols led to the formation of α -amino ϵ -caprolactam. Subsequent deamination of α -amino- ϵ -caprolactam catalyzed by either chemically using hydroxylamine-*O*-sulfonic acid or catalytically using transition metal catalysts afforded ϵ -caprolactam. Efforts towards development and optimization of the catalyst-free cyclization of L-lysine as well as the transition-metal-catalyzed deamination of α -amino- ϵ -caprolactam will be described in detail in the thesis.

Copyright by

Jinsong Yang

2007

To my parents and my wife
For their constant love and support

ACKNOWLEDGMENTS

First, I would like to thank my supervisor, Professor John W. Frost, for his patience, guidance and inspiration during my time in the group. His creativity, his vision, his pertaining to detail and perseverance will influence me for my entire life. In addition, I want to thank the members of my graduate committee, Professor Babak Borhan, Professor Gregory Baker, and Professor Milton Smith for their input in the preparation of the thesis.

I am grateful for Dr. Karen Draths for her kindness and precious suggestions and advise. Meanwhile I am appreciative of current and former group members for their support and help including Dr. Dongming Xie, Dr. Jihane Achkar, Dr. Ningqing Ran, Dr. Wei Niu, Dr. Jiantao Guo, Dr. Wensheng Li, Dr. Heather Steuben, Dr. Padmesh Venkitasubramanian, Adam Bush. I am especially grateful to Xiaofei Jia, Dr. Jian Yi, Dr. Mapitso Molefe, Dr. Man kit Lau, Brad Cox, Justas Jancauskas, and Lee Stephen Sing Kin Whose friendship makes my life here so much easier and more enjoyable.

This thesis is dedicated to my parents, Xiuzhen Wu and Guangfan Yang, my brother Jian Yang and my dear wife, Zhiqiu Wang whose unconditional support and love carried me through in my past years. Finally, My deepest gratitude to my friends Dr. Tao Wu, Shujuan Xu, Zhenwei Lu, Liping Wang, Dr. Yonghui Zhang, and Dr. Jinlong Wang for their giving and sharing.

TABLE OF CONTENTS

LIST OF TABLES	ix
LIST OF FIGURES.....	xi
LIST OF ABBREVIATIONS.....	xiv
CHAPTER 1.....	1
1.1. Introduction	1
1.2. Overview of sustainable chemistry.....	3
1.2.1. Renewable raw materials.....	4
1.2.2. Heterogeneous catalysts	14
1.3. Syntheses of caprolactam.....	21
CHAPTER 2.....	34
SYNTHESIS OF ϵ -CAPROLACTAM FROM L-LYSINE.....	34
2.1. Introduction	34
2.2. Background	35
2.3. Design	35
2.4. Results.....	37
2.4.1. Cyclization.....	37
2.4.1.1 Cyclization of L-lysine	37
2.4.1.2. Ring closure to form medium-sized lactams	41
2.4.2. Deamination.....	43
2.4.2.1. Reductive deamination with hydroxylamine- <i>O</i> -sulfuric acid.....	43
2.4.2.2 Catalytic hydrogenolysis in water.....	47
2.4.2.3 Reductive deamination of α -amino- ϵ -caprolactam with Pt catalyst.....	51
2.4.2.3.1. Effect of reaction temperature.....	53
2.4.2.3.2. Effect of hydrogen pressure	54
2.4.2.3.3. Catalyst concentration	55
2.4.2.3.4. Reaction time	56
2.4.2.3.5. Effect of substrate concentration.....	57
2.4.2.3.6. Optimizing use of solvents.....	57
2.4.2.3.7. Catalyst supports	58
2.4.3. Synthesis and purification of β -lysine.....	59
2.5. Discussion	60
CHAPTER 3. HYDRODENITROGENATION (HDN) WITH TRANSITION METAL SULFIDES	

3.1 Background	67
3.2. Introduction	68
3.2.1 Overview of hydrodenitrogenation (HDN)	68
3.2.2. Reaction mechanisms of C-N bond cleavage	70
3.2.3. Active sites and the role of H ₂ S, H ₂ and H ₂ S/H ₂	74
3.2.4. Periodic trends of transition metal sulfides	77
3.2.5. Bimetallic sulfide catalysts.....	78
3.3 Results.....	80
3.3.1 Screening of noble metal catalysts.....	81
3.3.2 HDN activities of sulfided bimetallic catalysts	83
3.3.3 Effect of sulfur concentration	85
3.3.4 Effect of catalyst concentration	87
3.3.5. Solvent effects	87
3.3.6 Effect of total pressure of H ₂ S/H ₂	89
3.3.7 Effect of H ₂ S/H ₂ ratio	90
3.3.8 Role of alkali salt addition.....	91
3.3.9 Effect of surface oxidation of support on the HDN activity.	92
3.3.10 Effect of water addition.....	96
3.3.11 Optimization of reaction conditions with Pt-Re catalysts.....	96
3.3.1.3. Comparison with other noble metals and Ni-Mo catalyst.....	101
3.4. Discussions.....	103
CHAPTER 4.....	110

DEAMINATION OF α -AMINO- ϵ -CAPROLACTAM WITH GOLD CATALYST

4.1. Overview	109
4.2. Introduction	110
4.2.1. Adsorption on gold surface	111
4.2.2. Preparation of highly dispersed gold catalysts	112
4.2.3. Selection of suitable supports	115
4.3. Experimental	117
4.3.1. Catalyst preparation	117
4.3.2. Catalyst characterization by transmission electron microscopy.....	119
4.4. Results.....	119
4.4.1. Preliminary results	119
4.4.2. Screening of supports.....	121
4.4.3. Effect of presulfidation.....	123
4.4.4. Optimization HDN conditions using Au-S/NiO.....	126
4.4.4.1. Reaction temperature.....	126
4.4.4.2. Reaction time	127
4.4.4.3. Effect of H ₂ S/H ₂ ratio	127
4.4.4.4. Effect of presulfidation temperature	128
4.5 Discussions.....	130

CHAPTER 5.....	137
Experimental	137
General chemistry.....	137
Reagents and solvents.....	138
General methods.....	138
Chromatography.....	138
Spectroscopic measurement.....	139
Chapter 2.....	140
Cyclization of L-lysine in the presence of Al ₂ O ₃	140
Cyclization of L-lysine without Al ₂ O ₃	140
Synthesis of 2,7-diaminoheptanoic acid monohydrochloride (homolysine)	141
Deamination of α -amino- ϵ -caprolactam with hydroxylamine- <i>O</i> -sulfonic acid	142
Deamination of L-lysine in water.....	143
Deamination of α -amino- ϵ -caprolactam in Water.....	143
Preparation of 40% Pt/SiO ₂	144
Deamination of α -amino- ϵ -caprolactam of 40% Pt/SiO ₂	144
Catalytic HDN of α -amino- ϵ -caprolactam with Pt/C and H ₂	145
Synthesis of β -lysine.....	145
Chapter 3.....	146
Catalyst preparation.....	146
Preparation of 16 wt% Pt/C	147
Preparation of 16 wt% Pt-S/C.....	147
Preparation of bimetallic Pt-Re-S/C catalysts.....	148
Preparation of bimetallic Pt-Re-S/C catalysts by coimpregnation.....	148
Preparation of bimetallic Pt-Re-S/C catalysts by catalytic reduction.....	149
Preparation of 8 wt% Pt-Cs-S/C catalysts	149
Preparation of Pt-S/C-x catalysts with oxidated activated carbon	150
Catalytic HDN of α -amino- ϵ -caprolactam.....	151
Catalytic HDN of α -amino- ϵ -caprolactam with Pt/C and H ₂	151
Catalytic HDN of α -amino- ϵ -caprolactam with Pt/C and H ₂ S.....	152
Catalytic HDN of α -amino- ϵ -caprolactam with Pt-S/C and H ₂	152
Catalytic HDN of α -amino- ϵ -caprolactam with Pt-S/C and H ₂ S	153
Chapter 4.....	154
16 wt% Au-S/C preparation by IMP	154
Preparation of 8 wt% Au/TiO ₂ by DP	154
Preparation of 8 wt% Au/NiO by DP	155
Preparation of 8 wt% Au-S/NiO	155
Catalyst characterization by transmission electron microscopy (TEM).....	156
Catalytic HDN of α -amino- ϵ -caprolactam with Au-S/NiO and H ₂ S/H ₂	156
Direct conversion of L-lysine to caprolactam.....	157

LIST OF TABLES

Table 1. Cyclization of L-lysine hydrochloride in the presence of Al_2O_3	38
Table 2. Cyclization of L-lysine in mono alcohols	39
Table 3. Cyclization of L-lysine hydrochloride in triols and diols.	41
Table 4. Synthesis of 7- and 8-membered lactams	42
Table 5. Deamination of α -amino- ϵ -caprolactam with $\text{NH}_2\text{OSO}_3\text{H}$	46
Table 6. Deamination of L-lysine to pipercolinic acid in water ^{a,c}	50
Table 7. Deamination of α -amino- ϵ -caprolactam in water ^a	50
Table 8. Temperature effect of reductive deamination with Pt/C.....	54
Table 9. H_2 pressure effect for reductive deamination with Pt/C	55
Table 10. Catalyst concentration.....	56
Table 11. Reaction time.....	56
Table 12. Optimizing substrate concentration.	57
Table 13. Solvent effect.....	58
Table 14. Support effect.	58
Table 15. HDN activities of unsulfided catalysts	82
Table 16. HDN activities of sulfided catalysts	83
Table 17. HDN activities of sulfided bimetallic catalysts	85
Table 18. Temperature effect on HDN activity of Pt-Re-S/C catalyst.....	85
Table 19. Effect of thiophene concentration on HDN activity of Pt-S/C.....	86
Table 20. Effect of thiophene concentration on HDN activity of Pt-Re-S/C ^a	86
Table 21. Effect of catalyst concentration on HDN activities.....	87
Table 22. Solvent effects for deamination of α -amino- ϵ -caprolactam	89

Table 23. Effect of H ₂ S/H ₂ mixture total pressure	90
Table 24. Effect of changing H ₂ S/H ₂ ratio.....	91
Table 25. CsOH addition effect	92
Table 26. Effect of catalyst support surface oxidation by HNO ₃	95
Table 27. Examination of catalyst supports.....	95
Table 28. Effect of additives.....	95
Table 29. Effect of water addition.....	96
Table 30. HDN with bimetallic catalyst.....	98
Table 31. Ru Hydrodenitrogenation.....	102
Table 32. Rh Hydrodenitrogenation.....	102
Table 33. Pd Hydrodenitrogenation	102
Table 34. Re Hydrodenitrogenation	102
Table 35. Ir Hydrodenitrogenation.....	102
Table 36. Ni-Mo Hydrodenitrogenation.....	103
Table 37. Pt Hydrodenitrogenation	103
Table 38. Preliminary results of HDN with Au catalyst.	121
Table 39. Screening of supports.....	122
Table 40. HDN with Au supported on metal oxides.	122
Table 41. Presulfided catalysts.....	125
Table 42. Optimization of temperature	126
Table 43. Optimization of reaction time.....	127
Table 44. Optimization of H ₂ S concentration.....	128
Table 45. Effect of presulfidation temperature	130

LIST OF FIGURES

Figure 1. Selected organic chemicals from D-glucose.	2
Figure 2. Targets of the National Research Council of the USA for the biobased production of organic compounds and of liquid fuels by the year of 2090.....	5
Figure 3. Chemical and biocatalytic approaches to adipic acid.....	6
Figure 4. Commercially available derivatives from L-lactic acid.....	8
Figure 5. D-Fructose-derived furanoid products.....	10
Figure 6. Kelvar [®] and its analogues.	11
Figure 7. Versatile intermediate chemicals derived from furfural.....	12
Figure 8. Synthesis of phenol and <i>p</i> -hydroxybenzoic acid from benzene and glucose.....	13
Figure 9. Reaction pathways for hydrogen production by reaction of oxygenated hydrocarbons with water.	17
Figure 10. Industrial processes of propylene oxide.....	18
Figure 11. Influence of Au particle size on product yield during propylene epoxidation using O ₂ and H ₂	20
Figure 12. Classical production of ϵ -caprolactam.....	22
Figure 13. Formation of ammonium sulfate.....	22
Figure 14. Acidic oximation process.....	23
Figure 15. HPO (hydroxylamine-phosphate-oxime) process.	24
Figure 16. EniChem ammoximation process.....	24
Figure 17. Syntheses of ϵ -caprolactam from 1,3-butadiene.	26
Figure 18. Renewable synthesis of caprolactam.....	28
Figure 19. Synthetic strategies of caprolactam from L-lysine..	36
Figure 20. Synthesis of homolysine.	43

Figure 21. Cleavage of C-N bonds.....	44
Figure 22. Proposed mechanism of reductive deamination using $\text{NH}_2\text{OSO}_3\text{H}$	45
Figure 23. Catalytic hydrogenolysis.....	48
Figure 24. Ring opening of aziridines.	48
Figure 25. C-N bond cleavage of benzyl amine.....	49
Figure 26. Mechanism for formation of pipercolinic acid from L-lysine.	51
Figure 27. Reductive deamination with Pt/SiO_2	53
Figure 28. Synthesis of β -lysine.....	59
Figure 29. Deamination of L-lysine in water.	61
Figure 30. Possible intermediates for C-N hydrogenolysis with Pt catalyst.	63
Figure 31. Hofmann elimination mechanism.....	70
Figure 32. Nucleophilic substitution mechanism.....	71
Figure 33. Organometallic mechanism of C-N bond cleavage.....	71
Figure 34. Mechanism of hydrogenolysis of alkylamines via imine intermediacy.	72
Figure 35. Disproportionation mechanism.	72
Figure 36. Formation of a dialkylamine via an imine mechanism.....	73
Figure 37. HDN mechanism with transition metal sulfide.....	73
Figure 38. Structure of transition metal sulfides.....	75
Figure 39. Interconversion between sulfur vacancy and Brønsted acid site.....	75
Figure 40. (a) heterolytic splitting of H_2 ; (b) homolytic splitting of H_2 ; (c) H_2S competition for the same vacancy.....	77
Figure 41. The Co promotion by donation of electrons to Mo.	79
Figure 42. Schematic illustration of Pt-Re catalyst stabilization in the presence of sulfur.....	79
Figure 43. Indirect substitution of an amine to a thiol by metal catalysis.....	91
Figure 44. Elemental analysis of $\text{Pt-S}/\text{SiO}_2$	94

Figure 45. Transmission electron microscopy (TEM) images: (a) Pt-Re-S/C prepared from catalytic reduction and activated by reduction; (b) Pt-Re-S/C prepared by coimpregnation and activated by reduction; (c) Pt-S/C.	98
Figure 46. Elemental analysis of Pt-S/C.....	99
Figure 47. Element analysis of Pt-Re-S/C (Table 16, entry 2).	99
Figure 48. Element analysis of Pt-Re-S/C (Table 16, entry 4).	100
Figure 49. HDN of acetyl α -amino- ϵ -caprolactam.....	101
Figure 50. Chemoselective reduction of 4-nitrobenzaldehyde with Au/TiO ₂	111
Figure 51. Product distribution of the oxidation of propylene over Au/TiO ₂ as a function of Au particle size.	113
Figure 52. Flow chart of the deposition-precipitation method (DP).	115
Figure 53. Turnover frequencies for CO oxidation with hemispherical and spherical Au and Pt catalyst supported on TiO ₂	116
Figure 54. TEM images of Au catalyst. (a) Au/TiO ₂ prepared from deposition-precipitation method (DP). (b) Au-S/C prepared from impregnation method..	120
Figure 55. TEM images of Au catalysts. (a)Au/Fe ₂ O ₃ -DP. (b) Au/Co ₃ O ₄ -DP. (c) Au/NiO-DP.....	123
Figure 56. Dark field TEM images of Au catalysts. (a) Au/Fe ₂ O ₃ -DP. (b) Au/Co ₃ O ₄ -DP.	123
Figure 57. TEM images of Au catalysts. (a) Au-S/Fe ₂ O ₃ -DP. (b) Au-S/Co ₃ O ₄ -DP. (c) Au-S/NiO-DP.....	125
Figure 58. Dark Field TEM images of Au catalysts. (a) Au-S/Fe ₂ O ₃ -DP. (b) Au-S/Co ₃ O ₄ -DP. (c) Au-S/NiO-DP.....	125
Figure 59. TEM images of Au-S/NiO: (a) unsulfided material; (b) presulfided at 250 °C; (c) presulfided at 250 °C.....	129
Figure 60. TEM images of Au-S/NiO: presulfided at 300 °C.	129
Figure 61. TEM images of Au-S/NiO: presulfided at 400 °C.	130

LIST OF ABBREVIATIONS

Ac	acetyl
BET	Brunauer, Emmett, and Teller
BTX	benzene, toluene, xylene
Cbz	benzyloxycarbonyl
DHS	3-dehydroshikimic acid
DMF	N,N-dimethylformamide
DP	deposition precipitation
F-T	Fischer-Tropsch
GG	gas-phase grafting
h	hour
HDM	hydrodemetallization
HDN	hydrodenitrogenation
HDS	hydrodesulfurization
HDO	hydrodeoxgenation
HE	Hofmann elimination
HMDA	hexamethylenediamine
HMF	5-hydroxymethylfurfural
HPLC	high pressure liquid chromatography
HPO	hydroxylamine-phosphate-oxime
IMP	impregnation method
kg	kilogram
LG	liquid phase grafting
M	molar
min	minute
mL	milliliter

μL	microliter
mM	millimolar
μM	micromolar
NMR	nuclear magnetic resonance spectroscopy
PCA	protocatechuic acid
PLA	polylactic acid
PET	polyethylene terephthalate
TEM	transmission electron microscopy
THF	tetrahydrofuran
TLC	thin layer chromatography

CHAPTER 1

1.1. Introduction

Today the chemical industry is dominated by technologies that rely on starting materials derived from petroleum and natural gas. As a nonrenewable resource, petroleum is associated with geopolitical instabilities, declining availability, environmental problems and rising prices.^{1,2} The current chemical industry has been subject to close inspection owing to concerns about its reliance on fossil resources, its environmentally unfriendly production processes, and inevitably the generation of tons of toxic by-products and wastes that are not recyclable or degradable.³ As a result, the progressive shifting of chemical industry from fossil raw materials to renewable feedstocks becomes an unavoidable necessity. Terrestrial biomass offers a renewable and sustainable source of carbon available in polymeric (cellulose, starch, lignin, hemicellulose, protein) and monomeric forms (carbohydrate, amino acids, plant extractives), which could be used both as direct replacements for existing petrochemical building blocks and as a valuable source of new building blocks in chemical syntheses.⁴ Thanks to the development of biotechnology, especially fermentation techniques,³ it is now possible to convert biomass into industrially important chemicals with prices low enough to compete with petroleum-based processes. For example, D-glucose, which can be obtained from plant-derived starch and cellulose, is an attractive alternative to petroleum as a feedstock for many important chemicals such as ascorbic acid, lactic acid, succinic acid, amino acids, 1,3-propanediol, ethanol and several vitamins (Figure 1).

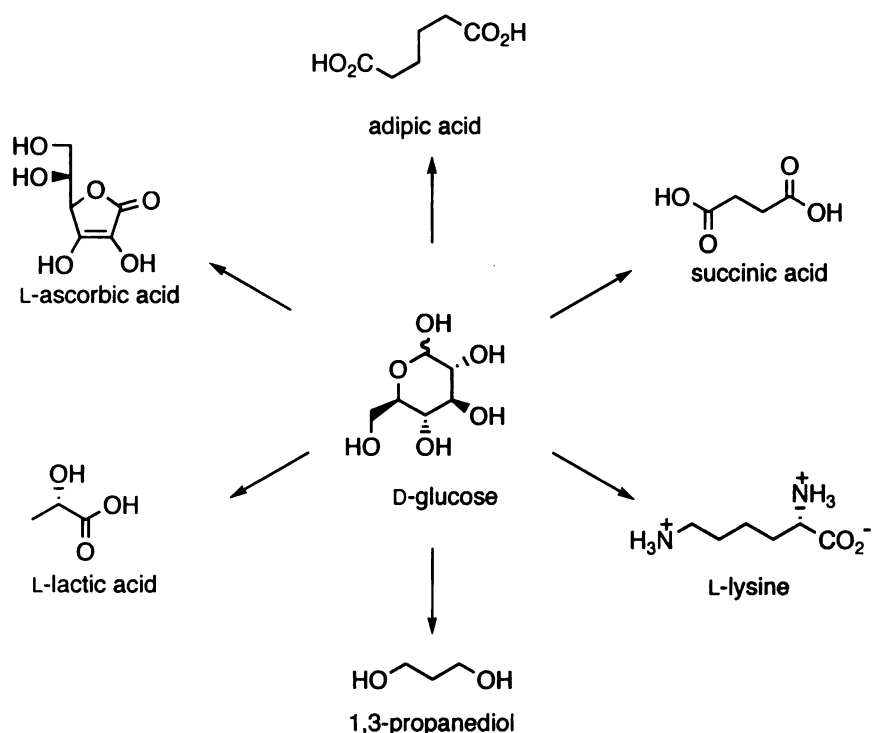


Figure 1. Selected organic chemicals from D-glucose.

As the monomer of nylon 6, ϵ -caprolactam is currently manufactured from petroleum-based benzene or toluene through multiple-step syntheses. Most processes for production of caprolactam entail the use of aggressive reagents such as oleum and sulfuric acids and generate large quantities of low-value ammonium sulfate salts. For the sustainable development of our society, it is necessary to devise environmentally benign methods of producing ϵ -caprolactam.

For completion of this thesis, alternative synthesis of this petroleum-derived bulk chemical ϵ -caprolactam from a renewable feedstock has been explored. In Chapter 2, strategies were developed to synthesize ϵ -caprolactam from L-lysine. L-Lysine underwent cyclization in refluxing high-boiling point alcohols to provide α -amino- ϵ -caprolactam. Subsequent chemical deamination of α -amino- ϵ -caprolactam with hydroxylamine-*O*-

sulfonic acid afforded ϵ -caprolactam. To obviate the use of stoichiometric amounts of deamination reagent, catalytic deamination of α -amino- ϵ -caprolactam with Pt on carbon was explored but low yields were encountered. In Chapter 3, effort towards preparation of transition metal sulfides and optimization of hydrodenitrogenation conditions are reported. The effects of presulfiding catalysts, temperature, reaction time, pressure, solvent, and H_2/H_2S ratio were examined. The highest yield of caprolactam was achieved using presulfided Pt on carbon. In Chapter 4, preparation and characterization of Au nanoparticle catalysts by transmission electron microscopy (TEM) are described. Optimization of reaction conditions by screening catalyst supports together with presulfiding, changing reaction temperature, reaction time and H_2S/H_2 ratios led to improved yields of ϵ -caprolactam when presulfided Au on NiO was employed as the hydrodenitrogenation catalyst, which is almost the same as the yield achieved with sulfided Pt on C.

1.2. Overview of Sustainable Chemistry

In the manufacture of the commodity chemicals caprolactam, adipic acid, aniline, phenol and many epoxides and esters, which are produced in more than millions of tons per year globally, there are several environmentally unacceptable problems. Most of these materials consume excessive energy in their manufacture. Production often uses aggressive, corrosive and sometimes even explosive reagents and a large amount of waste is generated. The production of these commodity chemicals frequently requires multiple steps, uses stoichiometric amounts of reagents, and are derived from nonrenewable feedstocks. Thus, there is an increasing need to devise new methods of manufacture of these chemicals that can minimize the consumption of energy and nonrenewable materials

along with minimization of the generation of wastes and gases that are ozone depleters and/or contribute to global warming.

To achieve environmentally benign and sustainable processes, two promising approaches have been extensively explored. One is shifting from nonrenewable petroleum feedstocks to renewable raw materials to achieve sustainable development. The other is to replace traditional synthetic methods that use stoichiometric amounts of reagents and produce excessive amounts of waste with cleaner and simpler catalytic methods with high atom efficiency and low E-factor.^{5,6}

1.2.1. Renewable Raw Materials.

At present, the share of renewable raw materials in feedstock consumption of the chemical industry is 10% both in Germany and the USA.⁷ Through investigation, the National Research Council of the USA has anticipated a fast development of renewable feedstocks up to 2090 (Figure 2). It is expected that 10% liquid fuel and 25% of the production of organic products will be replaced by renewable feedstocks in 2020 (Figure 2). By 2090, 50% of liquid fuel and up to 90% of organic chemicals in US should be provided by biomass (Figure 2).⁸

Ironically, about 50 years ago, petroleum-based products gradually replaced similar products once made from biological materials. Now, biobased products are starting to compete with the petroleum-derived products that once supplanted them.

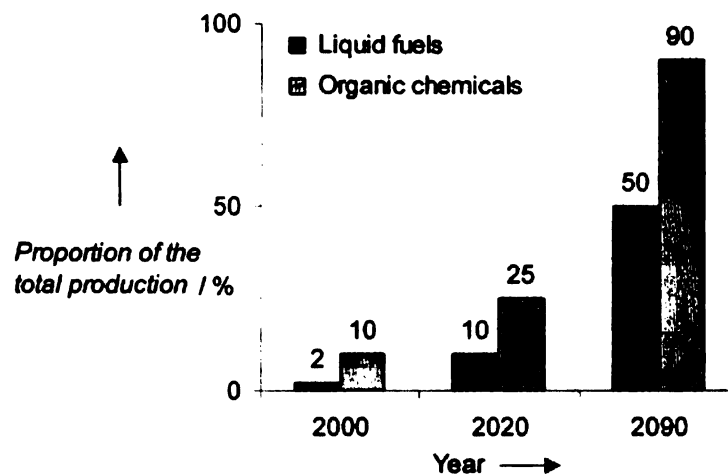


Figure 2. Targets of the National Research Council of the USA for the biobased production of organic compounds and of liquid fuels by the year of 2090. The proportion of the total production of each is given in percentage.

Currently, carbohydrates are the largest portion of renewable raw material used.⁹ The main attention should be focused on efficient use of carbohydrates and their subsequent conversion to useful chemical products and energy. Glucose (cellulose, starch), arabinose (hemicelluloses), and glycerol (plant oils) are the carbohydrate raw materials used for organic chemicals because they are inexpensive and accessible in large quantities. As the most abundant monosaccharide, D-glucose, which is accessible by hydrolysis of starch and cellulose, will be a key renewable starting material because a variety of biotechnological or chemical products can be readily derived from glucose (Figure 1). Current utilization of renewable feedstocks for chemical production is still at an early stage. Some selected examples of converting renewables to chemicals (especially polymer precursors) on an industrial scale are now outlined.

Adipic acid. One example is the microbial synthesis of adipic acid from D-glucose for use in the production of nylon 6,6. Adipic acid is one of the top 50 large-volume chemicals with an annual production at 2.5 millions tons worldwide in 1999. More than

80% of adipic acid is used for production of nylon 6,6 and the rest goes to plasticizers, lubricants and polyurethanes.

Most current processes for production of adipic acids start from benzene-derived cyclohexane via an intermediacy of cyclohexanol, cyclohexanone or a mixture of the two (known as KA oil) (Figure 3). Conversion of cyclohexanol or cyclohexanone to adipic acid involves using stoichiometric amount of concentrated nitric acid with copper and vanadium catalysts and subsequently generates a large quantity of nitrous oxide, which is a known greenhouse gas and depletes the ozone layer.¹⁰ Approximately 400,000 metric tons of N₂O are emitted each year during the production of adipic acid, which accounts for 5-8% of the world atmospheric emission of N₂O. Therefore, development of more environmentally friendly procedures for the production of adipic acid is highly desirable.

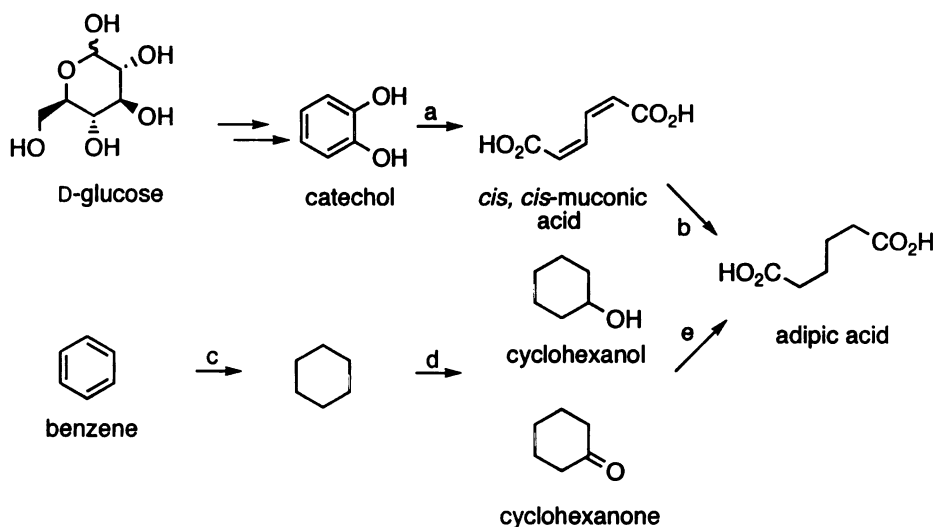


Figure 3. Chemical and biocatalytic approaches to adipic acid. Key: (a) *E. coli* WN1/pWN2.248; (b) H₂, 50 psi., 10% Pt/C; (c) Ni-Al₂O₃, H₂, 370-800 psi., 150-250 °C; (d) Co, O₂, 120-140 psi., 150-160 °C; (e) Cu, NH₄VO₃, 60% HNO₃, 60-80 °C.

Other industrial methods for making adipic acid include dihydrocarboxylation or carbomethoxylation of butadiene. A green route has been developed to oxidize

cyclohexene directly to adipic acid using aqueous H_2O_2 under solvent and halide free conditions.¹¹ This certainly provides a possible solution to the N_2O emission problem if the high cost of H_2O_2 can be significantly reduced in the future. Using dry air only as an oxidant, Thomas' group has devised two benign methods to produce adipic acid.¹² In one approach, the terminal methyl groups of hexane are selectively oxidized to carboxylic acids using aluminophosphate molecular sieves catalyst containing Co(III) ions. The second method involves oxidation of cyclohexane using aluminophosphate molecular sieves containing Fe(III). Use of these heterogeneous catalysts allows easy separation and recycling of the catalyst, avoids the use of nitric acid as well as the production of N_2O .

A biocatalytic process for adipic acid synthesis that eliminates all of environmental problems associated with the current industrial process has been achieved by Frost and coworkers.¹³ D-Glucose is converted to *cis,cis*-muconic acid by a biocatalyst. Hydrogenation of *cis,cis*-muconic acid at mild conditions with Pt on carbon affords adipic acid. Expression of a gene encoding catechol 1,2-dioxygenase in a catechol-producing *E. coli* strain enables the synthesis of *cis,cis*-muconic acid from D-glucose. An improved route to adipic acid via catechol utilized an *aroE* auxotroph *E. coli* WN1 expressing *aroZ*-encoded 3-dehydroshikimic acid (DHS) dehydratase for the conversion of DHS to protocatechuic acid (PCA), *aroY*-encoded PCA decarboxylase for the conversion of PCA to catechol, and *catA*-encoded catechol 1,2-dioxygenase for the conversion of catechol to *cis,cis*-muconic acid.¹⁴ This route affords 37 g/L of *cis,cis*-muconic acid from D-glucose in 23% yield (mol/mol). Catalytic hydrogenation of *cis,cis*-muconic acid over Pt on carbon (50 psi H_2) gives adipic acid in 97% yield. This biocatalytic approach uses a renewable feedstock, mild conditions and emits no N_2O . What's more, this route can also

provide catechol, a chemical building block used to synthesize flavors (such as vanillin), pharmaceuticals (L-DOPA) and antioxidants (4-*tert*-butylcatechol).

L-lactic acid. Another interesting example is L-lactic acid, which is primarily used in food and related industries.¹⁵ Generally, L-lactic acid is produced by microbial synthesis. For example, microbes like *Lactobacillus bulgaricus* synthesize 100 g/L of L-lactic acid in 95% yield from corn (starch) or starch-derived glucose.¹⁶ Recently, much attention has been paid to L-lactic acid due to two emerging products: as a precursor of the biodegradable polymer polylactic acid (PLA) and for the manufacture of the solvent ethyl lactate (Figure 4).^{17,18}

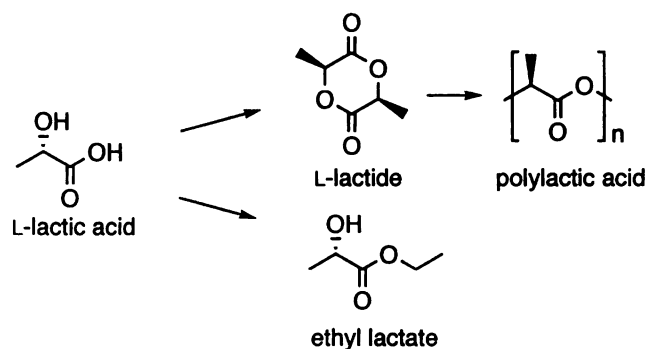


Figure 4. Commercially available derivatives from L-lactic acid.

Ethyl lactate is a useful derivative of lactic acid that has been commercialized. It finds wide use in inks, specialty coatings and cleaning because of its high performance. Right now, ethyl lactate is used in soy oil-solvent blends by Vertec Biosolvents Inc. As an environmentally-benign solvent that is readily biodegradable, ethyl lactate has the potential to displace petroleum-derived organic solvents such as dimethylformamide, toluene and N-methylpyrrolidone, provided its production cost (~ \$4/kg) can be reduced in

the future with advances in bioprocessing steps associated with separation and purification.

Poly(lactic acid) (PLA) is produced industrially by the ring opening of L-lactide (Figure 4), a dimer of lactic acid. Poly(lactic acid) is suitable for use in food packaging or surgical implants because it is biodegradable (to lactic acid, CO₂) and degrades within 45-60 days.

Due to growing demand for poly(lactic acid), the production of lactic acid is increasing rapidly. A joint venture between Cargill and Dow was opened in Blair, Nebraska in 2002 with a capacity of 140,000 metric tons per year.¹⁹ Today, poly(lactic acid) made from corn is already competitive with some petroleum-derived polymers such as poly(ethylene terephthalate) (PET) because of its combination of performance in applications, cost, and environmental benefits. In the future, using lignocellulosic feedstocks can further lower the manufacturing cost of poly(lactic acid) and may make it competitive with polypropylene and polystyrene as well.

Furans. Several sugar-derived furans are industrially attractive because they can potentially replace petroleum-based six-carbon monomers for production of polyamides (nylon 6, nylon 6,6) and polyesters. 5-Hydroxymethylfurfural (HMF) and furfural (2-furfuraldehyde) are readily accessible from plant-derived pentosans and fructose by acid-catalyzed dehydration.²⁰ As six-carbon monomers, furfural, 5-hydroxymethylfurfural and their derivatives could replace adipic acid, alkyldiols or hexamethylenediamine to produce polyamides or polyesters. HMF has been used for the manufacture of phenolic resins.²¹ As shown in Figure 5, a number of industrially useful chemicals can be prepared from HMF through well-developed methods, including 2,5-bis(hydroxymethyl)furan 4

(reduction), 5-hydroxymethyl-2-furoic acid **1** (oxidation), 2,5-furandicarboxylic acid **3** (oxidation) (Figure 5). Currently, fossil fuel-derived terephthalic acid is the most important dicarboxylic acid, produced on a millions of tons scale and mainly used for the production of polyester. Polymers, especially polyesters and polyamides have been prepared from furans such as 2,5-furandicarboxylic acid (FDCA) and other 5-hydroxymethylfurfural derivatives instead of terephthalic acid.²²

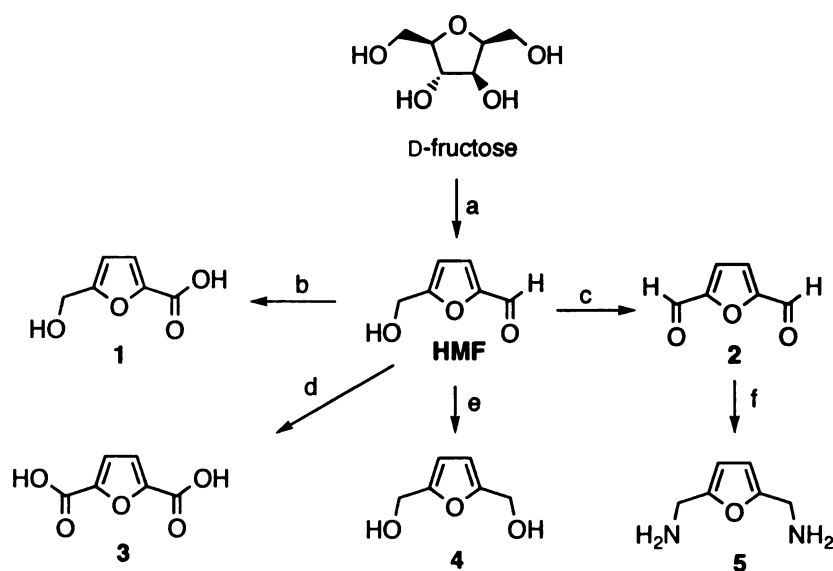


Figure 5. D-Fructose-derived furanoid products. Key: (a) H^+ , 90%; (b) Ag_2O , 100 °C, 75%; (c) $BaMnO_4/1,1,2$ -trichloroethane, 93%; (d) $Pb, Pt/O_2/pH\ 7$, quantitative (e) Pt/H_2 , quantitative; (f) NH_2OH/HCl , Raney Ni/H_2 , 33%.

For example, reaction of 2,5-furandicarboxylic acid **3** and diamine **5** results in furanoic polyamide **7** (Figure 6) that can potentially replace petroleum-based polyamides. Polymerization of 2,5-furandicarboxylic acid **3** with aromatic diamines leads to **6**, an analogue of Kelvar[®] (Figure 6). Currently, none of those polymers is economically

competitive with existing products due to the relative higher cost of starting material fructose. As a result, HMF is not produced on an industrial scale yet.

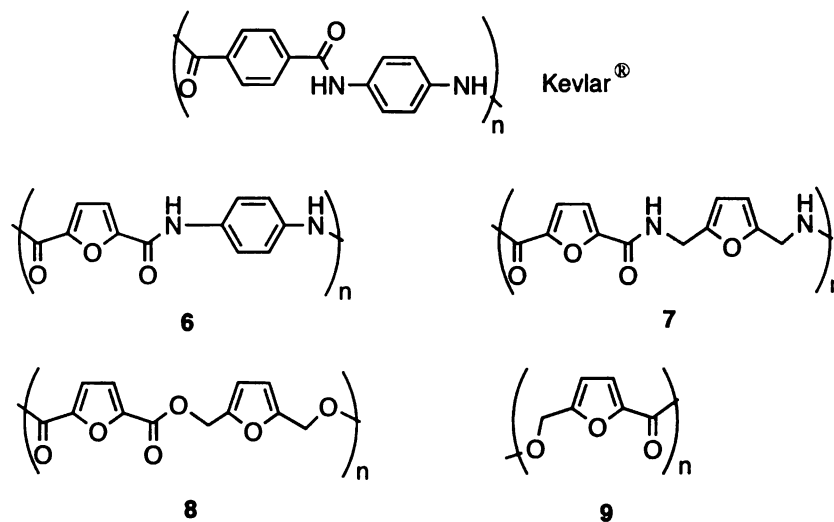


Figure 6. Kevlar® and its analogues.

In contrast, furfural is produced in about 250,000 tons per year from hydrolysis of pentoses. The well-developed chemistry of furfural provides access to several useful building blocks (Figure 7): furfuryl alcohol **11** (hydrogenation), furanacrylic acid **14** (Perkin reaction), furoic acid **13** (oxidation), furan **15** (through catalytic decarbonylation) and tetrahydrofuran **16** (hydrogenation), which provides a biobased alternative to petroleum-derived 1,4-butanediol.²³ Other established chemicals, such as fumaric acid, maleic acid, and levulinic acids, can also be prepared from furfural by ring-cleavage chemistry.²⁴

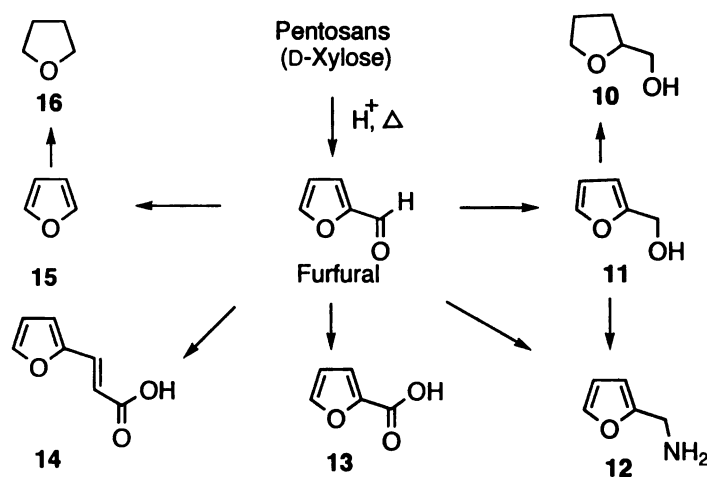


Figure 7. Versatile intermediate chemicals derived from furfural.

Phenol and p-hydroxybenzoic acid. Phenol is used to make synthetic resins, solvents, lubricating oils, dyes, pharmaceuticals, pesticides and perfumes. The predominant route for manufacturing phenol is via benzene-derived cumene hydroperoxide rearrangement (Figure 8). In fact, the Hock oxidation method accounts for about 97% of the 8.9 million tons of phenol production worldwide. The production of phenol consumes about 20% of the global benzene production. Benzene is an important industrial solvent and precursor for drugs, rubbers, plastics and dyes. However, benzene is volatile and carcinogenic.²⁵ Long term exposure to benzene can cause acute myeloid leukemia and non-Hodgkin's lymphoma.²⁶ What's more, benzene is produced from BTX (benzene-toluene-xylene) fraction of the nonrenewable fossil fuel.²⁷ To obviate the use of feedstock derived from fossil fuels, a new route to phenol by aromatization of D-glucose-derived shikimic acid (Figure 8) has been established.²⁸ Due to the increasing fears for potential of another bird flu pandemic, shikimic acid has recently attracted increasing attention as the base starting material for producing the anti-influenza drug Tamiflu (Figure 8).²⁹ Shikimic acid was extracted from the Chinese star anise before a technique was developed by Frost and

coworkers for the microbial synthesis of shikimic acid from D-glucose.³⁰ Reaction of shikimic acid in near-critical water gives phenol in 51% isolated yield.²⁶ Reaction of shikimic acid in refluxing acetic acid containing 1 M sulfuric acid at 120 °C yields *p*-hydroxybenzoic acid (Figure 8.) in 57% yield.²⁶ *p*-Hydroxybenzoic acid is used as a food preservative and as a key component for production of liquid crystal polymers such as Xydar, which find wide use in high-performance applications as sensors, switches and other electronic compounds at elevated temperatures.³¹ *p*-Hydroxybenzoic acid is currently synthesized by Kolbe-Schmitt reaction of potassium phenoxide with dry CO₂ at 240 °C followed by acidification with mineral acid. Given the increasing rise in the price of benzene and other fossil-derived starting materials, syntheses of phenol and *p*-hydroxybenzoic acid from nontoxic renewables are attractive alternative routes to these important chemicals.

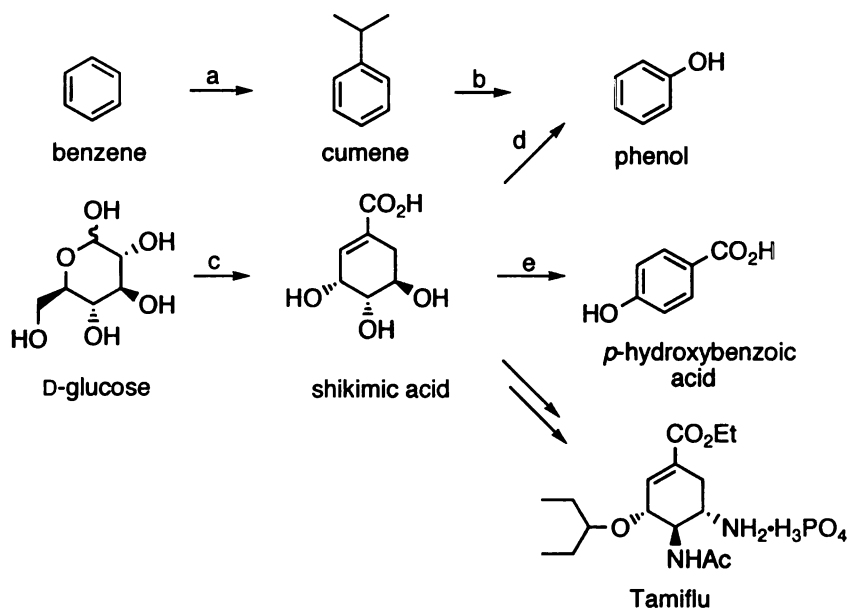


Figure 8. Synthesis of phenol and *p*-hydroxybenzoic acid from benzene and glucose. Key: (a) propene, AlCl₃; (b) 1) O₂, 100 °C, 2) H₂SO₄; (c) *E. coli* SP1.1/pKD12.138 or SP1.1pts/pSC6.090; (d) H₂O, 350 °C; (e) 1 M H₂SO₄ in AcOH.

1.2.2. Heterogeneous catalysts

As discussed before, catalytic reactions offer significant benefits in achieving environmentally benign syntheses. Catalysis can lower energy requirements, increase reaction selectivity, decrease use of processing and separation reagents, and allow for the use of less toxic materials. In general, there are heterogeneous, homogeneous and biological catalysts. Heterogeneous catalysis, in particular, provides for ease of separation of product from the catalyst and therefore eliminates the need for separation through extraction or distillation. Heterogeneous catalysts currently used are frequently classified into three different types: metals alone, metals plus other components (metal oxide, metal sulfides, metal nitrides, metal borides) and supported metals. Metal oxides are used mainly for selective oxidation of hydrocarbons and selective reduction of NO_x with NH₃. Metal sulfides are used for hydrodesulfurization (HDS) and hydrodenitrogenation (HDN) of petroleum. Metals are most widely used for a variety of reactions such as hydrogenation and oxidations.

Catalytic metals are mainly limited to 12 elements in groups VIII and IB of the periodic table (Fe, Co, Ni, Cu, Rh, Pd, Ag, Pt, Ru, Ir, Os and Au). Among them, the most catalytically active metals are Ni, Pd, Pt and Rh. Nickel is used extensively in hydrogenation and is frequently used in the form of Raney nickel. Palladium is good for hydrogenation of most unsaturated organic molecules except benzenes. It is frequently used for hydrogenolysis off protecting groups. Platinum catalyzes the hydrogenation of most functional groups except esters, acids and amides. Rhodium is good for the hydrogenation of most functional groups with a minimum of hydrogenolysis activity.

Many of the methods for preparing heterogeneous catalysts have been reviewed.³² A brief summary of preparation methods is as follows. Skeletal metals are formed by leaching away one metal from an intimate alloy of two or more metals. One example of these is Raney nickel. Metallic powders are made from several ways. They can be prepared by reducing salts (normally chlorides of metals) with a reducing gas such as hydrogen. They can also be made from thermal decomposition of metal carbonyls or metal salts of organic acids in a vacuum. Metal sulfides may be prepared by passing a sulfur-containing compound over the metal under a hydrogen atmosphere. Such catalysts are normally immune to nonmetallic poisons.

Particle size is an important parameter in heterogeneous catalysis. Two classes of heterogeneous catalytic reactions have been defined³³ according to the effects of the particle size: one is structure sensitive where rates per exposed atom depend on the particle sizes such as hydrogenolysis of C-C bond. The other is structure insensitive where rates are not dependent on the particle sizes of catalysts such as dehydrogenation of cyclohexane to benzene. Since the relative populations of exposed atoms at edges, corners and planes of the metal crystallites change as the particle size changes, structure-sensitive reactions are believed to occur on active sites whose numbers change with the particle sizes.

Measurement of particle size distributions can be done with chemisorption, chemical reactions³⁴ and electron micrographs. One classical example of the use of chemical reactions to characterize the catalyst surface has been reported by Sinfelt and his co-workers.³⁵ During their investigation, both structure-sensitive and structure-insensitive reactions were used to characterize catalysts composed of different mol ratios of Cu to Ni.

As the concentration of Cu in Cu-Ni alloy increases from zero to 100%, the reaction rate of cyclohexane dehydrogenation (structure insensitive) remains constant until the very highest concentration of Cu. Alternatively, the reaction rate of ethane hydrogenolysis, which is structure-sensitive, continuously decreases. Since the dehydrogenation of cyclohexane presumably occurs on the active sites of single Ni atoms, its reaction rate remains constant until the concentration of Cu becomes too high to significantly dilute the Ni. Ethane hydrogenolysis depends on the active sites of a certain minimal size (or ensembles). The numbers of Ni clusters on the catalyst surface decreased rapidly as the result of addition of Cu onto the catalyst surface.

Energy production from biomass. Record-high oil, gasoline and natural gas prices combined with possible global-warming have driven people to look for new clean-energy technologies. Biofuels and hydrogen seem to be the most promising solutions. Hydrogen is currently produced from nonrenewable natural gas and petroleum³⁶ but could in principle, be derived from renewable resources, such as water and biomass. However, It is difficult to generate hydrogen efficiently from water. Technologies available for generating hydrogen from biomass, such as steam-reforming of bio-oils³⁷ or enzymatic decomposition of sugars,³⁸ usually require complex processing or suffer from low hydrogen generation rates. Dumesic's group has demonstrated that hydrogen can be produced at 500 K in a single-reactor aqueous phase reforming process using a Pt-based catalyst.³⁹ Dumesic and his coworkers proposed the mechanism shown in Figure 9 to explain the formation of the alkanes and hydrogen. The reactant undergoes dehydrogenation on the surface of the metal to generate the adsorbed species before the subsequent C-C bond cleavage or C-O bond cleavage. On the surface of catalyst

employed, Pt-C bonds are stronger than Pt-O bonds. This may indicate that the adsorbed species probably prefers to bind on the catalyst surface through Pt-C bond instead of Pt-O bond, which lead to the cleavage of C-C bonds and generation of CO and hydrogen (Figure 9). CO reacts with water to form CO₂ and hydrogen by the so-called water-shift reaction. Two reactions have been identified to affect the selectivity of hydrogen production from hydrocarbons (Figure 9). “Series selectivity” entails reaction of hydrogen produced with CO or CO₂ leading to alkanes and water by methanation or a Fischer-Tropsch (F-T) reaction (Figure 9). The other reaction is the “parallel selectivity” problem which involves cleavage of C-O bond and hydrogenation of the resulting intermediate resulting in the formation of undesired alkanes (Figure 9). Thus, the key to high hydrogen production is to find the catalyst that favors the C-C bond cleavage over C-O bond cleavage.

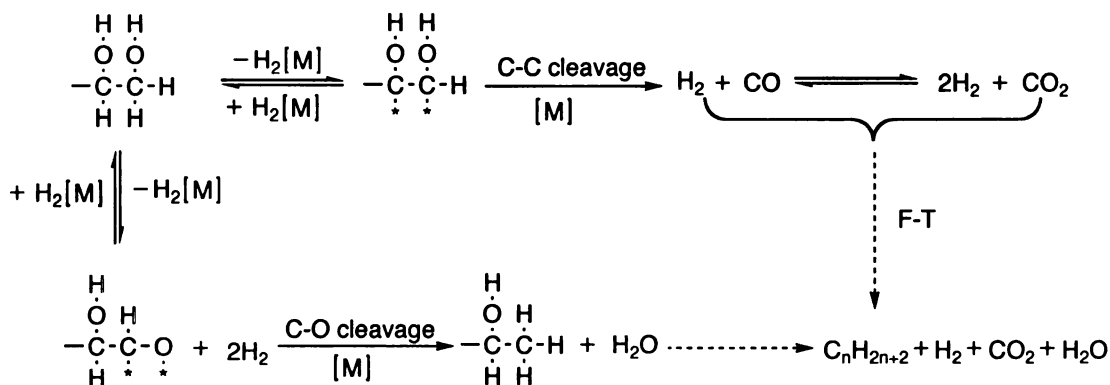


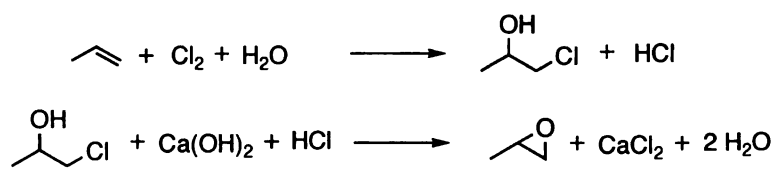
Figure 9. Reaction pathways for hydrogen production by reaction of oxygenated hydrocarbons with water. Key: [M] = metal surface; * surface metal site; F-T= Fischer-Tropsch reaction.

A theoretical study based on the self-consistent periodic DFT (density functional theory) calculations, together with transition-state theory, predicts that on the Pt (111)

surface and at temperature higher than 550 K the rate constant for C-C bond cleavage is higher than that of C-O bond cleavage. These calculations also predict that C-C bond cleavage in ethanol on Pt (111) is much faster than in ethane on Pt (111).⁴⁰ These calculations explain why hydrogen production can be favored. This theoretical analysis suggests that a promising aqueous-phase technology for producing H₂ fuel from renewable biomass. With further research, it is possible that this catalytic methodology can be applied industrially in the future.⁴¹

Propylene oxide. Propylene oxide is one of the most important bulk chemicals, which is used for producing polyurethane and polyols. It is produced globally at 5 millions tons per year and provides a market of about \$11 billion per year. Current industrial production of propylene oxide involves a two-stage reaction using either chlorine (chlorohydrin process) (Figure 10) or organic peroxide (Halcon process) (Figure 10).

Chlorohydrin process



Halcon process



Figure 10. Industrial processes of propylene oxide.

The chlorohydrin process causes serious environmental pollution and the Halcon process produces stoichiometric quantities of low value co-products such as styrene or *t*-

butyl alcohol. Although H_2O_2 is an environmentally benign oxidant and can oxidize propylene to propylene oxide in high selectivity, the price of H_2O_2 is too high to be economically competitive.⁴² Molecular oxygen is an ideal oxidant due to its low cost and generation of water as the byproduct. Hoelderich and coworkers have reported the liquid-phase generation of propylene oxide by reaction of propylene with oxygen and hydrogen in aqueous methanol over Pd on TS-1 (a titanium silicalite catalyst), giving conversion and selectivity over 40% in batch reactions.⁴³ Liu and colleagues have examined the direct oxidation of propylene by molecular oxygen without hydrogen by a Pd catalyst in methanol in an autoclave reactor and achieved over 60% selectivity at 43% conversion of propylene.^{44,45}

Gold-catalyzed epoxidation of propylene using hydrogen and oxygen has been investigated extensively for the past decade.⁴⁶ Four factors have been identified to be important for the preparation of efficient Au catalysts in the direct propylene epoxidation. The first factor is the methods employed for Au deposition. Impregnation resulted in complete oxidation of propylene to H_2O and CO_2 while deposition precipitation led to epoxidation with selectivity higher than 90% (Figure 11). The second factor is the appropriate selection of support materials. Anatase TiO_2 (one of the three mineral forms of TiO_2) is the only single metal oxide that can make Au selective below 100 °C, but the conversion of propylene remains low. However, use of titanosilicate supports lead to the stabilization of propylene oxide at higher temperature and also increases the propylene oxide yield as desorption of propylene oxide is favored at high reaction temperature.⁴⁷ For example, conversion of propylene was only 1% in the case of Au catalysts supported on anatase and microporous TS-1 but conversion increased to 4% for ordered mesoporous Ti-

MCM-41 (Ti-containing mesoporous molecular sieve) and hydrophobic Ti-HMM (Ti-containing hybrid mesoporous material) and to about 5% for three-dimensional sponge-like mesoporous titanosilicates with epoxidation selectivity greater than 90%. The third important factor is the size of Au particles (Figure 11). Only those Au catalysts with particle sizes between 2-5 nm show efficient epoxidation activity. When the mean diameter of Au particles is smaller than 2 nm, propylene is reduced to propane (Figure 11). When the Au particle sizes are bigger than 5 nm, the formation of H₂O and CO₂ is favored (Figure 11).

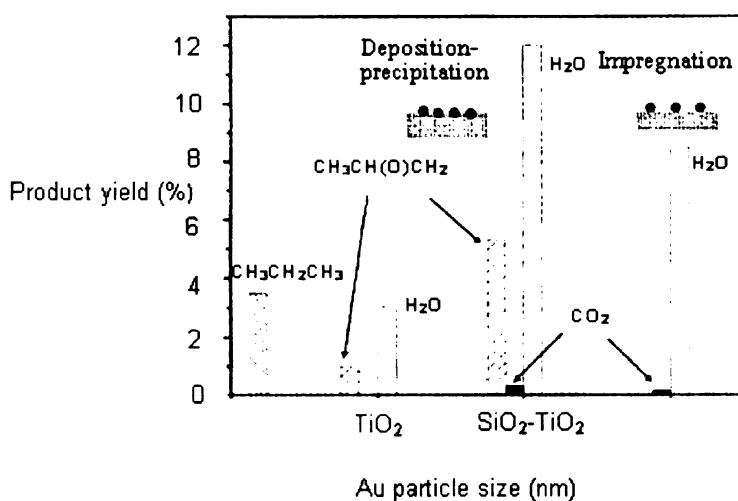


Figure 11. Influence of Au particle size on product yield during propylene epoxidation using O₂ and H₂.

The fourth factor affecting the catalyst is the additive. Many alkaline and alkaline earth salts work as promoters and play an important role in the selectivity of epoxidation.⁴⁸ For example, mixing of CsCl with Au supported on Ti-MCM-41 increased the propylene

epoxide selectivity to 97% with a propylene conversion less than 2%. Addition of BaNO₃ into Au on titanosilicate support improved propylene conversion to 4% with propylene oxide selectivity of about 90%.⁴⁹ An efficient regeneration of Au catalyst on titanosilicate using a trace amount of trimethylamine resulted in a propylene conversion up to 8.5% and a propylene oxide selectivity of 91%. This result is very close to the current industrial standard (a propylene conversion of 10%, a propylene oxide selectivity of 90%). Trimethylamine-promoted, one-step epoxidation of propylene using oxygen and hydrogen over supported Au catalysts thus serves as an example of a chemical process that can both meet the industrial standards and be environmentally compatible.⁵⁰

1.3. Syntheses of Caprolactam

As the monomer of nylon 6, approximately 4 million tons of ϵ -caprolactam are produced each year.⁵¹ Nylon 6 is widely used for its high strength-to-weight ratio, good chemical and thermal stability, and durability. Most current manufacturing processes for caprolactam start from either toluene or benzene, via the intermediacy of cyclohexanone, cyclohexanone oxime and followed by a Beckmann rearrangement to afford ϵ -caprolactam (Figure 12).

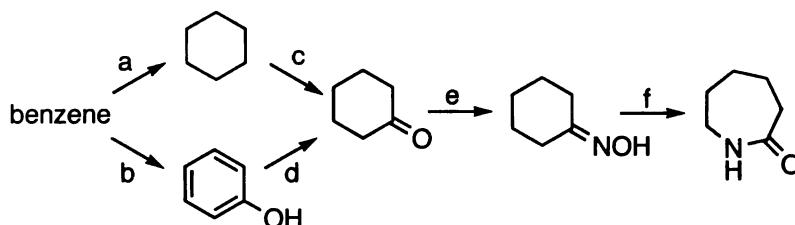


Figure 12. Classical production of ϵ -caprolactam. Key: (a) H_2/Ni ; (b) 2-propene, HZSM-12; (c) i) O_2 , ii) Cu/Zn ; (d) H_2/Pd ; (e) i) $(\text{NH}_2\text{OH})_2\text{H}_2\text{SO}_4$, ii) NH_3 ; (f) i) $\text{H}_2\text{SO}_4\cdot\text{SO}_3$, ii) NH_3

The major issues with current production of caprolactam involve the use of hydroxylamine sulfate and oleum in the ammoximation (Figure 13) and Beckmann rearrangement respectively (Figure 13). Neutralization of the liberated acid from hydroxylamine sulfate with ammonia results in the formation of large quantities of low-value ammonium sulfate as a byproduct (up to 4.5 kg of ammonium sulfate per kg of caprolactam).

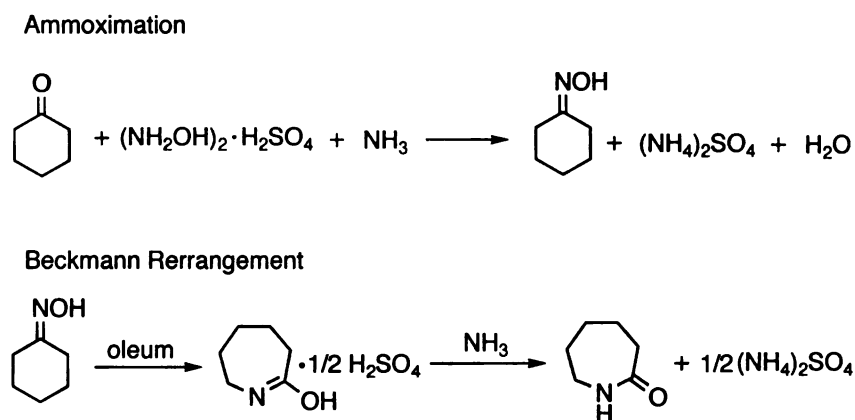
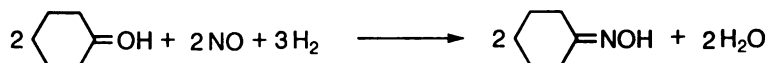


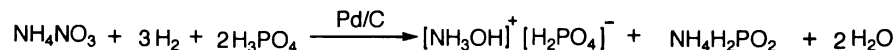
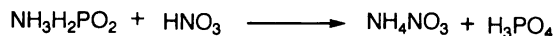
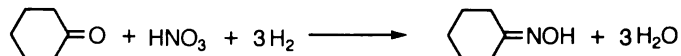
Figure 13. Formation of ammonium sulfate

The formation of large quantities of ammonium sulfate is economically and environmentally problematic for caprolactam producers. To minimize the formation of ammonium sulfate, many processes have been explored that entail developing new catalysts or using new starting materials. Most of the effort has been put into preventing the formation of ammonium sulfate salt during the ammoximation (Figure 13).

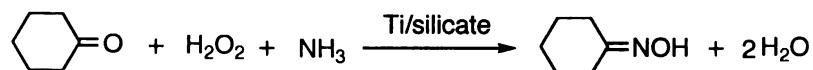
Step 1:**Step 2:****Overall:****Figure 14. Acidic oximation process**

BASF made its contribution by developing the acidic oximation process shown in Figure 14. In the first step of the acidic oximation process, nitric oxide is catalytically reduced in a solution of ammonium hydrogen sulfate over platinum on graphite to give ammonium hydroxylammonium sulfate, which drives the transformation of cyclohexanone to cyclohexanone oxime. The resulting ammonium hydrogen sulfate is recovered for the generation of hydroxylamine. Hence, no further neutralization of ammonium hydrogen sulfate is required. This acidic oximation process reduces the amount of ammonium sulfate from the previous 2.5-2.7 tons to only 0.1 ton per ton of cyclohexanone oxime.

Another popular process developed by DSM is the hydroxylamine-phosphate-oxime (HPO) process (Figure 15), during which the ammoximation is conducted in a hydroxylamine phosphoric acid buffer. After separation of the oxime, the remaining ammonium phosphate buffer is concentrated and recycled into the hydroxylamine synthesis. Hydroxyl ammonium phosphate is formed by reduction of ammonium nitrate

Step 1:**Step 2:****Step 3:****Overall****Figure 15. HPO (hydroxylamine-phosphate-oxime) process.**

and phosphoric acid with hydrogen in the presence of a palladium catalyst. Nitrate ions consumed are replaced by addition of nitric acid (Figure 15, step 3). The HPO process avoids the formation of ammonium sulfate in the ammoximation step. However, both BASF's acidic oximation process and DSM's HPO process still need to use hydroxylamine. The generation and handling of hydroxylamine require extensive capital investment. One innovation, called the EniChem ammoximation process, has actually bypassed the need of hydroxylamine (Figure 16). In this process, cyclohexanone is reacted with ammonia and hydrogen peroxide at 90 °C in the presence of a titanosilicate catalyst (Figure 16). This process was first developed by EniChem (now Syndial, Italy). However, the main drawback of this process is the high price of the catalyst along with the high and volatile price of hydrogen peroxide.

**Figure 16. EniChem ammoximation process.**

The final step of caprolactam synthesis is a Beckmann rearrangement, during which oleum is commonly used to initiate this transformation (Figure 13). Neutralization of the released acid with ammonia has resulted in about 1.8 tons of ammonium sulfate per ton of caprolactam. To avoid the formation of ammonium sulfate, there has been extensive investigation into the optimization of the classical Beckmann rearrangement. A variety of catalysts have been tested for the reaction, namely zeolitic molecular sieves and nonzeolitic catalysts. The majority of the work done by different groups focuses on the relation of the catalysis acidity and yield, the location of the rearrangement, and the best reaction conditions. An important process called the Gas-phase Beckmann Rearrangement, first introduced by Dupont in 1938, has been developed worldwide ever since. This process uses heterogeneous catalysts instead of sulfuric acid and generates no ammonium sulfate. Contrary to the general belief that the Beckmann rearrangement is catalyzed only by acid, a high silica MFI zeolite that possesses no acidity was found to be the best catalyst for the reaction.

Sumitomo successfully increased the selectivity of the catalyst, made it suitable to be industrially used and commercialized a process for a Beckmann rearrangement free of ammonium sulfate for the first time. The process operates at 350 °C with a small positive pressure and methanol as the promoter in a fluid bed reactor. Combining the ammoximation (from EniChem) and fluidized-bed Beckmann rearrangement, Sumitomo has successfully commercialized a zero ammonium sulfate route to produce caprolactam.⁵² However, as we mentioned before, the disadvantages of this process are the high cost of catalysts, hydrogen peroxide and the fluidized-bed reactor.⁵³

The other promising alternative to the heterogeneous processes is the production of caprolactam based on non-aromatic starting materials such as butadiene or adiponitrile. Two relevant approaches have been considered. The first results from a collaboration between DSM and Dupont called the ALTAM process (Figure 17).⁵⁴

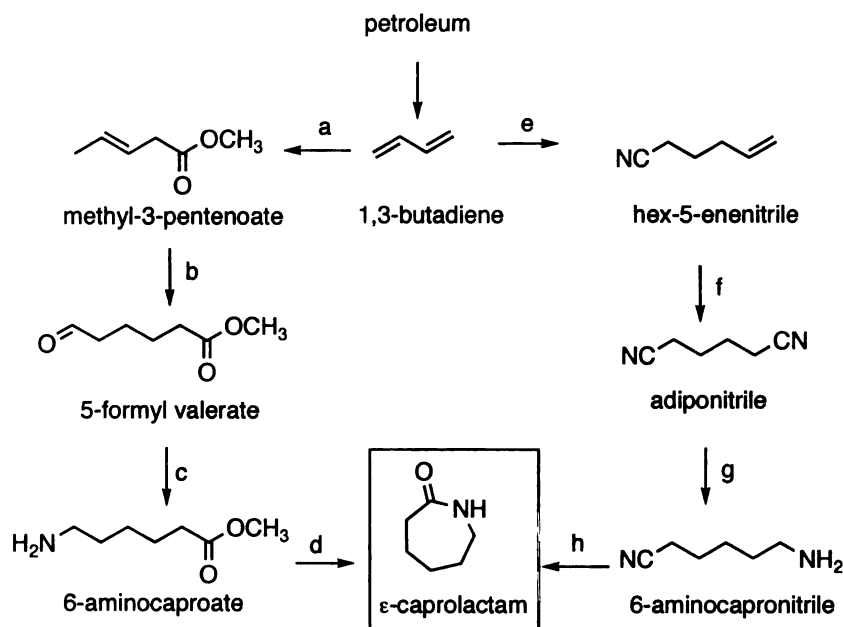


Figure 17. Syntheses of ϵ -caprolactam from 1,3-butadiene. Key: (a) CO, MeOH, Ni-zeolites; (b) CO, H₂, Co, Rh; (c) NH₃/H₂, Ru; (d) 250 °C; (e) HCN; (f) HCN; (g) Ni/Co, H₂; (h) TiO₂, H₂O.

In the first step, butadiene is carbonylated in the presence of methanol at high pressure (> 7 MPa) to produce the pentenoate ester. The methyl pentenoate is subjected to hydroformylation with syngas in the presence of a ligand-promoted rhodium catalyst to afford 5-formyl valerate. The resulting valerate ester undergoes reductive amination over a ruthenium catalyst to 6-aminocaproic acid, which is then cyclized to caprolactam at an elevated temperature (250 °C) in the absence of catalyst.⁵⁵

Another approach, developed by Dupont with BASF and Rhodia separately,⁵⁶ uses adiponitrile as an intermediate (Figure 17). Adiponitrile can be prepared from butadiene and hydrogen cyanide over a nickel phosphate catalyst, which was a process first developed by Dupont for production of hexamethylenediamine (HMDA), one monomer for nylon 6,6. The next step is partial hydrogenation of adiponitrile at high pressure (6.9 MPa) and 80 °C over Raney nickel in liquid ammonia. The final step is hydrolytic cyclization of the resulting 6-aminohexanitrile at moderate temperature (240 °C) and high pressure (10 MPa) over TiO₂ to give caprolactam (Figure 17).⁵⁷ Butadiene-based processes certainly provide another option in the future. However, the butadiene routes involve several separations and recycling steps of products and byproducts, severe reaction conditions, low productivity of catalyst and fluctuating pricing of butadiene. The future of butadiene-based routes depends on a relative cheaper feedstock cost to benzene exists and persists.

There are certainly significant improvements in developing butadiene-based routes and heterogeneously catalyzed routes based on zeolitic molecular sieves and non-zeolitic materials to reduce the generation of ammonium sulfate or avoid using toxic and corrosive reagents in caprolactam production. However, all above routes are still based on petroleum feedstocks (benzene or butadiene). In the long run, it is only reasonable to replace fossil feedstocks with renewables that are processed by catalytic reactions to achieve environmentally sustainable development. This concept has been demonstrated by the example of adipic acid syntheses development. Adipic acid is an important building block for nylon 6,6 and urethanes.⁵⁸ It is currently produced from hexanone or hexanol involving aggressive nitric acid oxidation generating a large amount of nitrous

oxide, a green house gas. Alternative catalytic syntheses have been developed to eliminate the use of nitric acid by direct conversion of cyclohexane in air.^{59,60} Still, all syntheses rely on petroleum-derived benzene as the feedstock. A biocatalytic process for adipic acid synthesis that eliminates all environmental problems associated with the current industrial process has been achieved by Frost and coworkers.⁶¹ This aroused our interest in exploring the possibility of devising a process to catalytically prepare caprolactam from a renewable feedstock as well. In this thesis, a benzene-free synthesis of caprolactam has been explored where caprolactam is synthesized from glucose-derived L-lysine via intermediacy of α -aminocaprolactam (Figure 18).

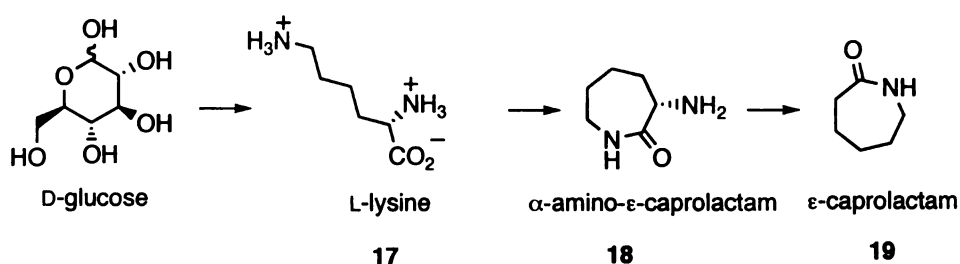


Figure 18. Renewable Synthesis of Caprolactam.

References

- 1 (a) Campbell, C. J.; Laherrère, J. H. *Sci. Am.* **1998**, *60*. (b) Lovins, A. B.; Datta, E. K.; Bustnes, O. D.; Koomey, J. G.; Glasgow, N. J. *Winning the Oil Endgame*; Rocky Mountain Institute: Snowmass, Colorado, **2004**. (c) Lichtenthaler, F. W. *R. C. Chimie* **2004**, *7*, 65.
- 2 (a) Mullin, R. *Chem. Eng. News.* **2004**, *82*(42), 29. (b) Tullo, A. H. *Chem. Eng. News.* **2004**, *82*(11), 20.
- 3 (a) Weissermel, K.; Arpe, H.-J. In *Industrial Organic Chemistry, 3rd ed.*; VCH: New York, 1997: p. 310. (b) Committee on Biobased Industrial Products.; Board on Biology.; Commission on Life Sciences.; National Research Council., In *Biobased Industrial Products: Priorities for Research and Commercialization.*; Washington, D. C. National Academy Press, 1999.
- 4 (a) Frost, J. W.; Lievense, J. Prospects for Biocatalytic Synthesis of Aromatics in the 21st- Century. *New J. Chem.* **1994**, *18*, 341. (b) Eissen, M.; Metzger, J. O.; Schmidt, E.; Schneidewind, U. *Angew. Chem. Int. Ed.* **2002**, *41*, 414. (c) Lichtenthaler, F. W. *Acc. Chem. Res.* **2002**, *35*, 728.
- 5 Trost, B. M. *Science* **1991**, *254*, 1471.
- 6 Sheldon, R. A. *CHEMTECH* **1994**, 38.
- 7 Anon. *Chem. Eng. News.* **2002**, *22*, 55.
- 8 *Biobased Industrial Products: Priorities for Research and Commercialization*, National Academy Press, Washington, D.C, **2000**.
- 9 Kamm, B.; Gruber, P. R.; Kamm, M. "Biorefineries-Industrial Processes and Products. Status Quo and Future Directions" Vol. 2. Wiley-VCH Verlag GmbH & Co. KGaA, Weinheim, **2006**,
- 10 (a) Thiemens, M. H.; Trogler, W. C. *Science* **1991**, *251*, 932. (b) Dickenson, D. E.; Cicerone, R. J. *Nature* **1986**, *319*, 109.
- 11 Sato, K.; Aoki, M.; Noyori, R., *Science*, **1998**, *281*, 1646.
- 12 (a) Raja, R.; Sankar, G.; Thomas, J. M., *Angew. Chem. Int. Ed.* **2000**, *39*, 2313. (b) Dugal, M.; Sankar, G.; Raja, R.; Thomas, J. M., *Angew. Chem. Int. Ed.* **2000**, *39*, 2310.

- 13 Draths, K. M.; Frost, J. W. *J. Am. Chem. Soc.* **1994**, *116*, 399.
- 14 Niu, W.; Draths, K. M.; Frost, J. W. *Biotechnol. Prog.* **2002**, *18*, 201.
- 15 Datta, R. In *Kirk-Othmer Encyclopedia of Chemical Technology*, 4th ed.; Kroschwitz, J. I.; Howe-Grant, M. Eds.; Wiley: New York, **1997**; Vol. 13. p1042.
- 16 Datta, R.; Tsai, S-H.; Bonsignore, P.; Moon, S-H.; Frank, J. R. Technological and economic potential of poly(lactic acid) and lactic acid derivatives. *FEMS Microbiol. Rev.* **1995**, *16*, 221.
- 17 Hester, A. IB. *Ind Bioprocess.* **2000**, *22*, 3.
- 18 Watkins, K. A. *Chem. Eng. News.* **2002**, *80*, 15.
- 19 (a) McCoy, M. *Chem. Eng. News.* **2003**, *81*, 18. (b) Ritter, S. K. *Chem. Eng. News.* **2002**, *80*, 20.
- 20 Moreau, C.; Belgacem, M. N.; ZGandini, A., *Topics Catal.* **2004**, *27*, 11.
- 21 Koch, H.; Pein, J. *Polym. Bull.* **1985**, *13*, 525.
- 22 Mitiakoudis, A.; Gandini, A.; Cheradame, H. *Polym, Commun.* **1985**, *26*, 246.
- 23 Mc Killip, W. J.; Collin, G.; Hoke, H.; Zeitsch, K. J. "Furan and derivatives", *Ullmann's Encyclopedia of Industrial Chem.* **2000**, http://www.mrw.interscience.wiley.com/ueic/articles/a12_119/frame.html.
- 24 Gandini, A.; Belgacem, M. N. *Prog. Polym, Sci.* **1997**, *22*, 1203.
- 25 Lewis, R J. *Carcinogenically Active Chemicals*; Van Nostrand Reinhold: New York, 1991; pp 68.
- 26 O'Connor, S. R.; Farmer, P. B.; Lauder, I. J. *J. Pathol.* **1999**, *189*, 448.
- 27 (a) Stadelholfer, J. W. *Industrial Aromatic Chemistry*; Springer-Verlag: New York, 1988. (b) Szmant, H. H. *Organic Building Blocks of the Chemical Industry*; Wiley: New York, 1989.
- 28 Gibsons, J. M.; Thomas, P. S.; Thomas, J. D.; Baker, J. L.; Chandran, S. S.; Harrup, M. K.; Draths, K. M.; Frost, J.W. *Angew. Chem. Int. Ed.* **2001**, *40*, 1945.

- 29 (a) Federspiel, M.; Fischer, R.; Henning, M.; Mair, H-J.; Oberhauser, T.; Rimmler, G.; Albiez, T.; Bruhin, J.; Estermann, H.; Gandert, C.; Gockel, V.; Gotzo, S.; Hoffmann, U.; Huber, G.; Janatsch, G.; Lauper, S.; Odette, T. -S.; Trussardi, R.; Zwahlen, A. G. *Org. Process Res. Dev.* **1999**, *3*, 266. (b) Kim, C. U.; Lew, M. Williams, M. A.; Liu, H.; Zhang, L.; Swaminathan, S.; Bischofberger, N.; Chen, M. S.; Mendel, D. B.; Ty, C. Y.; Laver, W. G.; Stevens, R. C. *J. Am. Chem. Soc.* **1997**, *119*, 681. (c) Rohloff, J. C.; Kent, K. M.; Postich, M. J.; Becker, M. W.; Chapman, H. H.; Kelly, D. E.; Lew, W.; Louie, M. S.; McGee, L. R.; Prisbe, E. J.; Schulze, L. M.; Yu, R. H.; Zhang, L. *J. Org. Chem.* **1998**, *63*, 4545.
- 30 (a) Drath, K. M.; Knop, D. R.; Frost, J. W. *J. Am. Chem. Soc.* **1999**, *121*, 1603. (b) Knop, D. R.; Draths, K. M.; Chandran, S. C.; Barker, J. L.; von Daeniken.; Weber, W.; Frost, J. F. *J. Am. Chem. Soc.* **2001**, *123*, 10173. (c) Chandran, S. C.; Yi, J.; Draths, K. M.; von Daeniken, R.; Weber, W.; Frost, J. W. *Biotechnol. Prog.* **2003**, *19*, 808.
- 31 Kirsch, M. A.; Williams, D. J. *Chemtech.* **1994**, *24*, 40.
- 32 (a) Schwartz, J. A.; Contescu, C.; and Contescu, A. *Chem. Rev.* **1995**, *95*, 477. (b) Peterson, R. J. *Hydrogenation Catalysts*, Noyes Data, Park Ridg, NJ, 1977.
- 33 Boudart, M.; *Adv.Catal.* **1969**, *20*, 153.
- 34 (a) Augustine, R. L.; *Heterogeneous Catalysis for the Synthetic Chemist*, Dekker, New York, 1996. (b) Notheisz, F.; Bartok, M.; Ostgard, D.; Smith, G. V. *J. J Catal.* **1986**, *101*, 212.
- 35 Sinfel, J. H.; Carter, J. L.; Yates, D. J. C. *J. Catal.* **1972**, *24*, 283.
- 36 Rostrup-Nielsen, J. R. *Phys. Chem. Chem, Phys.* **2001**, *3*, 283.
- 37 Garcia, L.; French, R.; Czernik, S.; Chornet, E. *Appl. Catal. A.* **2000**, *201*, 225.
- 38 Woodward, J.; Orr, M.; Cordray, K.; Greenbaum, E. *Nature* **2000**, *405*, 1014.
- 39 Cortright, R. D.; Davda, R. R.; Dumesic, J. A. *Nature* **2002**, *418*, 964.
- 40 Alcalá, R.; Mavrikakis, M.; Dumesic, J. A. *J. Catal.* **2003**, *218*, 178.
- 41 Chornet, E.; Czernik, S. *Nature* **2002**, *418*, 928.
- 42 Xi, Z.; Zhou, N.; Sun, Y.; Li, K. *Science* **2001**, *292*, 1139.

- 43 Hoeldrich, W. F.; Laufer, W. *Appl. Catal. A: Gen.* **2001**, *213*, 163.
- 44 Liu, Y. Y.; Murata, K.; Inaba, M. *Catal. Lett.* **2004**, *93*, 109.
- 45 Dauciu, T.; Beckman, E. J.; Hancu, D.; Cochran, R. N.; Grey, R.; Hajnik, D. M.; Jewson, J. *Angew. Chem. Int. Ed.* **2003**, *42*, 1140.
- 46 Hayashi, T.; Tanaka, K.; Haruta, M. *J. Catal.* **1998**, *178*, 566.
- 47 a) Uphade, B. S.; Akita, T.; Nakamura, T.; Haruta, M. *Appl. Catal. A: Gen.* **2001**, *215*, 137. b) Uphade, B. S.; Akita, T.; Nakamura, T.; Haruta, M. *J. Catal.* **2002**, *209*, 331. c) Sinha, A. K.; Seelan, S.; Akita, T.; Haruta, M. *Appl. Catal. A: Gen.* **2003**, *240*, 243.
- 48 (a) Hayashi, T.; Wada, M.; Haruta, M.; Tsubota, S. US Patent 5,932,750 (1999). (b) Uphade, B. S.; Okumura, M.; Tsubota, S.; Haruta, M.; *Appl. Catal. A: Gen.* **2000**, *190*, 43.
- 49 Sinha, A. K.; Seelan, S.; Tsubota, S.; Haruta, M.; *Top. Catal.* **2004**, *29*, 95.
- 50 Chowdhury, B.; Bravo-Suárez, J. J.; Daté, M.; Tsubota, S.; Haruta, M. *Angew. Chem. Int. Ed.* **2006**, *45*, 412.
- 51 *Chemical Week* **2003**, 165 (29), 26.
- 52 Alex, S. *Chemical Week* **2000**, 162(40), 50.
- 53 Eul, W.; Moeller, A.; Steiner, N. *Kirk-Othmer Encyclopedia of Chemical Technology*; Wiley: New York, <http://www.mrw.interscience.wiley.com/kirk/articles/hydrhess.a01/sect11-fs.html>.
- 54 Bellussi G.; Perego C. *Cattech*, **2000**, *4*, 4.
- 55 (a) Fischer, R.; Harder, W.; Merger, F.; Priester, C. U.; Vagt, U. US Patent 4,963, 672, 1990. (b) Dockner, T.; Sauerwald, M.; Fischer, R.; Hutmacher, H. M.; Priester, C. U.; Vagt, U. US Patent 4,767, 856, 1987.
- 56 (a) Sanches, K. M. US Patent 5,151,543, 1992. (b) Gilbert, L.; Laurain, N.; Leconte, P.; Nedez, C. EP Patent 748797 A1, 1998. (c) Achhammer, G.; Fuchs, E. US Patent, 5, 874,575, 1999. (d) Eiermann, E.; Narbeshuber, T. WO Patent

9928296, 19999 (e) Brunelle, J -P.; Seigneurin, A.; Sever, L. WO Patent 0005203 A1 2000. (f) Eiermann, M.; Ansmann, A.; Flick, K. WO Patent 9947500 A1, 1999.

- 57 Technology Process Summary, *Eur. Chem. News* **1976**, 28, 734.
- 58 Davis, D. D. Ullmanns Encyclopaedia of Industrial Chemistry, Vol. A1, VCH, **1985**, 269.
- 59 Dugal, M.; Sankar, G.; Raja, R.; Thomas, J. M. *Angew. Chem. Int. Ed.* **2000**, 39, 2310.
- 60 Thomas, J. M.; Raja, R.; Sankar, G.; Johnson, B. F. G.; Lewis, D. W. *Chem. Eur. J.* **2001**, 7, 2973.
- 61 Niu, W.; Draths, K. M.; Frost, J. W. *Biotechnol. Prog.* **2002**, 18, 201.

CHAPTER 2

SYNTHESIS OF ϵ -CAPROLACTAM FROM L-LYSINE

2.1. Introduction

ϵ -Caprolactam, the monomer for the production of nylon 6 fibers and plastics, is projected to grow at 2.9% per year, and reach 4.5 million metric tons by 2010.¹ The current production of ϵ -caprolactam suffers from the use of problematic reagents and generation of large quantities of low-value side products.² Due to the pressures of both competitiveness and environmental concern, the syntheses of ϵ -caprolactam has undergone significant innovation either based on new starting materials or more efficient and safer catalysts.^{3,4,5} However, all current production and innovations are exclusively based on petroleum feedstock. Recently, the rise of oil prices has hurt the profitability of ϵ -caprolactam producers. Therefore, a synthesis of ϵ -caprolactam from a renewable source is highly desirable.

To this end, synthesis of ϵ -caprolactam from D-glucose-derived L-lysine has been investigated, which involves the cyclization of L-lysine and subsequent deamination of the resulting α -amino- ϵ -caprolactam. A new method of L-lysine cyclization in the absence of catalyst has been developed involving the optimization of reaction temperature and solvents. This method has also been applied to the synthesis of other medium-sized lactams. After successfully masking the ϵ -amine group as an amide by cyclization, different strategies have been explored to selectively remove the α -amino group of α -amino- ϵ -caprolactam. Deamination of α -amino- ϵ -caprolactam was explored

chemically using hydroxylamine-*O*-sulfonic acid (NH₂OSO₃H) and catalytically over Pt on carbon.

2.2. Background

The production of L-lysine ranks the second amino acids to L-glutamic acid at 7.5 ×10⁸ kg/year.⁶ The L-lysine market has increased by about 8% to 9% annually in the past few years, and is expected to grow by about 7% to 8% per year.⁷ The rapid growth in demand of L-lysine and other amino acids is mainly due to their utilization as feed additives. As a limiting amino acid, lysine is primarily used as a feed additive for swine and poultry to improve feed efficiency and promote growth. Increasing demand and competition have led to innovations in lysine production, which has resulted in higher productivity and a substantial cost reduction. For example, the manufacturing cost of lysine has decreased by more than twofold in the last two decades.⁷ L-Lysine was targeted as a starting material because of its structural similarity to ε-caprolactam, accessibility from plant-derived feedstocks (starch) and low production cost. L-Lysine has all the functional groups necessary for the formation of ε-caprolactam. Given the increasing price of benzene and other petroleum-derived starting materials and likely reductions of lysine's price, synthesis of ε-caprolactam from this renewable source can be both economically competitive and sustainable.

2.3. Design

There are three possible approaches to synthesize caprolactam from lysine (Figure 19). The first route entails cyclization followed by deamination of the intermediate of α-aminocaprolactam (Figure 19). Another possibility is a one-step reaction directly from L-

lysine to caprolactam. The third approach starts with deamination of lysine to 6-aminocaproic acid followed by cyclization (Figure 19). Our preliminary results showed that poor selectivity was observed for deamination of L-lysine while the yield of the one-step synthesis was too low to be practical. Ultimately, attention was then focused on route a: cyclization of L-lysine to α -amino- ϵ -caprolactam, successfully masking the ϵ -amino group, followed by selective removal of the α -amino group to result in the desired caprolactam product. Two major techniques are needed to make the above synthesis practical: efficient cyclization and selective deamination.

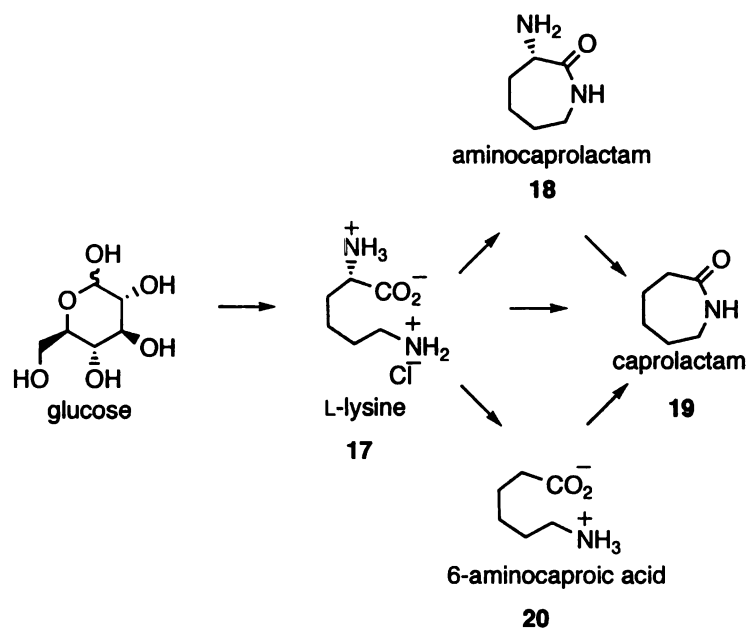


Figure 19. Synthetic strategies of caprolactam from L-lysine. a) cyclization followed by deamination; b) one-step synthesis; c) deamination and then cyclization.

2.4. Results

2.4.1. Cyclization

2.4.1.1 Cyclization of L-lysine

L-lysine is the ideal precursor for synthesis of caprolactam because that it has the same carbon chain with the necessary functional groups needed for the formation of the lactam. The challenge of this route is how to selectively remove the secondary α -amino group without affecting the ϵ -amino group of L-lysine. Our strategy is to simply mask the ϵ -amino group by forming an amide through cyclization of the L-lysine. Among different methods developed for the cyclization of amino acids,⁸ alumina-catalyzed cyclization seemed most suitable for our goal.^{9d} L-Lysine is cyclized to the corresponding lactam in refluxing toluene catalyzed by silica or alumina. The advantages of this process are the high reaction yield (90%) with low cost and high abundance of the reagents. However, considering the high volume of the industrial production of caprolactam, using a huge amount of Al_2O_3 and toxic solvents such as toluene can be problematic when scaling up this process.

To avoid the use of petroleum-derived toluene while retaining the ability to remove water as an azeotrope, cyclizations of L-lysine hydrochloride were examined in various alcohols (Table 1). These solvents also allowed the impact of reaction temperature on the cyclization to be determined. All reactions were initiated with neutralization of L-lysine hydrochloride (0.25 M) with NaOH. The resulting NaCl precipitate was filtered out of solution after the reaction. A Dean-Stark trap was used to remove the water generated during the reaction with the exception of diols or triols (

Table 3), where the first 10% of the solvent volume was removed when the reaction was brought to reflux. After acidification, α -amino- ϵ -caprolactam hydrochloride could be crystallized from water (Table 2, entry 3) although a significant reduction of yield was encountered.

The cyclization of L-lysine was first examined in the presence of Al_2O_3 in refluxing ethanol, 1-propanol, 1-butanol, and 1-pentanol. No cyclization was detected in ethanol (Table 1, entry 1) or 1-propanol (Table 1, entry 2). A 92% yield of α -amino- ϵ -caprolactam was observed in 1-butanol (Table 1, entry 3). In 1-pentanol, a 96% yield of α -amino- ϵ -caprolactam was realized along with a reduction in the reaction time (Table 1, entry 4). Further increase of reaction temperature by refluxing in 1-hexanol resulted in an almost quantitative yield (Table 1, entry 5).

Table 1. Cyclization of L-lysine hydrochloride (17) in the presence of Al_2O_3

entry	17/NaOH/ Al_2O_3 (mmol)	reaction conditions	18 (% yield ^a)
1	30/30/270	1-ethanol (120 mL) 78°C, reflux, 12 h	0
2	30/30/270	1-propanol (120 mL) 97°C, reflux, 12 h	0
3	30/30/270	1-butanol (120 mL) 117 °C, reflux, 6 h	92
4	30/30/270	1-pentanol (120 mL) 137 °C, reflux, 4 h	96 ^a
5	30/30/270	1-hexanol (120 mL) 156 °C, reflux, 4 h	96 ^a

a) Crude ^1H NMR product yields were determined relative to a calibration curve based on the ratios of integrated resonances at $\delta=4.29$ for varying concentrations of α -amino- ϵ -caprolactam 10 relative to the integrated resonance at $\delta=0.00$ for sodium 3-(trimethylsilyl)propionate-2,2,3,3- d_4 in D_2O .

The impact of omitting Al_2O_3 during cyclization of L-lysine was examined. Cyclization of L-lysine in yields ranging from 21-51% have been reported in near-critical

and supercritical water.^{8h,i} Catalyst-free cyclizations of 6-aminocaproic acid to form ϵ -caprolactam have also been reported in ethanol heated to 200 °C.⁹ Reaction of L-lysine in ethanol (200 °C) did afford a 65% yield of α -amino- ϵ -caprolactam (Table 2, entry 10). By comparison, an 80% yield of α -amino- ϵ -caprolactam was obtained when L-lysine was cyclized in refluxing 1-butanol (Table 2, entry 1), although a much longer reaction time was required relative to Al₂O₃-catalyzed cyclization (Table 1, entry 3). The same pattern was observed for cyclization of L-lysine in 1-pentanol where a 93% yield was achieved (Table 2, entry 2 vs Table 1, entry 4). Increasing the reaction temperature via use of

Table 2. Cyclization of L-lysine in mono alcohols

entry	17/NaOH/Al ₂ O ₃ (mmol)	reaction conditions	18 (% yield ^{a,b})
1	30/30/0	1-butanol (120 mL) 117°C, reflux, 240 h	80 ^a
2	30/30/0	1-pentanol (120 mL) 137°C, reflux, 64 h	93 ^a
3	30/30/0	1-hexanol (120 mL) 157 °C, reflux, 8 h	89 ^a
4	300/300/0	1-hexanol (1.2 L) 157 °C, reflux, 8 h	91 ^a /75 ^b
5	30/30/0	1-heptanol (120 mL) 176 °C, reflux, 8 h	59 ^a
6	30/30/0	1-octanol (120 mL) 195 °C, reflux, 1 h	63 ^a
7	30/30/0	diethylene glycol monoethyl ether (120 mL) 195 °C, reflux, 1 h	32 ^a
8	30/30/0	1-nonanol (120 mL) 215 °C, reflux, 0.5 h	26 ^a
9	30/30/0	1-decanol (120 mL) 231 °C, reflux, 0.25 h	22 ^a
10	30/30/0	ethanol (120 mL) 200 °C, 2 h	65 ^a

a) Crude ¹H NMR product yields were determined relative to a calibration curve based on the ratios of integrated resonances at d=4.29 for varying concentrations of α -amino- ϵ -caprolactam **10** relative to the integrated resonance at d=0.00 for sodium 3-(trimethylsilyl)propionate-2,2,3,3-d₄ in D₂O. b) Yield of product purified by crystallization.

refluxing 1-hexanol at both smaller scale (Table 2, entry 3) and larger scale (Table 2, entry 4) reduced the time for the uncatalyzed cyclization of L-lysine.

Further increase of the reaction temperature above 160 °C (Table 2, entries 5-9) did significantly shorten the reaction time but also resulted in significant reduction of the reaction yield due to the secondary reactions such as decomposition or polymerization. For example, when refluxing in 1-decanol (Table 2, entry 9), the reaction finished in 15 min to give only 22% of the desired product. The products of the secondary reaction have not been examined in detail. Comparison between cyclization in 1-octanol (Table 2, entry 6) and diethylene glycol monoethyl ether (Table 2, entry 7) deserves some consideration. Refluxing L-lysine at the same temperature for the same amount of time, 1-octanol almost doubled the reaction yield in that of diethylene glycol monoethyl ether. It may indicate that polarity or the hydroxyl group of the solvent may play an important role in the cyclization of L-lysine, possibly due to hydrogen bonding or even activation of the acid group by formation of the ester. This observation aroused our interest to explore the cyclization in diols and triols (Table 3). Interestingly, the highest yield (96%) and shortest time (2 h) for the conversion of L-lysine to α -amino- ϵ -caprolactam were observed in refluxing 1,2-propanediol (Table 3, entry 1). 1,2-propanediol is obtained from the hydrogenation of lactic acid, which is obtained from fermentation on large scale for food and polymer applications. As observed before, the reaction yield in the cyclization of L-lysine decreased when the reaction temperature is above a certain temperature. In fact, all L-lysine was consumed after refluxing in glycerol (290 °C) for less than 10 min and no desired product was observed (Table 3, entry 4).

Table 3. Cyclization of L-lysine hydrochloride in triols and diols.

entry	17/NaOH/Al ₂ O ₃ (mmol)	reaction conditions	18 (% yield ^a)
1	300/300/0	1,2-propanediol (1.2 L) 187 °C, reflux, 2 h	96 ^a
2	30/30/0	ethylene glycol (120 mL) 197 °C, reflux, 1 h	94 ^a
3	30/30/0	1,3-propanediol (120 mL) 214 °C, reflux, 1 h	77 ^a
4	30/30/0	glycerol (120 mL) 290 °C, reflux, 0.1 h	0 ^a

a) Crude ¹H NMR product yields were determined relative to a calibration curve based on the ratios of integrated resonances at d=4.29 for varying concentrations of α-amino-ε-caprolactam **10** relative to the integrated resonance at d=0.00 for sodium 3-(trimethylsilyl)propionate-2,2,3,3-d₄ in D₂O.

2.4.1.2. Ring closure to form medium-sized lactams

Medium-sized ring lactams (7- to 10-membered) find widespread use in organic chemistry as key intermediates in the synthesis of natural products or pharmaceutically important compounds. However, still lacking is an efficient ring closure method to form medium sized lactams.¹⁰ With success in cyclization of L-lysine in refluxing 1,2-propanediol, attention was turned to the synthesis of other medium sized lactams, especially 7- and 8-membered lactams that are difficult to make. For comparison, cyclizations have also been run in ethanol in a pressure reactor that was heated to 200 °C.^{9a} These results are summarized in Table 4. Cyclization of 6-amino hexanoic acid in ethanol (200 °C) and 1,2-propanediol (187 °C) proceeded in 98% (Table 4, entry 1) and 96% (Table 4, entry 2) yield, respectively.

Table 4. Synthesis of 7- and 8-membered lactams

entry	substrate	substrate/NaOH (mmol)	reaction conditions	lactams (% yield ^a)
1	6-amino hexanoic acid	30/0	ethanol ^b (120 mL) 200 °C, 2 h	98 ^a
2	6-amino hexanoic acid	30/0	1,2-propanediol (120mL) 187 °C, reflux, 2 h	96 ^a
3	L-lysine-HCl	30/30	ethanol ^b (120 mL) 200 °C, 2 h	65 ^a
4	L-lysine-HCl	30/30	1,2-propanediol (120 mL) 187 °C, reflux, 2 h	95 ^a
5	7-amino heptanoic acid	10/0	ethanol ^b (120 mL) 200 °C, 2 h	10 ^a
6	7-amino heptanoic acid	10/0	1,2-propanediol (120mL) 187 °C, reflux, 2 h	12 ^a
7	homolysine-HCl	30/30	ethanol ^b (120 mL) 200 °C, 2 h	7 ^a
8	homolysine-HCl	30/30	1,2-propanediol (120 mL) 187 °C, reflux, 2 h	9 ^a

a) Product yields were determined ¹H NMR. b) Reactions were run in the high-pressure reactors.

Similarly, ring closure of L-lysine in both refluxing 1,2-propanediol and ethanol (200 °C) (Table 4, entries 3 and 4) provided the desired α -amino ϵ -caprolactam in good to excellent yields. However, a significantly lower yield was observed for cyclization in ethanol (Table 4, entry 3). This may be traced back to the possibility of polymerization. The extra secondary amine group of α -amino- ϵ -caprolactam (compared with caprolactam) can attack the amide group of another α -amino- ϵ -caprolactam and open the lactam ring and thus forming a dimer or oligomers. Cyclization of 7-amino heptanoic acid and homolysine has also been explored both in ethanol (200 °C) and 1,2-propanediol to make 8-membered lactams.

Since homolysine is not commercial available, it was synthesized according to a modified acetamidomalonic ester approach (Figure 20),¹¹ in which ethyl acetamidomalonate is reacted with 5-bromopentylphthalimide **23** in the presence of

sodium hydride, followed by hydrolysis (Figure 20). The intermediate 5-hydroxypentylphthalimide **22** was not isolated, but treated with phosphorous tribromide directly to give 5-bromo pentylphthalimide **23**. The monohydrochloride homolysine **25** was isolated in 32% overall yield without optimization.

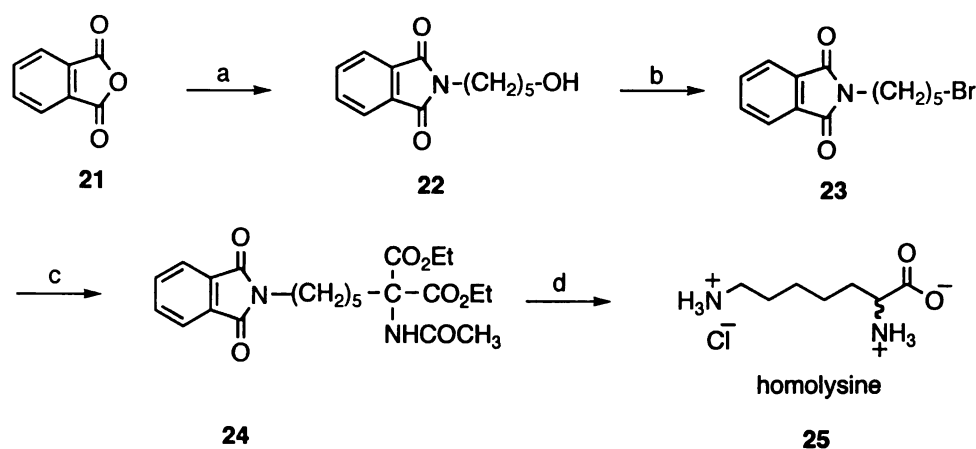


Figure 20. Synthesis of homolysine. Key: a) $\text{NH}_2(\text{CH}_2)_5\text{OH}$, toluene, reflux. b) PBr_3 , $100\text{ }^\circ\text{C}$, overall 70%. c) $\text{CH}_3\text{CONHCH}(\text{CO}_2\text{Et})_2$, NaH in DMF, 54%. d) 6N HCl, reflux, 84%.

With homolysine in hand, preparation of 8-membered lactams has been examined with our standard cyclization methods (Table 4, entries 5-8). Unfortunately, low reaction yields were obtained (8-12%). In conclusion, a convenient and catalyst-free method has been developed for the synthesis of 7-membered lactams.

2.4.2. Deamination

2.4.2.1. Reductive deamination with hydroxylamine-O-sulfuric acid

With a convenient preparation of α -amino- ϵ -caprolactam, attention was then turned to the selective deamination of the α -amino group of α -amino- ϵ -caprolactam. Practical methods for the cleavage of carbon-nitrogen bonds are limited. The chemistry

of these reactions is dominated by two fundamental properties of the nitrogen atom (Figure 21):¹² (1) the ability to form a positively charged tetravalent group that can activate the adjacent carbon-hydrogen bonds for abstraction and serve as a good leaving group and (2) the capacity of combining another nitrogen atom to form the very stable N₂ molecule (Figure 21).

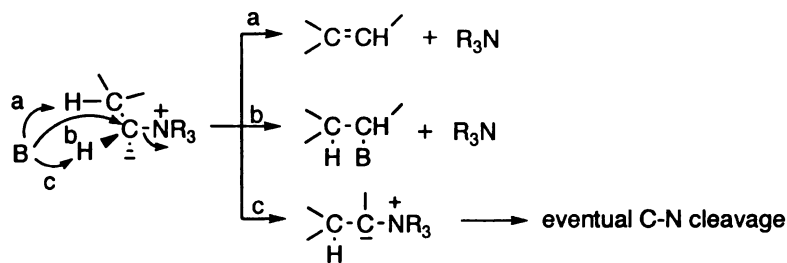


Figure 21. Cleavage of C-N bonds.

Taking advantage of the enthalpic advantage of forming N₂, Doldouras' group developed a reductive deamination method using hydroxylamino-*O*-sulfonic acid (NH₂OSO₃H) in the presence of aqueous base.¹³ This method was further improved by Ramamurthy's group using aqueous methanol as solvent and up to 20 equivalents of hydroxylamine-*O*-sulfonic acid.¹⁴ According to the mechanism proposed by the Doldouras' group (Figure 22),¹³ reaction of the primary amine with hydroxylamino-*O*-sulfonic acid in basic condition led to formation of hydrazine (Figure 22), followed by dehydration with a nitrene (Figure 22), then the resulting diazene (Figure 22) lost nitrogen gas to afford the desired saturated hydrocarbon. The N-amination step (the formation of the hydrazine) was thought likely to be the rate-determining step because the other steps were expected to be relatively rapid and did not involve any significant side reactions. Also, decomposition of hydroxylamine-*O*-sulfonic acid in aqueous

solution above room temperature would be a reason why a large excess of hydroxylamine-*O*-sulfonic acid was required for the reaction.¹⁵ So, the key to obtaining high reaction yield is to minimize the decomposition of hydroxylamine-*O*-sulfonic acid and assure the formation of hydrazine. It seems reasonable to run the reaction at lower temperature.

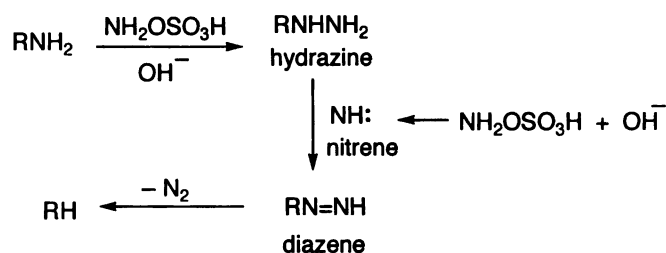
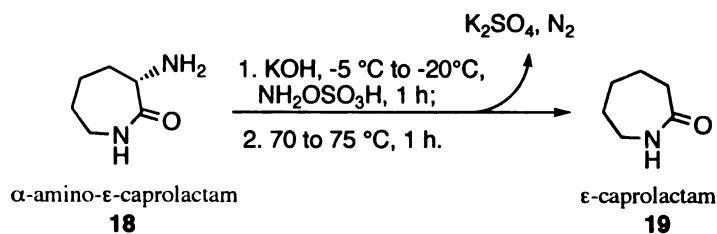


Figure 22. Proposed mechanism of reductive deamination using $\text{NH}_2\text{OSO}_3\text{H}$.

Hydroxylamine-*O*-sulfonic acid was employed to cleave off the α -amino group of α -amino- ϵ -caprolactam. Variations of reaction temperature, concentration of α -amino- ϵ -caprolactam, $\text{NH}_2\text{OSO}_3\text{H}/\alpha$ -amino- ϵ -caprolactam ratio and solvents were explored. In a typical example: α -amino- ϵ -caprolactam (2.56 g, 20 mmol) was dissolved in 100 mL water in a flask connected to a gas buret, and the solution cooled to $-5\text{ }^\circ\text{C}$. After addition of KOH (4.48 g, 80 mmol) and the first half of $\text{NH}_2\text{OSO}_3\text{H}$ (4.52 g, 40 mmol), the reaction solution was stirred at $-5\text{ }^\circ\text{C}$ for 1 h. The reaction solution was then heated to $70\text{-}75\text{ }^\circ\text{C}$ and stirred at this temperature for 1 h. The solution was again cooled to $-5\text{ }^\circ\text{C}$ followed by addition of more KOH (4.48 g, 80 mmol) and $\text{NH}_2\text{OSO}_3\text{H}$ (4.52 g, 40 mmol). After stirring at $-5\text{ }^\circ\text{C}$ for 1 h, the reaction solution was heated to $70\text{-}75\text{ }^\circ\text{C}$ and stirred at the temperature for 1 h. The completion of reaction was checked by ^1H NMR. After concentration to dryness, the crude product was purified by sublimation.

Table 5. Deamination of α -amino- ϵ -caprolactam with $\text{NH}_2\text{OSO}_3\text{H}$ 

entry	18 /KOH/ $\text{NH}_2\text{OSO}_3\text{H}$ (mmol)	H_2O / MeOH / EtOH (mL)	yield ^{a, b} (%)
1	20/800/400	240/160/0	61
2	20/800/400	120/80/0	62
3	20/800/400	60/40/0	64
4	20/160/80	60/40/0	65
5	20/160/80	60/0/40	70
6	20/160/80	100/0/0	75 ^c

a) product yields are after purification by sublimation; b) yields are based on L-lysine starting material. Intermediate α -amino- ϵ -caprolactam was not purified prior to deamination; c) entry 6 was run at $-5\text{ }^\circ\text{C}$ and all other entries were run at $-20\text{ }^\circ\text{C}$.

Due to the yield reduction encountered during the recrystallization of α -amino- ϵ -caprolactam, α -amino- ϵ -caprolactam from cyclization of L-lysine in 1,2-propanediol was separated from NaCl byproduct, concentrated and used directly in the deamination without further purification. Deamination yields in Table 5 thus were based on the starting L-lysine hydrochloride. Extension of the reaction conditions similar to those in previous literature^{13,14} reported for amino acid deamination with $\text{NH}_2\text{OSO}_3\text{H}$ gave low yields (data not shown), even when reactions were run in highly diluted systems (0.003 M) and up to 20 equivalents of $\text{NH}_2\text{OSO}_3\text{H}$ was employed. An increase of temperature and generation of a large amount of gas were observed during addition of $\text{NH}_2\text{OSO}_3\text{H}$, which indicated the decomposition of $\text{NH}_2\text{OSO}_3\text{H}$. To minimize the decomposition of $\text{NH}_2\text{OSO}_3\text{H}$, the reaction temperature was lowered from room temperature to $-20\text{ }^\circ\text{C}$ (Table 5, entries 1-5) and $-5\text{ }^\circ\text{C}$ (Table 5, entry 6), which resulted in a substantial yield

improvement. A four-fold increase in concentration (Table 5, entry 1 vs entry 3) did not adversely affect the reaction yield. A five-fold reduction in equivalents of KOH and $\text{NH}_2\text{OSO}_3\text{H}$ used in the reaction did not lower the reaction yield (Table 5, entry 3 vs entry 4). Aqueous methanol can be replaced by aqueous ethanol (Table 5, entry 5) and water was discovered to be suitable solvent (Table 5, entry 6). The highest deamination yield (75%) was achieved at a 0.2 M concentration of α -amino- ϵ -caprolactam with water as the reaction solvent (Table 5, entry 6). The $\text{NH}_2\text{OSO}_3\text{H}$ used for the deamination of α -amino- ϵ -caprolactam is best prepared by the reaction of hydroxylamine sulfate ($(\text{NH}_2\text{OH})_2\text{H}_2\text{SO}_4$) with fuming sulfuric acid ($\text{H}_2\text{SO}_4\cdot\text{SO}_3$). Conversion of L-lysine hydrochloride to ϵ -caprolactam thus ironically employed the same inorganic reagents that were used in the traditional manufacture of ϵ -caprolactam from cyclohexanone. Overall, synthesis of ϵ -caprolactam from glucose-derived L-lysine constitutes a fundamental departure from all reported syntheses of ϵ -caprolactam, which use petroleum-derived benzene or 1,3-butadiene as feedstock. However, using up to 4 equivalents of $\text{NH}_2\text{OSO}_3\text{H}$ and consequently generation of a large amount of salts make this process problematic. Thus, a catalytic deamination process is needed to make the biobased caprolactam synthesis economically competitive and environmentally friendly. To achieve this goal, catalytic hydrogenolysis has been explored.

2.4.2.2 Catalytic hydrogenolysis in water

The hydrogenolysis reaction is defined as the reductive cleavage of sigma bonds (such as C-O, C-N or C-halogen bonds) during catalytic hydrogenation. Good catalytic activity of the transition metals is only observed if A or B itself show sufficient bond

formation with the metal or when the A-B bond is situated in the neighborhood of an unsaturated function such as an aryl, vinyl or carbonyl group. The unsaturated function serves as a 'handle' that brings the A-B bond closer to the catalytic surface, thus promoting overlap between the σ and σ^* orbitals of A-B and the d and spd orbitals of the transition metal.

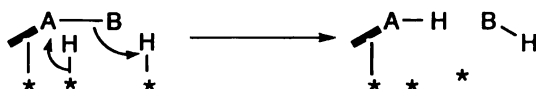


Figure 23. Catalytic hydrogenolysis.

Catalysts used for hydrogenolysis are dominated by palladium and Raney nickel. Sometimes platinum and rhodium have been applied while ruthenium shows some hydrogenolytic activity. Hydrogenolysis of the carbon-nitrogen bond closely resembles that of a carbon-oxygen bond, but takes place less readily. As expected, hydrogenolytic ring opening of aziridines occurs easily under very mild conditions (Figure 24),¹⁶ whereas benzyl amine derivatives are hydrogenolyzed at a reasonable rate (Figure 25).¹⁷ The debenylation of tertiary amines takes place over Pd/C at 25-50 °C in the presence of 2-4 atmosphere of H₂. The addition of some acid facilitates the hydrogenolysis as does the quaternization of the amine (Figure 25).

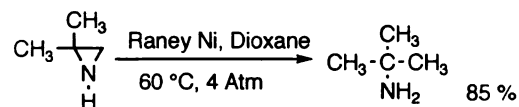


Figure 24. Ring opening of aziridines.

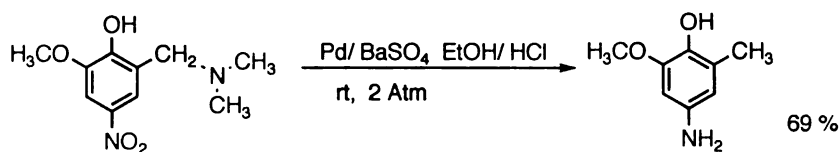
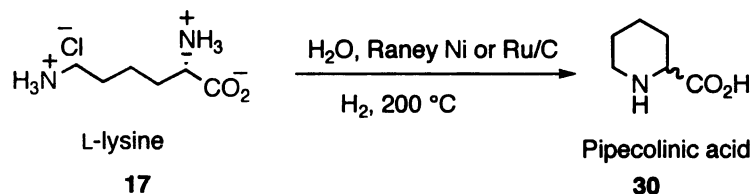


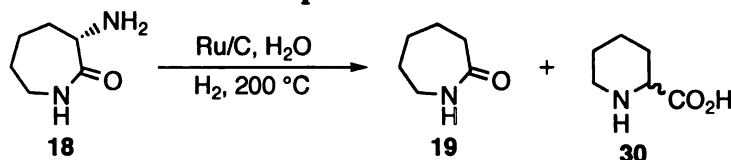
Figure 25. C-N bond cleavage of benzyl amine.

To avoid the generation of salts, the catalytic deamination of L-lysine or α -amino- ϵ -caprolactam has been explored with different kinds of metal catalysts. Preliminary deamination experiments of L-lysine were conducted using Raney nickel as the catalyst. Reaction at 100 °C recovered only unreacted starting material while oligomerization was observed when the temperature was increased to 250 °C. Reaction temperature was thus set at 200 °C. Since Raney nickel is pyrophoric, all reactions were run in water. Metal catalysts other than Raney nickel were also examined (Table 6) with similar conditions. As shown in Table 6, the formation of pipercolinic acid was observed. NiCl₂ (Table 6, entry 6) showed no deamination activity. Pd/C gave moderate yield (Table 6, entry 5). The highest yield (65%) was achieved using either Raney nickel or Ru/C. Reaction yields were significantly affected by H₂ pressure for both Raney nickel and Ru/C. In the case of Raney nickel, reaction yield increased with an increase of H₂ pressure (Table 6, entry 1 vs entry 2). On the other hand, the opposite trend was observed for Ru/C (Table 6, entry 3 vs entry 4). This procedure was extended to deaminate α -amino- ϵ -caprolactam using Ru/C as the catalyst, pipercolinic acid was again the major product but 3% desired product ϵ -caprolactam was afforded (Table 7, entry 1). The above results were not surprising since presumably α -amino- ϵ -caprolactam will be hydrolyzed back to L-lysine in the presence of water.

Table 6. Deamination of L-lysine to pipercolinic acid in water^{a,c}

entry	catalyst	temperature (°C)	H ₂ (psi)	reaction time (h)	(%yield) ^{a,b,c}
1	Raney Ni	200	100	8	33
2	Raney Ni	200	1000	8	65
3	Ru/C	200	100	8	65
4	Ru/C	200	1000	8	18
5	Pd/C	200	100	8	43
6	NiCl ₂	200	100	8	0

a) All reactions were run in water and L-lysine was at a concentration of 0.1 M; b) yields were determined by ¹H NMR; c) entries 1, 2 and 6, 100 mol% catalyst was used, in other entries only 5 mol% catalyst was used.

Table 7. Deamination of α-amino-ε-caprolactam in water^a

entry	catalyst	temp (°C)	H ₂ (psi)	time (h)	19/30 (%yield) ^b
1	Ru/C	200	100	8	3/63
2	Ru/C	200	1000	8	0/37

a) All reactions were run in water and α-amino-ε-caprolactam was at a concentration of 0.1 M; b) yields were determined by ¹H NMR; c) 5 mol% catalyst was used.

From the mechanism proposed by Ohtani and coworkers¹⁸ (Figure 26), it seems that formation of pipercolinic acid may consist of three steps: oxidation of the amine group to yield an imine, hydrolysis of the imine into an α-ketone acid or an aldehyde along with the release of ammonia (NH₃), followed by intramolecular condensation of the residual amino group with the carbonyl into two cyclic Schiff base intermediates, and reduction of the resulting Schiff base to afford pipercolinic acid. Considering the possibility of hydrolysis of imines (Figure 26) and α-amino-ε-caprolactam in the

presence of water, it is reasonable to run the deamination reactions in organic solvents or without any solvent at all (neat reaction).

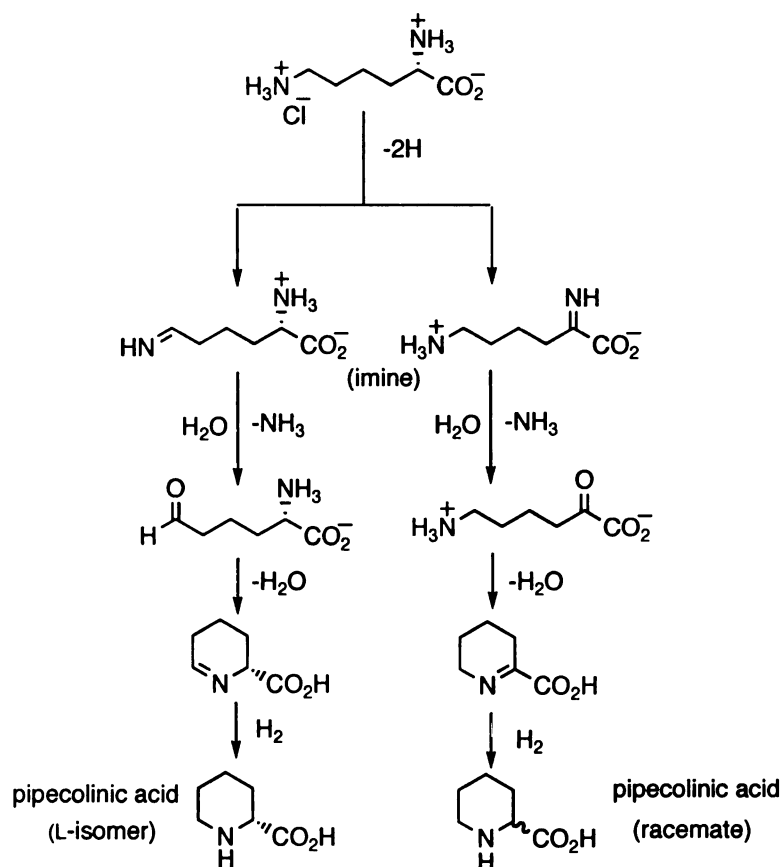


Figure 26. Mechanism for formation of pipecolic acid from L-lysine.

2.4.2.3 Reductive deamination of α -amino- ϵ -caprolactam with Pt catalyst

For the deamination of α -amino- ϵ -caprolactam, it is surprising that literature precedents to readily cleave C-N bonds other than aziridines, allylic amines and benzyl amines were limited. Maier's group reported that different amines can be reductively deaminated using 40% Pt/SiO₂ as a catalyst while amides are inert in these reaction conditions (Figure 27).¹⁹ This report deserves discussion here since this is the only reported high-yielding approach for deamination of unactivated amine. The Pt catalyst was prepared by impregnation of the SiO₂ support with catalyst precursor chloroplatinic

acid followed by calcinations and reduction to give the reduced catalyst containing 40% Pt and 60% SiO₂. Reductive deamination was conducted in a flow apparatus consisting of three U-tubes. Substrates were placed in the first U-tube, which was connected to the second U-tube containing Pt/SiO₂ catalyst. The last U-tube served as a product collector and was cooled to -78 °C with a dry ice-acetone mixture. Substrate and catalyst was preheated to the desired temperature (150-250 °C) and H₂ purged through the three U-tubes to carry the vaporized substrate to pass through the catalyst and the resulting deaminated product was collected in the third U-tube. This procedure requires no solvent or work-up. However, this approach can only apply to volatile substrates. For cyclohexamine, almost quantitative yield was achieved at 150 °C (This reaction was investigated by Mapitso Molefe in the Frost group). Catalytic activity of the prepared Pt/SiO₂ catalyst was verified by deamination of model substrate cyclohexamine. However, extension of the procedure to α -amino- ϵ -caprolactam at different temperatures from 150 °C to 250 °C failed to give any desired product ϵ -caprolactam. There may be two possible reasons for the failure. The 40% (wt%) Pt needed for the reaction to occur may indicate that a lot of active sites are needed. At the reaction temperature (150 °C to 250 °C), substrate α -amino- ϵ -caprolactam melted and perhaps blocked all the active sites and made it impossible for H₂ to adsorb on the surface of catalyst. To solve the competition between substrate and H₂ for the active sites, higher temperature, higher H₂ pressure, more efficient stirring and perhaps more active catalysts are needed.

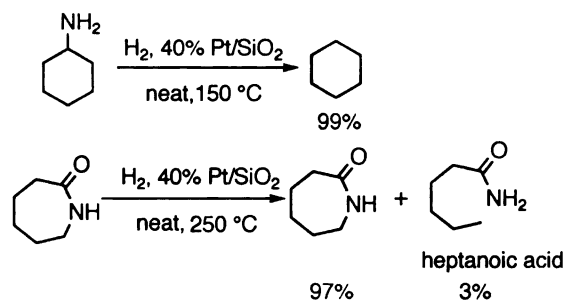


Figure 27. Reductive deamination with Pt/SiO₂.¹⁹

Attention was ultimately focused on high-pressure reactions using supported Pt catalyst, and in particular, carbon supported Pt because of the large surface area and cheap price of activated carbon. Batch reductive deamination of α -amino- ϵ -caprolactam was then examined with Pt/C catalyst inside a 500 mL Parr 4575 high-pressure reactor controlled by a Parr 4842 controller. Reaction conditions were optimized by varying reaction temperatures (250-350 °C), hydrogen pressures (0-400 psi), reaction time (1-8 h), catalyst concentrations (0.5-50 mol%), substrate concentrations (0.02-0.5 M), catalyst supports and solvents.

2.4.2.3.1. Effect of reaction temperature

First, the effect of reaction temperature on yield of deamination of α -amino- ϵ -caprolactam was examined with Pt/C catalyst and the results are summarized in Table 8. α -Amino- ϵ -caprolactam (0.1 M) and Pt/C (1 mol%) were stirred in THF (100 mL) in the presence of H₂ (100 psi) in a glass sleeve in a Parr high-pressure reactor for 8 h at different temperatures from 250 °C to 350 °C. Caprolactam yields were determined by ¹H NMR. At low temperature, both the conversion rate of α -amino- ϵ -caprolactam and caprolactam yield were low. Yield increased significantly with the increase of the

temperature (Table 8). Caprolactam yield peaked at 300 °C and further increase of the temperature resulted in reduction of yield (Table 8). Hence 300 °C was chosen as the optimal temperature for the following reactions.

Table 8. Temperature effect of reductive deamination with Pt/C

entry	catalyst (1 mol%)	temp (°C)	H ₂ (psi)	time (h)	caprolactam (% yield) ^{a,b}
1	Pt/C	250	100	8	4
2	Pt/C	280	100	8	9
3	Pt/C	290	100	8	12
4	Pt/C	300	100	8	14
5	Pt/C	310	100	8	11
6	Pt/C	320	100	8	10
7	Pt/C	350	100	8	8

a) all feeds were 0.1 M in THF; b) yields were the average of two runs and determined by ¹H NMR.

2.4.2.3.2. Effect of hydrogen pressure

Deamination of α -amino- ϵ -caprolactam at different H₂ pressures but otherwise identical reaction conditions are reported in Table 9. In the range of H₂ pressures examined, the caprolactam yield first increased with increasing H₂ pressures, reached the highest yield at 50 psi and then started to decrease with further increase of H₂ pressures. A 15% yield was achieved even in the absence of H₂. It seems that there is another hydrogen donor besides H₂, which can be solvent (THF). The other phenomenon that was hard to understand in the beginning was that high H₂ pressures did not increase reaction yield as expected. A possible explanation can be traced back to the competition between hydrogen and substrate on the surface of catalyst where deamination occurs. According to the precedent literature²⁰, several physical and chemical steps must take place for the reaction to occur. (1) hydrogen mass transfer from the gas to the liquid phase; (2) hydrogen and α -amino- ϵ -caprolactam mass transfer from the liquid phase to

the solid catalyst surface; (3) diffusion of hydrogen and α -amino- ϵ -caprolactam within the porous catalyst and (4) deamination of α -amino- ϵ -caprolactam to caprolactam via surface chemical reaction steps. When H₂ pressure is too high, hydrogen may occupy most of the active sites on the catalyst surface and make it difficult for α -amino- ϵ -caprolactam to transfer to the surface of catalyst and diffuse into it, thus decreasing the rate of conversion and consequently reducing the caprolactam yield.

Table 9. H₂ pressure effect for reductive deamination with Pt/C

entry	catalyst (1 mol%)	temp (°C)	H ₂ (psi)	time (h)	caprolactam (% yield) ^{a,b}
1	Pt/C	300	0	8	15
2	Pt/C	300	20	8	21
3	Pt/C	300	50	8	22
4	Pt/C	300	100	8	14
5	Pt/C	300	400	8	5

a) all feeds were 0.1 M in THF; b) yields were the average of two runs and determined by ¹H NMR.

2.4.2.3.3. Catalyst concentration

Adjustment of the catalyst concentration can have a great effect on the reaction rate and product distribution, depending on whether the reaction mechanism requires activation by one or more molecules of catalyst per reaction. Deamination of α -amino- ϵ -caprolactam using different concentration of Pt catalysts is summarized in the Table 10. Initially, the caprolactam yield increases in direct proportion to the catalyst concentration (Table 10, entries 1 and 2). Then the caprolactam yield starts to level off and decrease. The results may indicate two possibilities: on one hand, there is a diffusion problem. Catalyst catalyzes the reaction so fast that reactants are soon depleted in the liquid phase and diffusion of reactants controls the rate. On the other hand, exposure of product

caprolactam to excess catalyst may result in further undesired C-C bond cleavage and decrease the yield of caprolactam.

Table 10. Catalyst concentration.

entry	catalyst	con. (mol%)	temp (°C)	H ₂ (psi)	time (h)	caprolactam (% yield) ^{a,b}
1	Pt/C	0.5	300	50	8	11
2	Pt/C	1	300	50	8	22
3	Pt/C	5	300	50	8	19
4	Pt/C	25	300	50	8	10
5	Pt/C	50	300	50	8	0

a) all feeds were 0.1 M in THF; b) yields were the average of two runs and determined by ¹H NMR.

2.4.2.3.4. Reaction time

Using a combination of the best catalyst concentration (1 mol%), H₂ pressure (50 psi) and temperature (300 °C) as standard, deamination of α -amino- ϵ -caprolactam was examined in a variable of reaction time from 1 h to 8 h (Table 11). The reaction yield increased with extending the reaction time and leveled off after 4 h.

Table 11. Reaction time.

entry	catalyst (1 mol%)	temperature (°C)	H ₂ (psi)	time (h)	caprolactam (% yield) ^{a,b}
1	Pt/C	300	50	1	6
2	Pt/C	300	50	2	16
3	Pt/C	300	50	3	17
4	Pt/C	300	50	4	22
5	Pt/C	300	50	5	22
6	Pt/C	300	50	6	22
7	Pt/C	300	50	7	22
8	Pt/C	300	50	8	22

a) all feeds were 0.1 M in THF; b) yields were the average of two runs and determined by ¹H NMR.

2.4.2.3.5. Effect of substrate concentration

In optimization of the starting material concentration of the reaction, avoiding the possible polymerization of α -amino- ϵ -caprolactam or caprolactam is key. Deaminations of α -amino- ϵ -caprolactam at different substrate concentrations but otherwise identical reactions are reported in Table 12. An increase in the substrate concentration did not affect the reaction significantly. Decreasing the concentration 5 times from 0.1 M to 0.02 M only increases the reaction yield by 2 %. Since low substrate concentration will significantly lower the reaction productivity, the substrate concentration was then fixed at 0.1 M in the following reactions.

Table 12. Optimizing substrate concentration.

entry	sub.con. (mol/L)	catalyst (1 mol%)	temperature (°C)	H ₂ (psi)	reaction time (h)	caprolactam (% yield) ^a
1	0.02	Pt/C	300	50	8	23
2	0.1	Pt/C	300	50	8	21
3	0.5	Pt/C	300	50	8	16

a) yields were the average of two runs and determined by ¹H NMR.

2.4.2.3.6. Optimizing use of solvents

Solvent selection can play an important role in the reaction rates and product yield. Improvement can be realized by selecting the most appropriate solvent. Solvents are usually chosen based on compatibility with the reagents and substrate, solubility and polarity. Examination of solvents was conducted for the deamination of α -amino- ϵ -caprolactam (Table 11). Cyclohexane and THF gave almost the same caprolactam yield (entries 1 and 2)) while polar solvents such as BuOH (protic solvent) and DMF (polar

noprotic solvent) failed to offer any desired product. The adverse effect of polar solvents might indicate that the deamination of α -amino- ϵ -caprolactam using Pt/C may involve a non-polar intermediate. THF displayed the most suitable balance of solubility and reactivity.

Table 13. Solvent effect

entry	catalyst (1 mol%)	temperature (°C)	Solvent	H ₂ (psi)	time (h)	caprolactam (% yield) ^{a,b}
1	Pt/C	300	cyclohexane	50	4	19
2	Pt/C	300	THF	50	4	21
3	Pt/C	300	BuOH	50	4	0
4	Pt/C	300	DMF	50	4	0

a) all feeds were 0.1 M in THF; b) yields were the average of two runs and determined by ¹H NMR.

2.4.2.3.7. Catalyst supports

It is well known that there is synergetic effect between the noble metal catalyst and the support. The magnitude of the synergy could be significantly influenced by a proper combination of the active phase and support used. In this work, Al₂O₃ and SiO₂ were chosen as acidic supports, Zeolite Y as a basic support and activated carbon as a neutral one. Pt on different supports were prepared by impregnation of support with chloroplatinic acid followed by activation at 350 °C and reduction in H₂. The results are shown in Table 14. Activated carbon gave the highest yield (Table 14, entry 1), followed by SiO₂ and Al₂O₃, zeolite Y (Table 14, entry 4) showed no HDN activity.

Table 14. Support effect.

entry	catalyst (1 mol%)	temperature (°C)	H ₂ (psi)	time (h)	caprolactam (% yield) ^{a,b}
1	Pt/C	300	50	4	21
2	Pt/SiO ₂	300	50	4	9
3	Pt/Al ₂ O ₃	300	50	4	4
4	Pt/Zeolite Y	300	50	4	0

a) all feeds were 0.1 M in THF; b) yields were the average of two runs and determined by ¹H NMR.

2.4.3. Synthesis and purification of β -lysine.

With the difficulty in improving the deamination yield of α -amino- ϵ -caprolactam, attention was then changed to the synthesis of β -lysine, whose β -amino group is presumably thought to be more susceptible to elimination. Since β -lysine is not commercial available. It was synthesized according to a modified Arndt-Eistert reaction (Figure 28),²¹ which starts from Cbz-protected ornithine **26** (Figure 28), via the intermediacy of the corresponding diazoketone **27** (Figure 28), followed by Wolff rearrangement and deprotection of the carbamate **28** (Figure 28) in the presence of Pd/C to afford crude β -lysine **29** (Figure 28) in 35% overall yield.

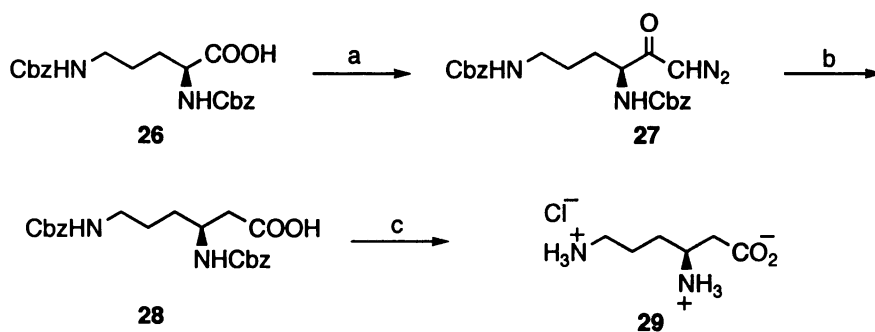


Figure 28. Synthesis of β -lysine. Key: (a) i) *i*-BuOCOCl, NMM, THF, -20 °C; ii) CH₂N₂, Et₂O, -5 °C- rt; iii) flash column, 78%. (b) cat. silver benzoate, NMM, THF/H₂O, in dark, 0 °C-rt; recrystallization (EtOAc/hexane), 45%. (c) Pd/C, EtOH, H₂ (100 psi), 50 °C; or Pd/C, formic acid, rt, quantitative.

Purification of β -lysine **29** was found to be challenging. Different purification techniques including Dowex-50 (H⁺), recrystallization and extraction were examined to obtain pure β -lysine **29** to examine the subsequent cyclization and deamination. None of above techniques was able to afford pure β -lysine. To minimize the formation of byproducts, the deprotection of Cbz group was optimized by using formic acid as hydrogen donor with Pt/C. This deprotection method successfully gave much cleaner

crude β -lysine and significantly simplified the following purification. Pure β -lysine was obtained after extraction of the acidified aqueous solution of crude β -lysine (pH=3) with chloroform, which was confirmed by both ^1H NMR and ^{13}C NMR.

Cyclization of β -lysine in EtOH at 200 °C successfully gave β -amino- ϵ -caprolactam. However, preliminary deamination studies of β -amino- ϵ -caprolactam either using Pt/C, Ru/Al₂O₃ or Pt-S/C as the catalyst (previous work by Brad Cox in Frost group) afforded very low yield of desired caprolactam together with complicated unidentified byproducts. These results were surprising to us, because the α -hydrogen of β -amino- ϵ -caprolactam is more acidic than the β -hydrogen of α -amino- ϵ -caprolactam and Hofmann elimination of a β -amino group is thermodynamically more favorable. This result may indicate that Hofmann elimination is not the major mechanism for deamination of α -amino- ϵ -caprolactam in our reaction conditions.

2.5. Discussion

All current syntheses of ϵ -caprolactam are based on petroleum, which is characterized by increasing prices and depleting supplies. The benzene prices have been rising continuously since 2003.²² High benzene prices hurt the producers of nylon-6 and other polyamides because most current commercial manufacture of ϵ -caprolactam are based on petroleum-derived benzene or 1,3-butadiene. It is reasonable to develop an alternative route to synthesize ϵ -caprolactam from renewable sources as in this case D-glucose-derived L-lysine, which is abundant and inexpensive.

ϵ -Caprolactam has been successfully synthesized from D-glucose-derived L-lysine hydrochloride in 75% overall yield. L-lysine hydrochloride is cyclized after neutralization in refluxing 1-hexanol or 1,2-propanediol to afford α -amino- ϵ -

caprolactam. Subsequent chemical deamination using with hydroxylamine-*O*-sulfonic acid and potassium hydroxide results in deamination and the formation of ϵ -caprolactam. Synthesis of ϵ -caprolactam from L-lysine constitutes a fundamental departure from previous syntheses of this monomer of nylon 6. However, using a stoichiometric amount of hydroxylamine-*O*-sulfonic acid and subsequently generation of large amounts of potassium sulfate are problematic considering the volume of ϵ -caprolactam global production. Catalytic deamination of α -amino- ϵ -caprolactam with metal catalysts certainly provides a promising solution to these problems. Cleavage of C-N bonds is a rarely addressed problem and related literature precedents are limited. Deamination of L-lysine in water using Raney Ni or ruthenium on carbon led to the formation of pipercolinic acid in 65% yield (Figure 29). It is interesting to find a convenient way to make pipercolinic acid but unfortunately it is not our target molecule. To avoid possible hydrolysis of imines (Figure 26) and polymerization of L-lysine or α -amino- ϵ -caprolactam in the presence of water, the catalytic deamination was then explored in non-aqueous solvents.

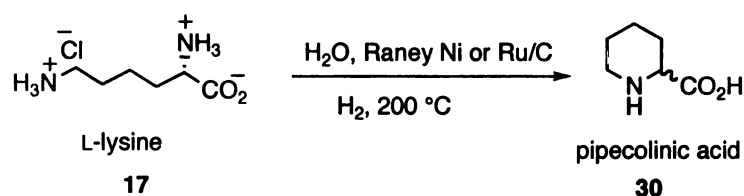


Figure 29. Deamination of L-lysine in water.

Maier group's work on reductive deamination with supported Pt catalysts deserves consideration since it provides some valuable insight about the possible solution to a selective C-N bond cleavage. They reported that a variety of nitrogen-containing

compounds, including primary and secondary amines, nitriles, nitro compounds and heterocycles, can be cleanly converted to the according parent hydrocarbon and ammonium with Pt/SiO₂ and hydrogen. More interestingly, our target molecule, ϵ -caprolactam was found to be stable in the presented reaction conditions (Figure 27). The major limiting factor for this method is that it requires the volatility of the substrates. 40% Pt/SiO₂ was prepared according to the literature¹⁹ and catalytic activity of Pt/SiO₂ was confirmed by successful application of the method to the deamination of cyclohexamine. However, direct extension of the method to α -amino- ϵ -caprolactam failed because it is not volatile. Modification of the method by mixing the catalyst with α -amino- ϵ -caprolactam and heating from 150 °C to 250 °C in the presence of H₂ generated no desired product while yielding tar (not identified). Failure of application of the Pt/SiO₂ catalyst to deamination of α -amino- ϵ -caprolactam can be explained by the mechanism shown in Figure 30. It is suggested that C-N hydrogenolysis is initiated by insertion of the catalyst into the α -C-H bond to form a σ -complex **31** (Figure 30) or an α , β -adsorbed intermediate **32** (Figure 30). Then hydrogen atoms that are activated by the catalyst surface will come to attack the activated C-N and result in the scission of the C-N bond. The large Pt content needed for the reaction may indicate that numerous active sites are required. Melted α -amino- ϵ -caprolactam at the reaction temperature (150-250 °C) could block all the active sites and make it impossible for hydrogen to absorb on the Pt surface. If the above assumption is right, probably a higher reaction temperature, higher hydrogen pressure and more dispersed catalysts are required to achieve the effective C-N bonds cleavage of α -amino- ϵ -caprolactam. With that, deamination of α -

amino- ϵ -caprolactam using carbon supported Pt was examined in the high-pressure reactor.

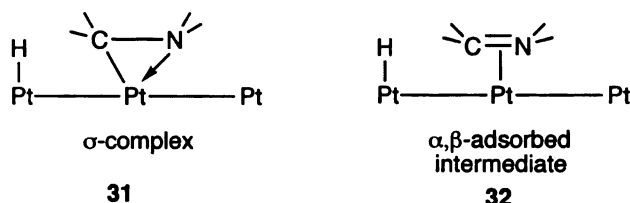


Figure 30. Possible intermediates for C-N hydrogenolysis with Pt catalyst.

Optimization of reaction conditions by varying reaction temperature, hydrogen pressure and catalyst concentration led to desired caprolactam in 22% yield. Temperature as high as 300 °C is necessary for this deamination to proceed. In order to better understand the mechanism of this reaction, the reaction mixture was isolated by flash chromatography. Multiple spots were observed in the TLC plate. One of major byproducts was identified to be EtNH₂, which can come from the decomposition of α -amino- ϵ -caprolactam or caprolactam. Control reactions were then performed to test the stability of substrate and product at the current reaction conditions. In the absence of Pt catalyst and otherwise identical reaction conditions, caprolactam was kept at 300 °C in THF in the presence of hydrogen (50 psi). After 8 h, about 20% caprolactam was converted to unidentified products. In the same conditions, about 25% α -amino- ϵ -caprolactam was lost. From the control reaction, it seems both α -amino- ϵ -caprolactam and ϵ -caprolactam are not stable at temperature as high as 300 °C. It is very likely unselective C-C bond cleavage results in the low reaction yield. Under our hydrogenolysis conditions the metal surface may insert into C-H and N-H bonds. The

most significant difference between carbon and nitrogen, the nitrogen lone pair, may lose its significance on a metal surface under our hydrogenolysis conditions, and thus chemisorbed carbon and nitrogen may behave similarly accounting for the lack of selectivity of the hydrogenolysis reactions, especially at higher temperatures. To selectively cleave the C-N bonds, a catalyst has to be found that can differentiate between carbon and nitrogen at high temperature, or a more active catalyst that will allow the efficient HDN reaction at lower temperature.

References

- 1 *Chemical Week*, **2007**, 169 (8), 26.
- 2 Dahlhoff, G.; Niederer, J. P. M.; Hoelderich, W. F. *Cat. Rev.* **2001**, 43, 381.
- 3 Hoffman, J. *Chemical Market Report*, **2000**, 258 (9), 3.
- 4 O'Driscoll, C. *Eur. Chem. News* **2005**, 82, 2152.
- 5 Ichihashi, H.; Sato, H. *Appl. Catal. A: General* **2001**, 221, 359.
- 6 Comara Greiner, E. O.; Gubler, R.; Yokose, K. *CEH Marketing Research Report: Amino Acids*; SRI Consulting: Menlo Park, CA, 2003.
- 7 Ajinomoto, http://www.ajinomoto.com/ar/i_r/pdf/fact/feeduse_amino.pdf.
- 8 Synthesis of lactam: (a) Collum, D. B.; Chen, S. C.; Ganem, J. *J. Org. Chem.* **1978**, 43, 4393. (b) Steliou, K.; Nowosielska, A. S.; Favre, A.; Poupart, M. A.; Hanessian, S. *J. Am. Chem. Soc.* **1980**, 102, 7578. (c) Mader, M.; Helquist, P. *Tetrahedron Lett.* **1988**, 29, 3049. (d) Blade-Font, A. *Tetrahedron Lett.* **1980**, 21, 2443. (e) Barth, F.; O-Yang, C. *Tetrahedron Lett.* **1990**, 31, 1121. (f) Curran, D. P.; Tamine, J. *J. Org. Chem.* **1991**, 56, 2746. (g) Russell, G. A.; Li, C.; Chen, P. *J. Am. Chem. Soc.* **1996**, 118, 9831. (h) Goto, M.; Nagaoka, S.; Matsuda, S.; Nagata, M.; Hiraki, J.; Masuhari, M. JP patent, 2003206276, 2003. (i) Goto, M.; Umeda, M.; Kodama, A.; Hirose, T.; Nagaoka, S.; Masuhari, M.; Hiraki, J.; *J. Chem. Eng. Jpn.* **2004**, 37, 353.
- 9 a) Mares, F.; Sheehan, D.; *Ind. Eng. Chem. Process. Des. Dev.* **1978**, 17, 9. b) Merger, F.; Fischer, R.; Priester, C.-U. US Patent 4963673, 1990. c) Dockner, T.; Saucrwald, M.; Fischer, R.; Hutmacher, H. -M.; Priester, C.-U. US Patent 4767856, 1988.
- 10 Nubbemeyer, U. *Top. Curr. Chem.* **2001**, 216, 125.
- 11 Payne, L. S.; Boger, J. *Syn. Commun.* **1985**, 15(14), 1277.
- 12 *The Chemistry of the Amino Group*; Interscience Publishers: London. **1968**, 409.
- 13 Doldouras, G. A.; Kollonitsch, J. *J. Am. Chem. Soc.* **1978**, 100, 341.
- 14 Ramamurthy, T. V.; Ravi, S.; Viswanathan, K. V. *J. Labeled. Compd. Rad.* **1988**, 25 (8), 809.

- 15 *Encyclopedia of Reagents for Organic Synthesis*; Wiley: New York, **1995**, 2764.
- 16 Campell, K. N.; Sommers, A. H.; Campell, B. K., *J. Am. Chem. Soc.* **1946**, 68,150.
- 17 Kieboom, A. P. G.; Rantwijk, F. Van. *Hydrogenation and Hydrogenolysis in Synthetic Organic Chemistry*, Delft Univeristy Press, **1977**.
- 18 Pal, B.; Ikeda, S.; Kominami, H.; Kera, Y.; Ohtani, B. *J. Catal.* **2003**, 217,152.
- 19 Guttieri, M. J.; Maier, W. F., *J. Org. Chem.* **1984**, 49, 2875.
- 20 Zhang. Z. G.; Jackson, J. E.; Miller, D. J., *Ind. Eng. Chem. Res.* **2002**, 41, 691.
- 21 Guichard, G.; Avele, S.; Seebach, D. *Helv. Chim. Acta.* **1998**, 81,187.
- 22 *Chem. Eng. News* **2004**, 82 (37), 15.

CHAPTER 3

HYDRODENITROGENATION (HDN) WITH TRANSITION METAL SULFIDES

3.1 Background

In the preceding chapter, deamination of α -amino- ϵ -caprolactam over carbon supported Pt at 300 °C in the presence of H₂ resulted in the desired deaminated product ϵ -caprolactam in low yield. At this high temperature, unselective C-C bond cleavage competes with C-N cleavage and results in the loss of reaction yield. To increase the selectivity of deamination, catalysts must be found that can differentiate between carbon and nitrogen or allow an efficient deamination reaction at much lower temperature. Prior work in the Frost group revealed that deamination of cyclohexylamine with a conventional sulfided Ni-Mo HDN catalyst gave a very high yield (>90%) of deaminated product. The extension of this catalyst to hydrodenitrogenation of α -amino- ϵ -caprolactam failed to afford any deamination product. This aroused interest in reexamining the HDN catalysts for deamination of α -amino- ϵ -caprolactam. In the last decade, novel catalysts based on noble metal sulfides have attracted attention. Hydrodenitrogenation of petroleum to remove contaminants such as heterocyclic amines, anilines and aliphatic amines usually employs Al₂O₃ supported Ni-Mo sulfide and Co-Mo sulfide. Hydrodenitrogenation of substituted cyclohexylamines, other alkylamines, substituted pyridine and quinoline has been studied using sulfided Ni-Mo catalyst or other transition metal sulfides. Hydrodenitrogenation of α -amino- ϵ -caprolactam has not been reported before. The primary objective of this chapter is to update information on

mechanisms of C-N bond cleavage and elucidate the catalytic sites, leading to more efficient catalysts and consequently higher HDN yield. Extensive efforts towards catalyst development and optimization of reaction conditions will be described.

3.2. Introduction

3.2.1 Overview of Hydrodenitrogenation (HDN)

Catalytic HDN is a process in which organonitrogen compounds are removed from oil fractions to produce more processible and environmentally more acceptable liquid fuels. HDN, together with hydrodesulfurization (HDS), hydrodeoxygenation (HDO) and hydrodemetallization (HDM) all fall under a process called hydrotreating, in which the feedstock reacts with hydrogen in the presence of a catalyst. Despite the commercial importance of HDN, people have not focused on HDN since relatively small quantities of nitrogen compounds are present in the conventional petroleum stocks. However, this situation has changed recently because of two major reasons: First, a declining oil supply in the face of increasing demand will ultimately require a need to process heavy and low-quality feedstocks, which contain higher percentages of nitrogen compounds. Second, stringent legislation for ultra low sulfur automotive gas oil places increasingly higher demands for high performance HDN catalysts because nitrogen containing compounds are poisonous to HDS catalysts. Consequently, there has been growing interest in the development of more effective HDN catalysts as evidenced by the rapidly expanding literature in this field.¹

Industrial hydrotreating catalysts mostly are sulfided Co-Mo and Ni-Mo catalysts supported on Al₂O₃. Recently, a new generation of noble metal based sulfide catalysts

have been explored due to their potentially high HDN activity and selectivity. Since oil fractions always contains S, H₂S will be produced during the process of hydrotreating, leading to sulfidation of the metal or metal oxide that is used as the catalyst. HDN catalysts need to be presulfided to achieve their active state. The presulfidation is normally done before the HDN reaction by exposing the catalyst to a mixture of H₂S/H₂ or other sulfur-containing compounds such as thiophene or CS₂ at high temperature. The presulfidation conditions such as temperature, heating rate and duration of treatment play an important role in catalyst activity and stability. The HDN catalysts will gradually lose their activity after a certain period. The loss of activity can be traced to sintering, decomposition of the active sites, blocking of the active sites by reactants and products, coking and deposition of metal sulfides. However, it is possible to regenerate the used catalysts if burn-off is carefully controlled to avoid catalyst overheating, which irreversibly destroys the active sites of the catalyst.

Both heterocyclic nitrogen-containing compounds (mainly those containing six-membered pyridine and five-membered pyrrole rings) and nonheterocyclic nitrogen compounds (aliphatic amines and anilines) are found as impurities in petroleum and are subject to HDN.² Under common HDN conditions, amines and anilines undergo HDN quite fast. Therefore, heterocyclic compounds (especially pyridine and quinoline) have become the primary model compounds for HDN studies. HDN of pyridine has been explored using carbon supported sulfides (NiMo, Zr, Ag, Nb, Mo, Rh, and Pd) or carbon supported metal catalysts (Rh, Ru, Pd, Ir and Pt).^{3,4} HDN of quinoline has been examined using carbon supported metal sulfides (W, Re, Ir, Os, Pt, Mo, Ru, Pd, V, Cr, Mn, Fe, Co, and Ni).⁵ HDN of alkylamines have been studied mechanistically over NiMo sulfide and

other transition metal sulfides.⁶ Beyond alkyamines, quinoline and pyridine, no literature precedent for HDN of α -amino- ϵ -caprolactam is available. To find appropriate catalysts and reaction conditions for HDN of our substrates (L-lysine or α -amino- ϵ -caprolactam), a summary of C-N bond scission mechanisms, the current understanding of the nature of the transition metal sulfides and possible ways to improve HDN catalyst activity and selectivity will be given.

3.2.2. Reaction Mechanisms of C-N Bond Cleavage

HDN on metal sulfides has been extensively studied and several mechanisms have been proposed.⁷ Since our substrates (L-lysine or α -amino- ϵ -caprolactam) are aliphatic amines, only mechanisms concerning C-N cleavage of aliphatic amines will be reviewed here. The mechanisms for HDN were first put forward by Nelson and Levry.⁸ They suggested that a Hofmann-type elimination (HE) and nucleophilic substitution are the main mechanisms for C-N bond cleavage of aliphatic nitrogen-containing molecules. The C-N cleavage is initiated by addition of a proton to the nitrogen lone pair resulting in the formation of a quaternary ammonium compound, which makes it a better leaving group. C-N bond cleavage can now occur via either elimination of a β -hydrogen to form the alkene (Figure 31) or via nucleophilic substitution of the amine group at the α -carbon atom by a sulfhydryl group to form an alkanethiol (Figure 32) followed by hydrogenolysis of a much weaker C-S bond. Both mechanisms have been supported by other research groups.⁹

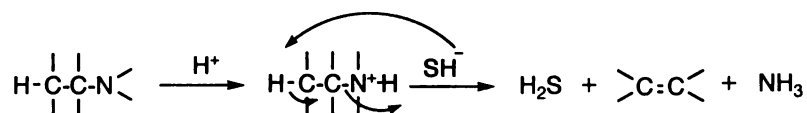


Figure 31. Hofmann elimination mechanism.

hydrogenation and C-S bond cleavage converts the alkylamine to the according alkane (Figure 34).¹¹

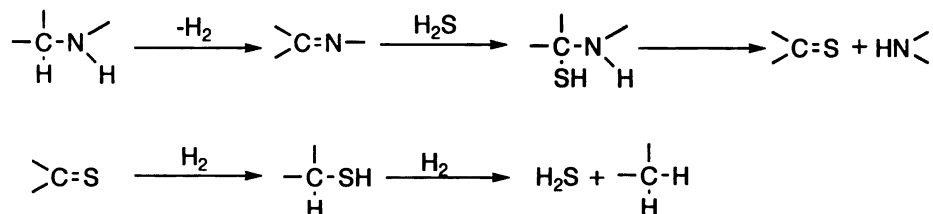


Figure 34. Mechanism of hydrogenolysis of alkylamines via imine intermediacy.

It should be mentioned that the HDN of amines is more complicated than other eliminations because a disproportionation reaction can occur between amines and results in the formation of substituted amines. It is actually another example of an S_N2 nucleophilic substitution mechanism. A substantial amount of dialkylamine was observed in the deamination of piperidine, hexylamine and pentylamine.¹² The nucleophilic substitution reaction between two alkylamine molecules results in the formation of dialkylamines and ammonia (Figure 35).

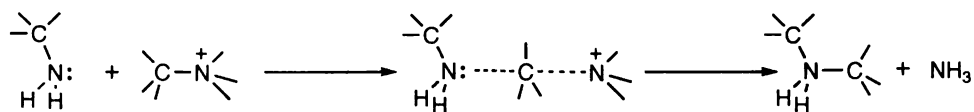


Figure 35. Disproportionation mechanism.

The formation of dialkylamines can also be explained by an imine mechanism as well. For example, in the HDN of ethylamine, the imine formed from dehydrogenation

will react with another ethylamine to give an intermediate, followed by elimination and hydrogenation to afford diethylamine (Figure 36).

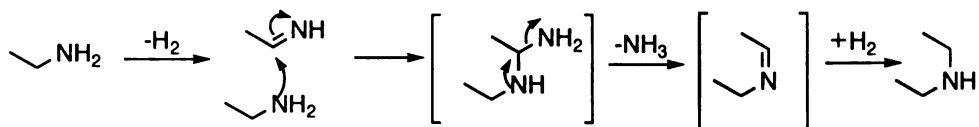


Figure 36. Formation of a dialkylamine via an imine mechanism.

Combining the chemistry and nature of the transition metal sulfide catalysts and the HDN mechanism proposed by Laine, Butt came up with a possible mechanism of piperidine hydrogenolysis in the presence of H_2S , which is shown in Figure 37.¹³ Reaction starts from chemisorption of the amine on the vacancy sites of the transition metal sulfide, via a 1,1' addition to form the metalloazocyclopropane species, followed by β elimination and C-N bond cleavage to give an alkene intermediate with a final hydrogenation to give pentylamine.

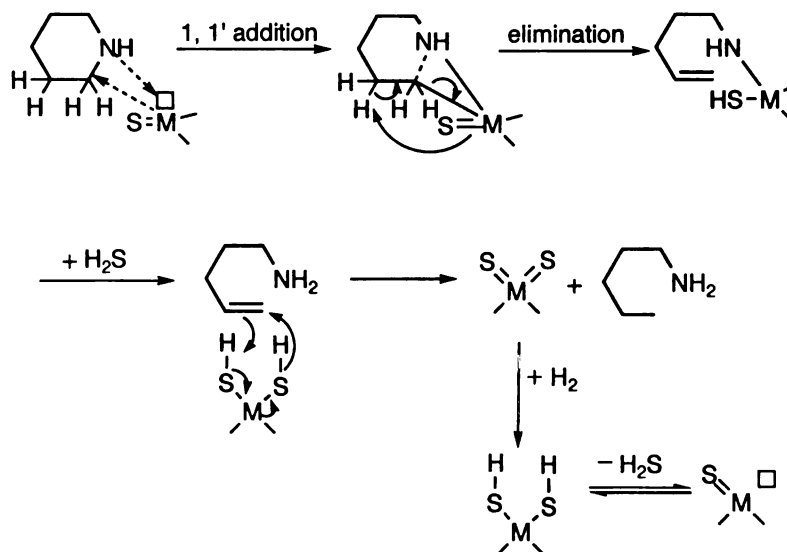


Figure 37. HDN mechanism with transition metal sulfide

The mechanistic basis of C-N bond cleavage on metal sulfides was significantly improved by studying the HDN reactivity of a series of amines with different structures and different numbers of hydrogen atoms on the carbon atoms adjacent to nitrogen atoms (H_α and H_β respectively). These amines were previously investigated on unsupported transition metal sulfides (Nb, Rh, Ru, Pd),¹⁴ or Mo or Nb carbides and MoS_2/SiO_2 ,¹⁵ or supported Pt sulfide.¹⁶ Those results suggested that the C-N cleavage depended on the catalyst properties and the structure of the amines to be processed (steric hindrance around the α carbon atom and the number of β hydrogens with respect to amine group).

The Portefaix group observed that the HDN rate of different pentylamines over sulfided NiMo/ Al_2O_3 increases proportionately to an increase in the number of β -hydrogens. This indicates that C-N bond cleavage of aliphatic amines over sulfided NiMo catalyst takes place by Hofmann elimination.^{9b}

The Catternot group showed that the HDN mechanism depends not only on the structure of the alkylamine to be transformed but also the acidity of the transition metal sulfide catalysts.¹⁴ They found that different metal sulfides have different acidities and thus different catalytic properties. Among the unsupported metal sulfides examined, the acidity decreases in the order $NbS_3 > MoS_2 > RuS_2 > Rh_2S_3$. The most acidic NbS_3 has the highest activity for the elimination and shows no activity for the nucleophilic substitution. The least acidic Rh_2S_3 turns out to be most active for the nucleophilic substitution but is inactive for the elimination.

3.2.3. Active sites and the role of H_2S , H_2 and H_2S/H_2

There are several species on the surface of the transition metal sulfide, the concentration of these species is related to the nature of the catalysts and also the reaction

conditions (Figure 38).¹⁴ These species include (i) vacancy sites formed by sulfur removal (ii) SH groups created either by hydrogen or by H₂S heterolytic adsorption, and (iii) bridged S²⁻ and S₂²⁻ anions. These vacancy sites are electron deficient and can coordinate with the amine via the lone pair of electrons on the nitrogen atom. The role of SH is dependent on the strength of the metal-sulfur bond. For example, a strong metal sulfur bond will weaken the S-H bond, resulting in increased acidity. On the other hand, a weak metal sulfur bond will strengthen the S-H bond and SH groups may act more as a nucleophile. The third species (S²⁻ and S₂²⁻) may act as bases and can abstract a β-hydrogen. These species have higher concentrations on poorly reducible metals (elements on the left side of periodic table, such as Nb and Mo) than on highly reducible metals (elements on the right side of periodic table, such as Ru and Pt).

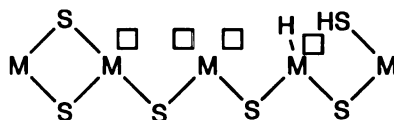


Figure 38. Structure of transition metal sulfide. □: vacancies.

It is well known that H₂S can increase the HDN activity of metal sulfides. To explain the beneficial effect of H₂S, several studies have postulated the existence of two kinds of active sites: vacancies (I) and acid-base sites (II) (Figure 39) on the surface of transition metal sulfides.¹⁷

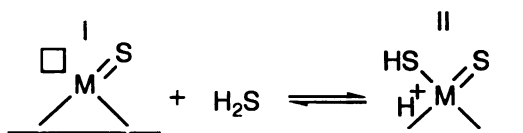


Figure 39. Interconversion between sulfur vacancy and Brønsted acid site.

Type I sites, which are sulfur vacancies associated with the metal atom, can facilitate hydrogenation and dehydrogenation. They might facilitate hydrogenolysis as well, such as breakage of a single C-N or C-S bond. Type II sites, usually consisting of H^+ on the surface from the dissociation of H_2S , are believed to facilitate hydrogenolysis and cracking. The above hypothesis indicates that the presence of H_2S in the reaction slightly reduces the number of sulfur vacancies and increases the number of Brønsted acid sites and sulfhydryl groups (SH). In the presence of H_2S , a slight reduction of hydrogenation and a significant increase in the rate of hydrogenolysis were observed when quinoline was hydrodenitrogenated using sulfided Ni-Mo/ Al_2O_3 . While the retardation of hydrogenation was traced to the competition between H_2S and nitrogen compounds on the hydrogenation sites (vacancies), the enhancement of the hydrogenolysis reaction was explained by the increase of surface acidity caused by H_2S .

Several reviews have covered HDN reactions.¹⁸ However, the role of hydrogen was ignored for a long time until 1983.¹⁹ The interaction of hydrogen with metals is the cause or basis of many phenomena ranging from chemisorption and activation of hydrogen on the surface of metal, its desorption on the metal and catalytic reactions involving hydrogen as a reactant. Furthermore, active surface hydrogen extends the catalyst life by slowing down the deactivation or formation of coke on the surface of the metals.

The adsorption and desorption of hydrogen on the metal sulfide was reported to involve several processes. It results in a gradual removal of sulfur as H_2S from metal sulfide catalysts leading to a decrease in the S/M ratio. At the same time, H_2 is absorbed

and activated on the metal sulfide where it can be transferred and participate in various reactions. Studies of the hydrogen adsorption on MoS₂ indicates that a heterolytic splitting of H₂ on the Mo-S catalyst surface gives a hydride and SH group while a homolytic dissociation of H₂ with the presence of S₂²⁻ species generates two SH groups.²⁰ H₂S can also dissociate on the same vacancy as follows (Figure 40, c).

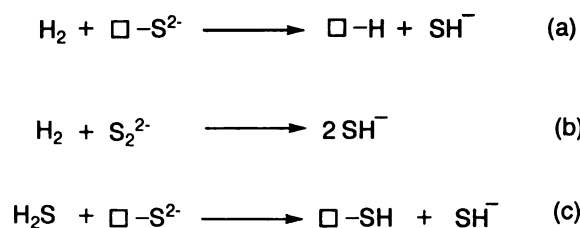


Figure 40. (a) heterolytic splitting of H₂; (b) homolytic splitting of H₂; (c) H₂S competition for the same vacancy.

By studying effects of the total pressure of H₂ and H₂S and the ratio of H₂S/H₂ on the HDN of pyridine and piperidine over commercial Ni-Mo/Al₂O₃, the Hanlon group found that it was not the absolute value of pressure of H₂S or H₂ but the ratio of H₂S/H₂ that affect the rate of hydrogenolysis.²¹

3.2.4. Periodic trends of transition metal sulfides

Studies of the periodic trends for transition metal sulfides have provided useful information about the role of the different kinds of active sites. These studies include hydrodesulfurization, hydrogenation and hydrodenitrogenation. When plotted versus the position of the elements in the periodic table, catalytic activity of transition metal sulfides usually exhibits volcano-shape curves. For HDN,²² the activity of the first-row transition metal sulfides is quite low. The second-row transition metal sulfides are much more

active with Ru, Rh and Pd standing out, While Ir, Os, Re and Pt normally show the highest activity among the third row transition metal sulfides. Both the bond energy model and the Sabatier principle are used to explain the volcano curves. It is suggested that the strength of metal sulfur bond is critical and the most active transition metal sulfides can be readily desulfurized to from the active vacancy sites and sulfhydryl groups. Periodic trends show the metal-sulfur bond decreases from the left to right, whereas the S-H bond strength increases in the same direction. On the contrary, the acidity of S-H groups decreases from the left to right. Ideally, a metal-sulfur bond should be strong enough to activate sulfur and at the same time weak enough to be easily transferred to reactant molecules. This ensures availability of the vacant sites for the substrates or another sulfur activation-transfer cycle.

Due to their high HDN activities, noble metal sulfides from the second row (Ru, Rh, Pd) as well as the third row (Re, Ir and Pt) were chosen as potential candidates for the HDN of α -amino- ϵ -caprolactam.

3.2.5. Bimetallic sulfide catalysts

Understanding of the fundamentals of periodic trends and the importance of the metal-sulfur bond strength leads to the development of catalysts with high HDN or HDS activity. One method is to adjust the metal-sulfur bond strength by adding a second metal into the monometallic sulfide. For example, addition of a second metal into Mo or Co-Mo catalysts led to a considerable increase in activity by offering a synergetic effect in HDN reactions.^{23,24} This promotion effect was proposed to be caused by an electron

donation from the second metal to Mo decreasing the Mo-S bond strength to an optimum range for HDS or HDN activity (Figure 41).²⁵

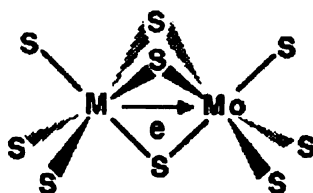


Figure 41. The Co promotion by donation of electrons to Mo.

Supported bimetallic catalysts have received considerable attention since the introduction of Pt-Re/ Al_2O_3 in 1968.²⁶ The addition of a second metallic element such as Re can improve the stability and selectivity of the Pt catalyst. In particular, undesired reactions such as C-C fissions and formation of ‘coke’ are suppressed. This advantageous byproduct suppression is used industrially in Pt-Re/ Al_2O_3 HDN catalysts. Sulfur, firmly bound to Re, blocks the cracking power of Re and dramatically diminishes the size of platinum relative to the total surface area (Figure 42)²⁷. The metallic dispersion and interaction between Pt and Re depend in great deal on the preparation, activation procedure and Re/Pt ratio. Different preparation and activation methods along with changes in Re/Pt ratio will be examined for the catalytic reactivity of Pt-Re catalysts. Using the experiences learned from Pt-Re catalysts, a combination of Pt with other noble metals will also be explored.

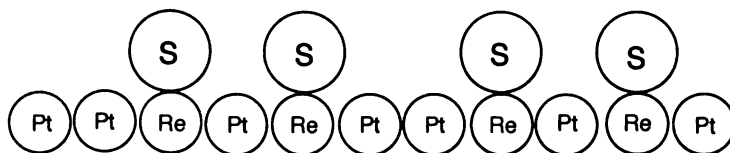


Figure 42. Schematic illustration of Pt-Re catalyst stabilization in the presence of sulfur.

3.3 Results

After examination of C-N bond cleavage mechanisms and possible methods to improve the HDN catalyst activities, we started to search for more promising HDN catalyst candidates and studied in detail the reaction conditions with a goal of higher yields.

Catalyst preparation

The catalysts were prepared by impregnation of active carbon with H_2PtCl_6 , $\text{RuCl}_3 \cdot \text{H}_2\text{O}$, $\text{RhCl}_3 \cdot 3\text{H}_2\text{O}$, PdCl_2 , NH_4ReO_4 or $(\text{NH}_4)_2\text{IrCl}_6$. The activated carbon (Norit RX3 Extra, Norit Americas Inc; BET (Brunauer, Emmett and Teller, three scientists who optimized the theory for measuring surface area) surface area $1370 \text{ m}^2\text{g}^{-1}$), which is not active under our reaction conditions, was chosen not only to mechanically stabilize the catalyst but also to minimize direct support interaction. The slurry of the support with the solution of catalyst precursor was dried under vacuum in a rotary evaporator. The catalyst mixture was crushed and sieved to 200 mesh. The resulting catalyst precursors were either reduced with H_2 ($400 \text{ }^\circ\text{C}$, 2 h) to afford carbon-support metal catalysts or presulfided by a $\text{H}_2\text{S}/\text{H}_2$ (10:90) mixture ($400 \text{ }^\circ\text{C}$, 2 h) to give carbon-supported metal sulfide catalysts.

Reaction unit and product analysis

All experiments were conducted in a Parr 4575 high-pressure reactor lined with a glass sleeve controlled by a Parr 4842 controller. A typical example is as follows: Under Ar, α -amino- ϵ -caprolactam, solvent (usually THF) and catalyst were added in a glass sleeve in a Parr high-pressure reactor and the vessel was assembled. The reaction chamber was flushed for 10 min with Ar and then pressurized with $\text{H}_2\text{S}/\text{H}_2$ to 100 psi.

The reaction chamber outlet valve was then opened to the atmosphere. This process was repeated two additional times. After repressurizing the reaction vessel with H₂S/H₂ to a desired pressure, the temperature of the stirred reaction vessel was increased to a designated temperature. The stirred reaction vessel was held at the temperature for 4-8 h. Upon cooling to rt, the pressurized reaction vessel's H₂S/H₂ atmosphere was vented through a bleach solution in a fume hood. After filtration, 1 mL of reaction solution was concentrated and caprolactam yields were determined by ¹H NMR based on a calibration curve.

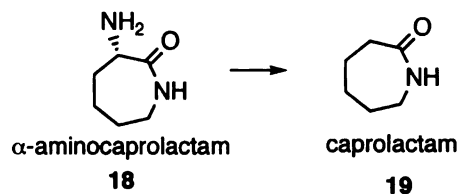
3.3.1 Screening of noble metal catalysts

Since the platinum group metals belong to the most active HDN catalysts, they were chosen to evaluate their deamination activity of α -amino- ϵ -caprolactam.

Hydrodenitrogenation of α -amino- ϵ -caprolactam in THF with carbon-supported VII (Re) and VIII (Ru, Rh, Pd, Ir, Pt) group metals were first conducted under my previous optimized conditions for Pt/C (300 °C, 4 h, H₂ (50 psi)). Results are summarized in Table 15. The highest activities were shown by Ru and Pd, followed by Pt and Rh while Re and Ir gave much lower yields than other metals. This is surprising since generally the third-row metals show higher HDN activity than those of the second-row. This contradiction can be explained by the high cracking ability of Ir and Re, which may cause the excessive unselective C-C bonds cleavage and consequently lower caprolactam yields.

in similar reaction conditions (same temperature, same total pressure). Pt-S/C, which was arguably the most selective catalyst for the HDN of α -amino- ϵ -caprolactam using our initially chosen conditions, became the primary catalyst for our following optimization of reaction conditions.

Table 16. HDN activities of sulfided catalysts

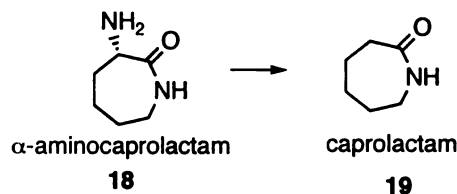


entry	catalyst (1mol%)	solvent	temp (°C)	time (h)	H ₂ S/H ₂ (psi/psi)	(19/18) (% yield)
1	Ru-S/C	THF	250	8	15/135	22/37
2	Rh-S/C	THF	250	8	15/135	15/0
3	Pd-S/C	THF	250	8	15/135	17/30
4	Re-S/C	THF	250	8	15/135	16/17
5	Ir-S/C	THF	250	8	15/135	16/18
6	Pt-S/C	THF	250	8	15/135	25/30

3.3.2 HDN activities of sulfided bimetallic catalysts

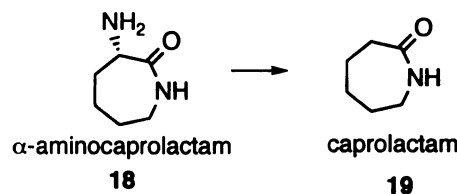
As discussed before, modification of HDN catalysts by addition of a second noble metal is one of the ways shown to improve reaction efficiency. Addition of a second metal into transition metal sulfides can adjust the metal sulfur bond strength and consequently affect the HDN activity. Pt-Re catalysts have been extensively used to suppress undesired C-C bond cleavage and increase the selectivity of Pt catalyst in industry. To investigate the effect of the combination of a second metal to our Pt catalyst, bimetallic catalysts were prepared by mixing chloroplatinic acid with one equivalent of another noble metal precursor, followed by drying and presulfidation according to the procedure described in the experimental section. As summarized in

Table 16 and Table 17, addition of a second metal increased the reaction selectivity but significantly lowered the reaction conversion. The most interesting result was given by Pt-Re-S/C (Table 17, entry 4). Addition of Re into Pt remarkably increased the reaction selectivity for conversion of α -amino- ϵ -caprolactam to ϵ -caprolactam. Specifically, 18% caprolactam yield was observed with 77% starting material left after reacting at 250 °C for 8 h (Table 17, entry 4). Unfortunately, extension of the reaction time to 24 h only gave 26% desired product when all starting material was consumed (data not shown). The high selectivity of the Pt-Re-S/C catalyst encouraged us to optimize the reaction conditions. Temperature effects were examined by stirring α -amino- ϵ -caprolactam with Pt-Re-S/C in a H₂S/H₂ atmosphere at different temperature ranging from 200 to 300 °C. No HDN activity was observed when the temperature was set to 200 °C (Table 18, entry 1), which indicated that HDN reactions require higher temperature to happen. When the reaction temperature was increased to 250 °C, 32% of caprolactam was achieved with 11% starting material left (Table 18, entry 2). The reaction yield peaked at 270 °C (35%) and started to decrease with further increases of the reaction temperature. Since the optimum selectivity was given at 250 °C, the temperature for later HDN reactions with platinum sulfide catalysts was fixed at 250 °C.

Table 17. HDN activities of sulfided bimetallic catalysts

entry	catalyst (1 mol%)	solvent	temp (°C)	time (h)	H ₂ S/H ₂ (psi)	yield (19/18)(%)
1	Pt-Ru-S/C	THF	250	8	15/135	18/36
2	Pt-Rh-S/C	THF	250	8	15/135	14/69
3	Pt-Pd-S/C	THF	250	8	15/135	17/16
4	Pt-Re-S/C	THF	250	8	15/135	18/77
5	Pt-Ir-S/C	THF	250	8	15/135	17/40

a) catalyst concentration was based on mol% of Pt.

Table 18. Temperature effect on HDN activity of Pt-Re-S/C catalyst

entry	catalyst (2 mol%)	solvent	temp (°C)	time (h)	H ₂ S/H ₂ (psi)	(19/18) (% yield)
1	Pt-Re-S/C	THF	200	8	15/135	0/95
2	Pt-Re-S/C	THF	250	8	15/135	32/11
3	Pt-Re-S/C	THF	270	8	15/135	35/0
4	Pt-Re-S/C	THF	300	8	15/135	32/0

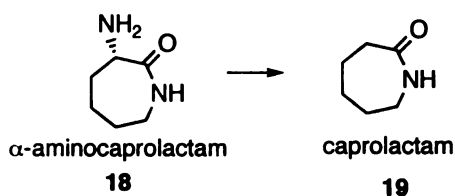
a) catalyst concentration was based on mol% of Pt.

3.3.3 Effect of sulfur concentration

It is well known that beneficial effects on HDN selectivity can be obtained by a partial and well controlled poisoning of the HDN catalysts with sulfur compounds. Thiophene was used as an alternative to hydrogen sulfide since thiophene can bind on the surface of catalyst much more tightly than hydrogen sulfide. To find the best sulfur concentration to achieve the high reaction selectivity, different concentrations of thiophene in a range of 4 mol% to 500 mol% were examined using Pt-S/C or Pt-Re-S/C

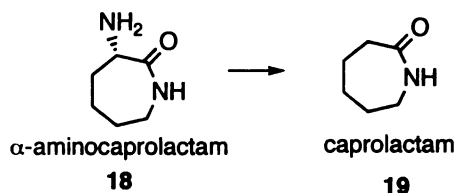
catalysts. Results are summarized in Table 19 and Table 20. Thiophene significantly inhibited the catalytic activity of both Pt-S/C and Pt-Re-S/C catalysts. Retardation of the HDN reaction can be traced to the competition between thiophene and α -amino- ϵ -caprolactam for the active sites. When the concentration of thiophene is too high, it can totally block all the active sites and completely shut down the reaction (Table 20, entry 4). It seems that moderate concentrations of thiophene (20 to 100 mol%) gives the optimal reaction selectivity.

Table 19. Effect of thiophene concentration on HDN activity of Pt-S/C



entry	catalyst (1 mol%)	thiophene (mol%)	solvent	temp (°C)	time (h)	H ₂ (psi)	(19/18) (% yield)
1	Pt-S/C	4	THF	250	8	150	11/45
2	Pt-S/C	20	THF	250	8	150	14/50
3	Pt-S/C	100	THF	250	8	150	7/65
4	Pt-S/C	500	THF	250	8	150	7/66

Table 20. Effect of thiophene concentration on HDN activity of Pt-Re-S/C^a



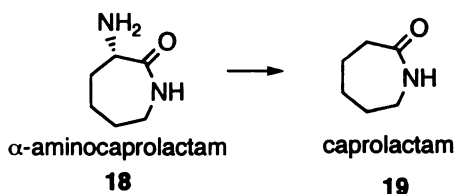
entry	catalyst (1 mol%)	thiophene (mol%)	solvent	temp (°C)	time (h)	H ₂ (psi)	(19/18) (% yield)
1	Pt-Re-S/C	4	THF	250	8	150	4/72
2	Pt-Re-S/C	20	THF	250	8	150	7/65
3	Pt-Re-S/C	100	THF	250	8	150	15/70
4	Pt-Re-S/C	500	THF	250	8	150	0/85

a) catalyst concentration was based on mol% of Pt.

3.3.4 Effect of catalyst concentration

Previous research indicated that the caprolactam yield was almost doubled (Table 4, entry 2 vs Table 3, entry 4) by increasing the concentration of Pt-Re-S/C from 1 mol% to 2 mol%. This result may suggest that multiple active sites may be needed for adsorption of substrate (nitrogen-containing compound) and effect the hydrogenolysis reaction. If this is true, increasing the reaction active sites by increasing catalyst concentration may be helpful for improvement of the reaction yield. To test this assumption, reactions with different concentrations of Pt-S/C (2 to 16 mol%) were examined to maximize the caprolactam yield (Table 21). As expected the yield increased with an increase of the catalyst concentration until the highest yield (44%) was achieved at 8 mol% of catalyst (Table 21, entry 3), increasing of the catalyst loading further did not significantly change the reaction yield (Table 21, entry 4).

Table 21. Effect of catalyst concentration of HDN activities



entry	catalyst	con. (mol%)	solvent	temp (°C)	time (h)	H ₂ S/H ₂ (psi/psi)	(19/18) (% yield)
1	Pt-S/C	2	THF	250	8	15/135	33/0
2	Pt-S/C	4	THF	250	8	15/135	40/3
3	Pt-S/C	8	THF	250	8	15/135	44/11
4	Pt-S/C	16	THF	250	8	15/135	43/4

3.3.5. Solvent effects

Solvent can affect the course and rates of reaction. In catalytic reactions, solvents can act as ligands. Some solvents are most likely to bind tightly to the metal and perhaps

divert the reaction from its intended goal. Some solvents are much less ligating and are widely used, such as THF or ethanol. Halogen solvents can form stable complexes with metal catalyst and greatly affect the reaction selectivity. Alkanes are normally non-coordinating. For the above considerations, a series of solvents were examined for the deamination reaction (Table 22). From the data shown in Table 22, it seems that solubility and the binding between solvent and metal plays an important role in the reaction activity. No formation of caprolactam was observed in acetonitrile. This may be due to the strong binding between acetonitrile and the metal that prevents amine adsorption of the surface of catalyst. The highest yield was achieved in THF. It seems that weakly bound solvents are useful for the reaction since they can easily be replaced by amines. Use of 2,5-dimethyl furan resulted in ten-fold reduction in the yield of caprolactam relative to use of THF as solvent (Table 22, entry 2 vs entry 3). Steric hindrance may keep the 2,5-dimethyl furan from ligating with Pt and thus can not affect the electronic affect the electronic properties of Pt significantly. THF can better donate the electrons to Pt and probably weaken the Pt-S bond strength and facilitate the HDN reaction. It suggests that the interaction between the solvent and metal can be critical for high hydrogenolysis activity.

Table 22. Solvent effects for deamination of α -amino- ϵ -caprolactam

entry	catalyst (4 mol%)	solvent	temp (°C)	H ₂ S/H ₂ (psi)	time (h)	caprolactam (% yield)
1	Pt-S/C	CH ₃ CN	250	15/135	8	0
2	Pt-S/C		250	15/135	8	40
3	Pt-S/C		250	15/135	8	4
4	Pt-S/C	hexanol	250	15/135	8	14
5	Pt-S/C		250	15/135	8	7
5	Pt-S/C		250	15/135	8	15

3.3.6 Effect of total pressure of H₂S/H₂

It is well known that there is competition among H₂, H₂S and α -amino- ϵ -caprolactam for the active sites on the catalyst surface. High pressures of H₂ and H₂S mixture can inhibit the deamination of α -amino- ϵ -caprolactam while low pressure of H₂ and H₂S may be deficient to facilitate cleavage of the C-N bond. Reactions were conducted by changing the total pressure of the H₂S/H₂ mixture (from 50 to 450 psi). Data in Table 23 showed that the caprolactam yield first increased and then decreased with the increase of the total H₂S/H₂ pressure in the range examined. This is consistent with our assumption that high H₂S/H₂ pressure decreases the availability of the vacancy sites and hinders the adsorption of α -amino- ϵ -caprolactam on the catalyst surface and thus inhibits the deamination of α -amino- ϵ -caprolactam.

Table 23. Effect of H₂S/H₂ mixture total pressure

entry	catalyst (4 mol%)	solvent	temp (°C)	H ₂ S/H ₂ (psi/psi)	time (h)	caprolactam (% yield)
1	Pt-S/C	THF	250	5/45	8	45
2	Pt-S/C	THF	250	10/90	8	47
3	Pt-S/C	THF	250	15/135	8	40
4	Pt-S/C	THF	250	45/405	8	34

3.3.7 Effect of H₂S/H₂ ratio

As discussed before, several studies indicated that the importance of the H₂S/H₂ ratio and temperature on the distribution of vacancy sites and SH groups.²⁸ The surface sulfidic species is believed to play a critical role in the C-N bond cleavage. Changing the ratio of H₂S/H₂ will change the above equilibrium and the number of vacancy sites and acid-base sites (Figure 39) leading to changes in the rate of hydrogenolysis.

The other possible reason for the importance of the H₂S/H₂ ratio can be explained by an indirect substitution mechanism. Substitution may be catalyzed by metallic sites as well as acidic sites. As shown in Figure 43, a sequence dehydration of the amine to an imine, hydrogen sulfide addition, ammonia elimination, hydrogenation of the thioketone to a thiol, which is then removed by following cleavage of weaker C-S bonds.

To investigate the effect of the H₂S/H₂ ratio for deamination of α -amino- ϵ -caprolactam, experiments were conducted in varying H₂S partial pressures from 5 to 40 psi while maintaining the total pressure of the H₂S/H₂ mixture at 100 psi. Data in Table 24 demonstrated that caprolactam yield did increase with an increase of H₂S/H₂ ratio until the highest yield (65%) was afforded using a H₂S/H₂ (20/80) mixture (Table 24, entry 3). Further increase of the H₂S concentration slightly lowered HDN yield probably due to the competition between H₂S and α -amino- ϵ -caprolactam for the vacancy sites.

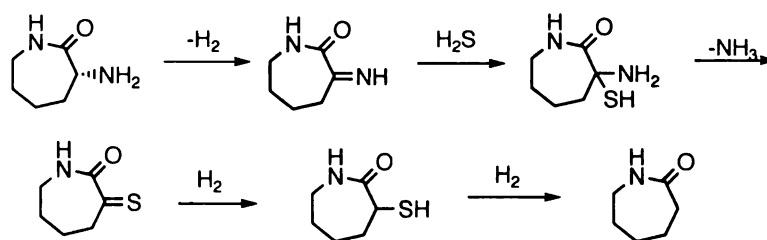


Figure 43. Indirect substitution of an amine to a thiol by metal catalysis.

Table 24. Effect of changing H₂S/H₂ ratio

entry	catalyst (8 mol%)	temp (°C)	H ₂ S/H ₂ (psi/psi)	time (h)	caprolactam (% yield)
1	Pt-S/C	250	5/95	8	58
2	Pt-S/C	250	10/90	8	60
3	Pt-S/C	250	20/80	8	65
4	Pt-S/C	250	40/60	8	52

3.3.8 Role of alkali salt addition

Based on our previous observation, it seems important to keep the Pt-S/C stable in the reaction to get high HDN activity. It was reported that modification of Ru catalysts with alkali metal salts, especially cesium hydroxide, improved the properties of the catalyst obtained.^{29,30} Ruthenium catalysts that showed higher catalytic activity in the presence of cesium existed in the oxidation state close to RuS₂ instead of ruthenium metal. It was suggested^{28,29} that even under hydrogen pressure the addition of an appropriate amount of cesium stabilized RuS₂ on the Al₂O₃ support, promoted the C-S bond cleavage, and prevented the ruthenium species from sintering to maintain higher dispersion. The above results inspired us to investigate the effect of CsOH addition into Pt catalysts. H₂PtCl₆ was treated with different ratios of CsOH (1 to 6 equivalents) and impregnated with activated carbon support. The resulting catalyst was presulfided by a

H₂S/H₂ (10:90) mixture before the reaction. The effect of the CsOH addition to the carbon-supported Pt sulfide catalysts was investigated in a high-pressure reactor under the following conditions (250 °C; 8 mol% catalyst (based on Pt); H₂S/H₂ (20/80 psi); THF). The results are summarized in Table 25. Although the catalytic activity of Pt-Cs catalysts did increase with the ratio of Cs/Pt, it was still lower than expected. According to the results of Ishihari and coworkers,²⁸ the heat of adsorption of H₂S on the Ru-Cs catalyst (126 KJ/mol) was quite larger than observed for the Ru catalyst (29 KJ/mol), indicating that the sulfur species bind more tightly on the surface of catalyst with addition of cesium. This explained why the Ru-Cs catalyst was further inhibited by H₂S. They also found that while addition of Cs to the Ru catalyst decreases the lability of active sites and increases their number. If the same holds true for our Pt-Cs catalyst, addition of cesium into Pt sulfide increases the Pt-S bond strength and makes it more difficult to generate SH groups, which is the nucleophile necessary for C-N cleavage, and thus reduces the HDN yield. An increase of caprolactam yield with the increase of Cs/Pt ratio can be explained by the increase in active sites.

Table 25. CsOH addition effect

entry	catalyst (8 mol%)	temp (°C)	H ₂ S/H ₂ (psi)	time (h)	caprolactam (% yield)
1	Pt-Cs-S/C	250	20/80	8	23
2	Pt-2Cs-S/C	250	20/80	8	27
3	Pt-6Cs-S/C	250	20/80	8	37

3.3.9 Effect of surface oxidation of support on the HDN activity.

Previous studies showed that catalytic activity of hydrotreatment catalysis can be tailored by oxidative and/or thermal treatment of the activated carbon support, which can

introduce oxygen containing groups on the surface of carbon, leading to a strong interaction between oxygen and the metal during the impregnation process and result in high dispersion of metal on the surface of the support.³¹ To investigate this effect, activated carbon was treated with different concentrations of boiling HNO₃ solutions (0.5, 1.0, 6.0 M), followed by extensive washing with distilled water. The resulted support was impregnated with H₂PtCl₆ solutions. The impregnated sample was then dried and presulfided with a H₂S/H₂ mixture. Then HDN reactions were run under our optimized conditions using the HNO₃ treated Pt-S/C catalyst. Results are shown in Table 26, oxidation of the activated carbon surface as a consequence of the treatments with HNO₃ showed negative effects for HDN. The higher the concentration of the HNO₃, the lower the caprolactam yield was observed (Table 26, entries 1-3). It is known that introduction of oxygen-containing groups will lead to a strong interaction between the support and metal precursor during the impregnation process. Oxidation of activated carbon as a consequence of HNO₃ treatment will also change the acidity of activated carbon. For example, the acidity strength of C-6 (carbon treated with 6 M HNO₃) is twice that of C-0 (carbon without treatment).³⁰ It seems that the reduction in the HDN yield can either be explained by a strong interaction between oxidized support and metal or an increase in the acidity of the support. To prove the above assumption, presulfided Pt catalysts on other supports such as Al₂O₃ and SiO₂ have been prepared and examined in the standard reaction conditions (Table 27). It is well known that the interaction between Al₂O₃ and SiO₂ and metal precursor is much stronger than that of carbon. Significant reduction of catalytic activity of Pt catalyst was observed as a result of replacing activated carbon with Al₂O₃ and SiO₂. Control reactions were conducted in the absence of Pt, and no desired

product was observed after all starting material was consumed (Table 27, entries 3-4). It seems that a strong interaction between the support and Pt sulfide has an adverse effect on the HDN reaction. Possibly the strong interaction between the metal precursor and the support provides less sulfidable species than carbon, resulting in less active sites for HDN, which is consistent with our elemental analysis of the Pt-S/SiO₂ and Pt-S/C catalysts. The sulfur/Pt ratio (about 0.2) for Pt-S/SiO₂ (Figure 44) is much lower than that of Pt-S/C (about 2.8) (Figure 46).

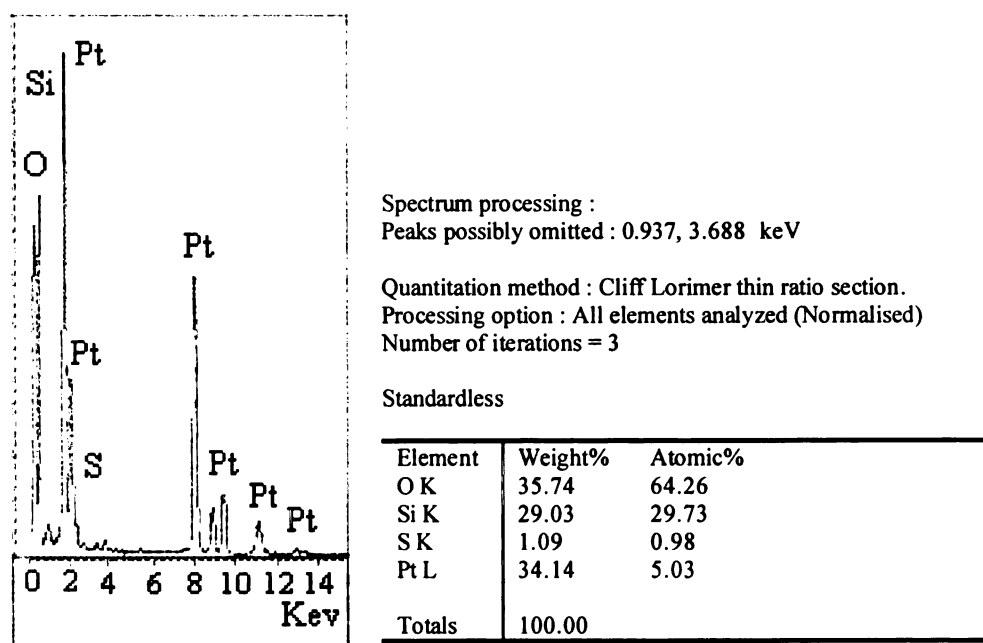


Figure 44. Elemental analysis of Pt-S/SiO₂.

However, the effect of acidity of support can not be ruled out. To adjust the acidity of the reaction system, phosphoric acid (Brønsted acid), InCl₃ (Lewis acid) and ammonia (in dioxane, weak base) have been added into the reaction respectively. Presumably, phosphoric acid will protonate the amine group of α -amino- ϵ -caprolactam and make it a better leaving group. However, phosphoric acid greatly inhibited the HDN activity of Pt-S catalyst (Table 28). This may be explained by the mechanism shown in

Figure 37. The HDN reaction is supposed to be initiated by absorption of amine group on the vacancy sites of the catalyst surface area. It will be very difficult for a protonated amine group to adsorb on the vacancy site and so it inhibits the HDN reaction. Lewis acids such as InCl_3 also gave low HDN activity. It probably activates the carbonyl group of α -amino- ϵ -caprolactam and makes it susceptible to be attacked by nucleophiles and thus decreases the selectivity of the HDN reaction. As far as ammonia, it slightly decreased the catalyst activity, possibly due to its competition with α -amino- ϵ -caprolactam in the adsorption of the vacancy sites. From these results, we can see that it is important to keep the vacancy sites on the Pt-S catalyst and the substrate amine group available for the HDN reaction to proceed efficiently.

Table 26. Effect of catalyst support surface oxidation by HNO_3

entry	HNO_3 (mol/L)	catalyst (8 mol%)	solvent	temp ($^\circ\text{C}$)	$\text{H}_2\text{S}/\text{H}_2$ (psi/psi)	time (h)	caprolactam (% yield)
1	0.5	Pt-S/C	THF	250	20/80	8	45
2	1	Pt-S/C	THF	250	20/80	8	35
3	6	Pt-S/C	THF	250	20/80	8	33

Table 27. Examination of catalyst supports

entry	catalyst (8 mol%)	solvent	temp ($^\circ\text{C}$)	$\text{H}_2\text{S}/\text{H}_2$ (psi/psi)	time (h)	caprolactam (% yield)
1	Pt-S/ SiO_2	THF	250	20/80	8	3
2	Pt-S/ Al_2O_3	THF	250	20/80	8	7
3	SiO_2	THF	250	20/80	8	0
4	Al_2O_3	THF	250	20/80	8	0

Table 28. Effect of additives

entry	catalyst (8 mol%)	additives	solvent	temp ($^\circ\text{C}$)	$\text{H}_2\text{S}/\text{H}_2$ (psi/psi)	time (h)	caprolactam (% yield)
1	Pt-S/C	H_3PO_4	THF	250	20/80	8	2
2	Pt-S/C	InCl_3	THF	250	20/80	8	14
3	Pt-S/C	NH_3	THF	250	20/80	8	44

3.3.10 Effect of water addition

Beneficial effects of water on HDN have been reported.^{32,33} In order to test the effect of water for the HDN of α -amino- ϵ -caprolactam, reactions were run with different concentrations of water in THF (2%, 10%, 100%). Results are summarized in Table 29, ϵ -caprolactam yield decreased with the increase of water concentration. It is known that caprolactam is polymerized at 270 °C in the presence of water or a base. The reduction of ϵ -caprolactam yield can be either due to hydrolysis of α -amino- ϵ -caprolactam or polymerization of ϵ -caprolactam.

Table 29. Effect of water addition

entry	catalyst (8 mol%)	H ₂ O/THF (mL)	temp (°C)	H ₂ S/H ₂ (psi)	time (h)	caprolactam (% yield)
1	Pt-S/C	2/98	250	20/80	8	59
2	Pt-S/C	10/90	250	20/80	8	36
3	Pt-S/C	100/0	250	20/80	8	4

3.3.11 Optimization of reaction conditions with Pt-Re catalysts

The advantage of Pt-Re/Al₂O₃ to Pt/Al₂O₃ for the catalytic reforming of petroleum has been well established.³⁴ This bimetallic catalyst shows a much improved activity maintenance and a much higher reforming yield. In the case of Re as a promoter, such improvement is achieved only after pretreatment with sulfur, which decreases the strong hydrogenolysis activity of the Pt-Re catalyst. The interaction between Pt-Re and dispersion of metal are greatly affected by the preparation and activation procedures.³⁵ So carbon-supported Pt-Re catalysts were prepared by coimpregnation or catalytic reduction methods. The activation was performed by calcinations or reduction treatment. These catalysts were presulfided using a flow of H₂S/H₂ (10/90) at 400 °C for 2 h (details

shown in the experimental section). Size and dispersion of metal particles were characterized by transmission metal spectroscopy (TEM). Based on observation from TEM, addition of Re did improve the dispersion of Pt (Figure 45). The particle size of Pt also decreased from 3-5 nm to less than 2 nm (Figure 45). HDN of α -amino- ϵ -caprolactam using Pt-Re catalysts was performed in our optimized conditions for Pt-S/C (250 °C, THF, H₂S/H₂ (20/80 psi)). Results are presented in Table 30. The preparation and activation procedures did make a difference for the caprolactam yield. It can be seen that the bimetallic catalyst prepared by catalytic reduction has higher deamination activity than when prepared by the coimpregnation method (Table 30, entry 1 vs entry 3). It is also true that the Pt-Re catalyst activated by reduction shows a higher deamination activity than when activated by calcinations (Table 30, entry 3 vs entry 4). The lower activity of calcined catalyst can be explained by inhibition or destroying of formation of Pt-Re ensembles by calcination, which is consistent with previous literature.³⁶ Changing the ratio of Pt/Re (from 0.5 to 2) failed to improve the reaction yield (Table 30, entries 5-6). Yield reduction was observed when Re was replaced with another metal such as Ru or Pd (Table 30, entries 7 and 8) while the same preparation and activation procedures were applied. It also can be seen that Pt-Re-S/C gave relatively lower caprolactam yield than Pt-S/C. This could be due to the larger dispersion of Pt in Pt-Re-S/C and with the fact that the reaction of hydrogenolysis is a demanding reaction that requires certain size metallic ensembles in order to proceed efficiently.³⁷ The other possibility is the change of sulfur/metal ratio. According to the elemental analysis data from Figures 16-18, the sulfur/metal ratio of the Pt-Re-S catalyst is much lower than that of the Pt-S/C (Figure

48). These results may indicate that the particle size of the Pt ensembles and sulfur/metal ratio is critical for the deamination activity of Pt catalysts.

Table 30. HDN with bimetallic catalyst

entry	catalyst	preparation method	activation method	caprolactam (% yield)
1	Pt-Re-S/C	coimpregnation	calcination	40
2	Pt-Re-S/C	coimpregnation	reduction	44
3	Pt-Re-S/C	cat. reduction	calcination	47
4	Pt-Re-S/C	cat. reduction	reduction	52
5	Pt-0.5Re-S/C	cat. reduction	reduction	42
6	Pt-2Re-S/C	cat. reduction	reduction	43
7	Pt-Ru-S/C	cat. reduction	reduction	41
8	Pt-Pd-S/C	cat. reduction	reduction	47

(a) reaction conditions: 250 °C, THF, 8 h, catalyst concentration (8 mol% based on Pt), 100 psi H₂S/H₂ (20: 80).

□

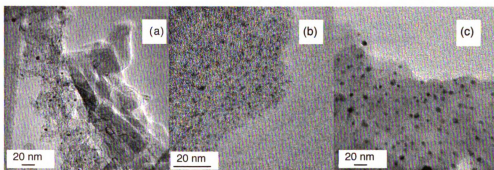
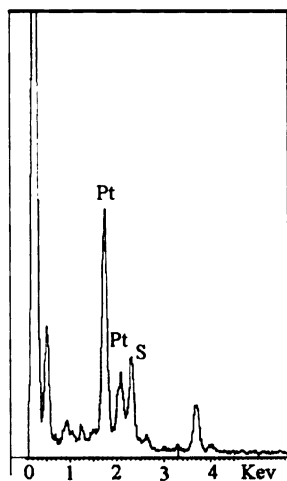


Figure 45. Transmission electron microscopy (TEM) images: (a) Pt-Re-S/C prepared from catalytic reduction and activated by reduction; (b) Pt-Re-S/C prepared by coimpregnation and activated by reduction; (c) Pt-S/C. (d) dark spots are the Pt particles.



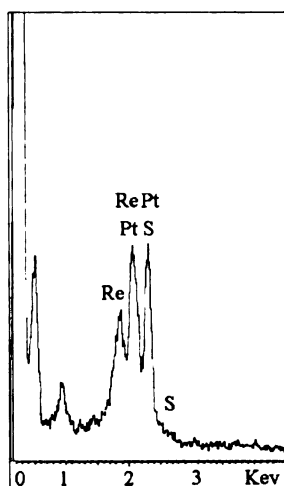
Spectrum processing :
 Peaks possibly omitted : 3.701, 4.018, 6.411 keV

Quantitation method : Cliff Lorimer thin ratio section.
 Processing option : All elements analyzed (Normalised)
 Number of iterations = 4

Standardless

Element	Weight%	Atomic%
S K	31.74	73.89
Pt L	68.26	26.11
Totals	100.00	

Figure 46. Elemental analysis of Pt-S/C.



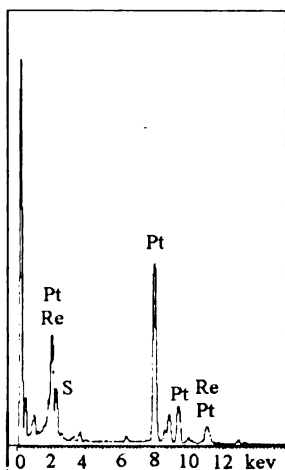
Spectrum processing :
 Peaks possibly omitted : 0.511, 0.933 keV

Quantitation method : Cliff Lorimer thin ratio section.
 Processing option : All elements analyzed (Normalised)
 Number of iterations = 3

Standardless

Element	Weight%	Atomic%
S K	18.66	57.95
Re L	22.43	11.99
Pt L	58.91	30.06
Totals	100.00	

Figure 47. Element analysis of Pt-Re-S/C (Table 16, entry 2).



Spectrum processing :
 Peaks possibly omitted : 3.313, 3.692, 6.402 keV

Quantitation method : Cliff Lorimer thin ratio section.
 Processing option : All elements analyzed (Normalised)
 Number of iterations = 3

Standardless

Element	Weight%	Atomic%
S K	11.88	44.85
Re L	16.81	10.93
Pt L	71.31	44.23
Totals	100.00	

Figure 48. Element analysis of Pt-Re-S/C (Table 16, entry 4).

3.3.1.2 Acetylation effect

To differentiate whether E_2 or S_N2 is the mechanism for the HDN using Pt-S/C under our reaction conditions. HDN of acetyl- α -amino- ϵ -caprolactam was examined with presulfided Pt catalyst (Figure 49). If E_2 is the mechanism, then since acetyl- α -amino group is supposed to be much better leaving group, a higher caprolactam yield should be expected. However, HDN of acetyl- α -amino- ϵ -caprolactam resulted in only 1% of caprolactam and most of starting material left. The result suggests that under our current reaction conditions it is not Hofmann elimination but rather S_N2 mechanism is the major contributor for the HDN reaction using carbon-supported Pt sulfide catalyst. However, this experiment can not rule out the possibility that coordination of amine with the vacant sites was lost due to the steric hindrance.

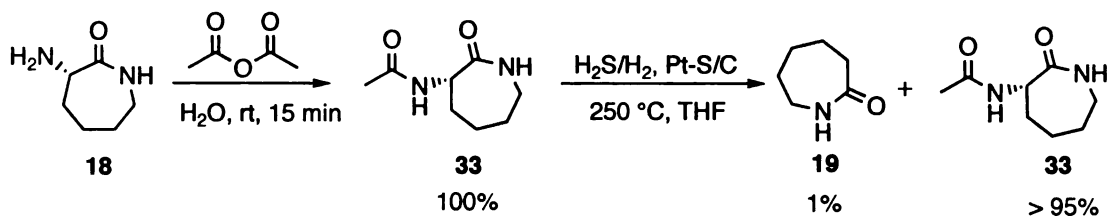


Figure 49. HDN of acetyl α -amino- ϵ -caprolactam

3.3.1.3. Comparison with other noble metals and Ni-Mo catalyst

With a reaction temperature, catalyst concentration, reaction time and solvent standardized (250 °C, 8 mol%, 8 h, and THF), attention was turned to use other carbon-supported noble metals (Ru (Table 31), Rh (Table 32), Pd (Table 33), Re (Table 34) and Ir (Table 35) and compared with the carbon-supported Ni-Mo catalyst (Table 36). HDN of α -amino- ϵ -caprolactam in THF were catalyzed by metal on carbon versus presulfided metal on carbon and use of H_2 versus $\text{H}_2\text{S}/\text{H}_2$ atmospheres (Table 31-Table 36). For all the metals examined, running the HDN with the catalyst under an initial $\text{H}_2\text{S}/\text{H}_2$ (20/80 psi) atmosphere gave higher yields of ϵ -caprolactam than use of strictly H_2 . This trend held irrespective of whether the catalyst had been presulfided. The highest HDN yields (Table 31-Table 36) were achieved when the catalyst was presulfided and run under initial $\text{H}_2\text{S}/\text{H}_2$ (20/80 psi) atmosphere. However, the highest yields were lower than the 65% yield of caprolactam achieved using presulfided Pt/C under an $\text{H}_2\text{S}/\text{H}_2$ (80/20 psi) atmosphere (Table 37, entry 4).

Table 31. Ru Hydrodenitrogenation

entry	catalyst (8 mol%)	temp (°C)	H ₂ S/H ₂ (psi/psi)	time (h)	caprolactam (% yield)
1	Ru/C	250	0/100	8	14
2	Ru/C	250	20/80	8	35
3	Ru-S/C	250	0/100	8	23
4	Ru-S/C	250	20/80	8	42

Table 32. Rh Hydrogenitrogenation

entry	catalyst (8 mol%)	temp (°C)	H ₂ S/H ₂ (psi/psi)	time (h)	caprolactam (% yield)
1	Rh/C	250	0/100	8	20
2	Rh/C	250	20/80	8	35
3	Rh-S/C	250	0/100	8	25
4	Rh-S/C	250	20/80	8	39

Table 33. Pd Hydrodenitrogenation

entry	catalyst (8 mol%)	temp (°C)	H ₂ S/H ₂ (psi/psi)	time (h)	caprolactam (% yield)
1	Pd/C	250	0/100	8	22
2	Pd/C	250	20/80	8	36
3	Pd-S/C	250	0/100	8	24
4	Pd-S/C	250	20/80	8	37

Table 34. Re Hydrodenitrogenation

entry	catalyst (8 mol%)	temp (°C)	H ₂ S/H ₂ (psi/psi)	time (h)	caprolactam (% yield)
1	Re/C	250	0/100	8	10
2	Re/C	250	20/80	8	16
3	Re-S/C	250	0/100	8	18
4	Re-S/C	250	20/80	8	26

Table 35. Ir Hydrodenitrogenation

entry	catalyst (8 mol%)	temp (°C)	H ₂ S/H ₂ (psi/psi)	time (h)	caprolactam (% yield)
1	Ir/C	250	0/100	8	3
2	Ir/C	250	20/80	8	13
3	Ir-S/C	250	0/100	8	18
4	Ir-S/C	250	20/80	8	33

Table 36. Ni-Mo Hydrodenitrogenation

entry	catalyst (8 mol%)	temp (°C)	H ₂ S/H ₂ (psi/psi)	time (h)	caprolactam (% yield)
1	Ni-Mo/C	250	0/100	8	6
2	Ni-Mo/C	250	20/80	8	22
3	Ni-Mo-S/C	250	0/100	8	13
4	Ni-Mo-S/C	250	20/80	8	35

Table 37. Pt Hydrodenitrogenation

entry	catalyst (8 mol%)	temp (°C)	H ₂ S/H ₂ (psi/psi)	time (h)	caprolactam (% yield)
1	Pt/C	250	0/100	8	19
2	Pt/C	250	20/80	8	24
3	Pt-S/C	250	0/100	8	34
4	Pt-S/C	250	20/80	8	65

3.4. Discussions

Hydrodenitrogenation of α -amino- ϵ -caprolactam has been examined thoroughly over supported Pt sulfide by varying solvents, temperatures, catalyst concentrations, H₂S/H₂ ratio etc, resulting in the highest caprolactam yield (65%) using presulfided Pt on carbon in a H₂S/H₂ (20/80 psi) atmosphere. With a reaction temperature, catalyst concentration, reaction time and solvent standardized (250 °C, 8 mol%, 8 h and THF), HDN activity of different carbon supported metal catalysts was compared (Ru, Rh, Pd, Re, Ir, and Ni-Mo). Hydrodenitrogenations were performed by the metal on carbon versus the presulfided metal on carbon and use of H₂ versus H₂S/H₂. For all the metals examined, H₂S/H₂ always gave higher caprolactam yields than use of straight H₂, no matter whether the catalyst had been presulfided or not.

To explain the beneficial effect of hydrogen sulfide and different HDN activities of the above transition metal sulfides, it is important to examine the detailed structure of the metal sulfide catalyst and possible mechanism for HDN of α -amino- ϵ -caprolactam. As mentioned before, the first step of the HDN mechanism requires the chemisorption of the amine on the vacancy sites of the transition metal sulfide catalysts. The second step that involves C-N bond cleavage depends on the nature of the catalyst. There are several species on the surface of the transition metal sulfides and the concentration of these species is related to the nature of the catalyst and also the reaction conditions (Figure 38). These species include (i) vacancy sites (ii) SH groups, and (iii) bridged S^{2-} and S_2^{2-} anions. The vacancy sites are electron deficient and can coordinate with the amines via the lone pair of electrons on the nitrogen atom. The role of SH is dependent on the strength of metal-sulfur bond. For example, a strong metal sulfur bond will weaken the S-H bond, resulting in a larger H^+ acidity. On the other hand, a weak metal sulfur bond will enforce the S-H bond and SH groups may act more as a nucleophile. According to Topsøe groups results,³⁸ it is predicted that the nucleophilic character of the SH group will increase from the sulfides of the elements on the left side of the periodic table to the right side noble metal sulfides while the acidity character will follow an opposite trend.

Thus the difference of HDN of the metal sulfides can be explained by their acidity or nucleophilic character. As mentioned before, the acidity of the metal sulfides will decrease from the left side of periodic table to the right, so the acidity of the second-row metals examined results in the following order: Ru sulfide > Rh sulfide > Pd sulfide. For the third row metals investigated, their nucleophilic character will increase from the left side to the right side, which means Pt sulfide is the most nucleophilic, followed by Ir

sulfide, and Re sulfide is the least nucleophilic. As shown from Tables 17 to 19, for the metals in the second row (Ru, Rh, Pd), the caprolactam yield sequence is in accordance with their acidity. The higher the acidity, the higher the caprolactam yield. Thus, for the second-row metals examined (Ru, Rh, Pd), Hofmann elimination may be the major mechanism. While for the third row metals (Ir, Re and Pt), the HDN activity sequence (Pt > Ir > Re) can be explained either by a E₂ or a S_N2 mechanism, depending on whether sulfhydryl group is acting as a nucleophile or a base. To differentiate between these two mechanisms (E₂ or S_N2), HDN of acetyl- α -amino- ϵ -caprolactam was examined with the presulfided Pt catalyst (Figure 49). If HDN is an E₂ mechanism and acetyl- α -amino group is a much better leaving group, a higher caprolactam yield should be expected. However, HDN of acetyl- α -amino- ϵ -caprolactam resulted in only 1% of caprolactam and most of starting material left. The result suggests that under our current reaction conditions it is not Hofmann elimination but rather an S_N2 mechanism is the major contributor for the HDN reaction using carbon-supported Pt sulfide catalyst. The weaker Pt-S bond leads to higher SH (nucleophile) concentration and thus higher HDN yields.

References

- 1 (a) Ho, T. C.; *Catal. Rev.-Sci. Eng.*, **1988**, *30*, 117. (b) Prins, R., "Handbook of Heterogeneous Catalysis", Vol 4, Wiley-VCH, Weinheim, 1997. (c) Laine, R. M.; *Catal. Rev.-Sci. Eng.*, **1983**, *25*, 459. (d) Startsev, A. N. *Catal. Rev.-Sci. Eng.*, **1995**, *37*, 353. (e) Delmon, B.; Froment, G. F.; *Catal. Rev.-Sci. Eng.*, **1996**, *38*, 69. (f) Schulz, H.; Schon, M.; Rahman. *Stud. Surf. Sci.* **1986**, *27*, 201.
- 2 Laine, R. M. *Catal. Rev.-Sci. Eng.*, **1983**, *25*, 459.
- 3 Ledoux, M. J.; Djellouli, B. *J. Catal.* **1989**, *115*, 580.
- 4 Vit, Z.; Zdrzil, M. *J. Catal.* **1989**, *119*, 1.
- 5 Eijsbouts, S.; de Beer, V. H. J.; Prins, R. *J. Catal.* **1988**, *109*, 217.
- 6 (a) Zhao, Y.; Kukula, P.; Prins, R. *J. Catal.* **2004**, *221*, 441. (b) Zhao, Y.; Prins, R. *J. Catal.* **2004**, *221*, 532. (c) Kukula, P.; Dulty, A.; Sivasankar, N.; Prins, R. *J. Catal.* **2005**, *236*, 14. (d) Cattenot, M.; Peeters, E.; Geantet, C.; Devers, E.; Zotin, J. L. *Catal. Lett.* **2005**, *99*, 171.
- 7 R. Prins, *Adv. Catal.* **2001**, *46*, 399.
- 8 Nelson, N.; Levy, R. B.; *J. Catal.* **1979**, *58*, 485.
- 9 (a) Porefaix, J. L.; Cattenot, M.; Guerriche, M.; Thivolle-Cazat, J.; Breysse, M. *Catal. Today* **1991**, *10*, 473. (b) Vivier, L.; Dominguez, V.; Perot, G.; Kasztelan, S.; *J. Mol. Catal.* **1991**, *67*, 267.
- 10 Hirschon, A. S.; Laine, R. M. *Fuel.* **1985**, *64*, 868.
- 11 Zhao, Y.; Prins, R. *J. Catal.* **2005**, *229*, 213.
- 12 (a) Zhao, Y.; Kukula, P.; Prins, R. *J. Catal.* **2004**, *221*, 441. (b) Oyama, S. T.; Lee, Y.; *J. Phys.Chem. B* **2005**, *109*, 2109. (c) Cattenot, M.; Portefaix, J. L.; Afonso, J.; Breysse, M.; Lacroix, M.; Perot, G. *J. Catal.* **1998**, *173*, 366.
- 13 Hadjiloizou, G. C.; Butt, J. B.; Dranoff, J. S. *Ind. Eng. Chem. Res.* **1992**, *3*, 2503.
- 14 Cattenot, M.; Portefaix, J. L.; Afonso, J.; Breysse, M.; Lacroix, M.; Perot, G. *J. Catal.* **1998**, *173*, 366.
- 15 Schwartz, V.; da Silva, V. T.; Oyama, T. *J. Mol. Catal. A.* **2000**, *163*, 251.

- 16 Cattenot, M.; Peeters, E.; Geantet, C.; Devers, E.; Zotin, J. L. *Catal. Lett.* **2005**, *99*, 171.
- 17 (a) Yang, S. H.; Satterfield, C. N. *Ind. Eng. Chem. Process Des. Dev.* **1984**, *23*, 20. (b) Kwart, H.; Katzer, J.; Horgan, J. J. *Phys.Chem.* **1982**, *86*, 2641.
- 18 (a) Perot, G. *Catal. Today* **1991**, *10*, 447. (b) Ren, S.; Wang, Z.; Hu, Y. *Ranliao Huaxue Xuebao* **1987**, *15*, 255.
- 19 PAÁL, Z.; Menon, P. G. *Catal. Rev.-Sci. Eng.*, **1983**, *25*, 229.
- 20 (a) Kalthod, D. G.; Weller, S. W., *J. Catal.* **1985**, *95*, 455. (b) Polz, J.; Zeilinger, H.; Muller, B.; Knozinger, H., *J. Catal.* **1989**, *120*, 22.
- 21 Hanlon, R. T. *Energy Fuel.* **1987**, *1*, 424.
- 22 (a) Vit, Z.; Zdrzil, M. *J.Catal.* **1989**, *119*, 1. (b) Eijsbouts, S.; De Beer, V. J. H.; Prins, R. *J.Catal.* **1988**, *109*, 217.
- 23 Hirschon, A.S.; Wilson Jr, R. B.; Laine, R. M., *Appl.Catal.* **1987**, *34*, 311.
- 24 Shabtai, J.; Guohe, Q.; Balusami, K.; Nag, N. K.; Massoth, F. E., *J. Catal.* **1988**, *113*, 206.
- 25 Harris, S.; Chianelli, R. R. *J. Catal.* **1986**, *98*, 17.
- 26 (a) Kluskdahl, H. E.; US Patent 3,415,737, 1968. (b) Jacobson, R. L.; Kluskdahl, H. E.; McCoy, C. S.; Davis, R. W; *Proc. Amer. Pet. Int. Div.* **1969**, *49*, 504.
- 27 Biswas, J.; Bickel, G. M.; Gary, P. G.; Do, D. D.; Barbier, J., *Catal. Rev.-Sci. Eng.*, **1988**, *30*, 161.
- 28 (a) Qu, L.; Prins, R.; *Appl.Catal. A* **2003**, *250*, 105. (b) Rana, M. S.; Sriniva, B. N.; Maity, S. K.; Murali Dhar, G.; Prasado Rao, T. S. R. *J. Catal.* **2000**, *195*, 31.
- 29 Ishihar, A.; Lee, J.; Dumeignil, F.; Yamaguchi, M.; Hirao, S.; Qian, E. W.; Kabe, T. *J. Catal.* **2004**, *224*, 243.
- 30 Ishihar, A.; Lee, J.; Dumeignil, F.; Yamaguchi, M.; Higashi, R.; Wang, A.; Qian, E. W.; Kabe, T. *J. Catal.* **2003**, *217*, 59.

- 31 Calafat, A.; Laine, J.; Lopez-Agudo, A.; Palacios, J.M. *J. Catal.* **1996**, *162*, 20.
- 32 Satterfield, C. N.; Carter, D. L. *Ind. Eng. Chem. Des. Dev.* **1981**, *20*, 538.
- 33 Gultekin, S.; Khaleeq, M.; Al-Saleh, M. A. *Ind. Eng. Chem. Res* **1989**, *28*, 729.
- 34 (a) Shum, V. K.; Butt, J. B.; Sachtler, W. M. H. *J. Catal.* **1985**, *96*, 371. (b) Parera, J. M.; Beltramini, J. N.; Querini, C. A.; Martinelli, E. E.; Churin, E. J.; Aloe, P. E.; Figoli, N. S. *J. Catal.* **1986**, *99*, 39. (c) Pieck, C. L.; Marecot, P.; Barbier, J. *Appl.Catal. A* **1996**, *145*, 323. (d) Augustine, S. M.; Alameddin, G. N.; Sachtler, W. M. H. *J. Catal.* **1989**, *115*, 217. (e) Biloen, P.; Helle, J. N.; Verbeek, H.; Dautzenberg, F.M.; Sachtler, W. M. H. *J. Catal.* **1980**, *63*, 112.
- 35 Pieck, C. L.; Gonzalez, M. B.; Parera, J. M. *Appl.Catal. A* **2001**, *205*, 305.
- 36 Pieck, C. L.; Marecot, P.; Barbier, J. *Appl.Catal. A* **1996**, *143*, 286.
- 37 Boudart, M.; Aldog, A.; Benson, J. E.; Dougharty, N. A.; Harking, G. G. *J. Catal.* **1966**, *6*, 92.
- 38 Nørskov, J. K.; Clausen, B. S.; Topsøe, H. *Catal. Lett.* **1992**, *13*, 1.

CHAPTER 4

DEAMINATION OF α -AMINO- ϵ -CAPROLACTAM WITH GOLD CATALYST

4.1. Overview

In Chapter 3, a fundamental understanding of the active sites and structure of transition metal sulfides and comparison of HDN activities of several transition metal sulfides indicate that the metal-sulfur bond strength plays a critical role in the HDN activity of those noble metal sulfides. It seems that the high HDN activity of the presulfided Pt catalyst is related with its weak Pt-S bond strength. It is well known that the Au-S bond strength is weaker than the Pt-S bond.¹ As discussed in the chapter 3, for the metal sulfide catalysts, weak metal-sulfur bond strength means that Au sulfide can be easily desulfurized to generate vacancy sites and sulfhydryl groups, which are known as active sites for hydrodenitrogenation reaction. Therefore, Au can be a better HDN catalyst than Pt. Recently a large number of papers have been published on Au catalyzed reactions and on the variables affecting the activity and mechanism have been studied in depth.² These studies stimulate our interest in exploring Au catalysts for HDN of α -amino- ϵ -caprolactam. With an aim of developing new suitable Au based catalysts for HDN reactions, a brief review of Au catalysts, especially important controlling factors will be presented, followed by syntheses of a series of Au catalysts on varying supports that were characterized by transmission electron microscopy (TEM).

4.2. Introduction

Gold has been long considered as catalytically inactive because bulk gold surfaces do not adsorb many molecules easily. However, this situation has been greatly changed with the discovery of the catalytic activity of highly dispersed Au catalysts.³ Supported Au particles have attracted increasing attention due to their unique catalytic properties and potential applications in many important chemical reactions. One milestone paper was published by Bond and coworkers in 1973 in which they demonstrated that an efficient hydrogenation of alkenes is possible at temperature as low as 100-217 °C using a supported gold catalyst.⁴ Largely through the efforts of Haruta and Hutchings,⁵ Au catalysts find wide applications in many other reactions such as selective propylene oxidation to propylene oxide, water gas shift reactions, NO reduction, selective hydrogenation of acetylene, oxidative-decomposition of amines and nucleophilic additions to π systems.⁶ Effects of gold in palladium catalysts on HDS activity have also been published.⁷ Au catalyzed HDN reactions have not been reported yet. One advantage of Au catalysts is their good selectivity in many reactions. For example, Corma's group showed that nitro compounds could be selectively reduced using supported Au catalyst in the presence of other reducible functional groups such as carbonyls group contrary to Pt and Pd catalysts.⁸

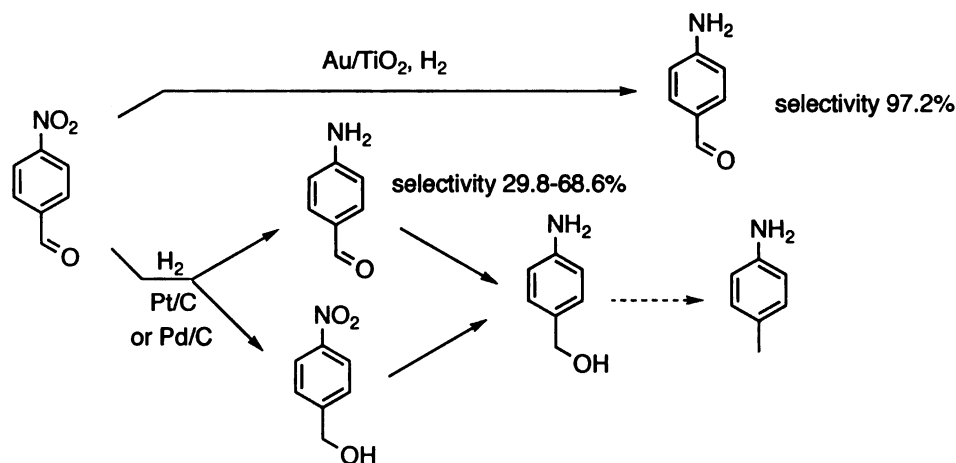


Figure 50. Chemoselective reduction of 4-nitrobenzaldehyde with Au/TiO₂.

The high selectivity of Au catalysts is very attractive and may provide a promising solution to improve the selectivity of HDN of α -amino- ϵ -caprolactam to caprolactam. To accomplish this goal, one has to understand at a fundamental level the major factors controlling Au catalytic activities. It is well known that the catalytic performance of Au catalysts is mainly determined by three major factors: the preparation methods,⁹ nature of the supports¹⁰ and size and dispersion of the Au particles.¹¹ A concise summary of Au surface adsorption, methods for preparation of highly dispersed Au catalyst and selection of catalyst supports will be introduced.

4.2.1. Adsorption on gold surface

Gold is inert towards most molecules. However, its surface reactivity changes significantly with surface structure. At room temperature only HCO_2H , H_2S and thiol compounds can adsorb on the smooth surface of Au. When defective surface structures are created through down sizing or scratching, the gold surface can adsorb many other molecules such as hexane, benzene, ether, ketones, H_2 , CO and O_2 . The strong affinity of

gold for sulfur is very interesting, which has been applied in molecular electronics and self-assembly and more relevant HDS reactions.¹² The formation of chemical bonds between sulfur and metal changes the electronic properties of the metal.¹³ Sulfur withdraws the electrons from the metal and reduces the electron density on the metals' surface, resulting in significant changes in the chemical and catalytic properties of these metal.¹³ For example, the electronic modifications caused by sulfur diminish the ability of these metals to adsorb small molecules (such as H₂, NO et al.). Studies of co-adsorption of both Au and S on the surfaces of different kinds of metals (Pt, Rh, Ru and Mo) show that repulsive interactions between Au and S limits the mobility of Au and thus changes the morphology of the Au on the surface of metals.¹³

Because of the bonding strength of adsorbents on the defective surface of Au is moderate and still weaker than that of Pd and Pt, Au catalysts are advantageous over other noble metal catalysts for the ability to elicit reactions at low temperature. As discussed before, for noble metal sulfide catalysts, weak metal-sulfur bond strength enhances reactivity. A Au sulfide can be more easily desulfurized to generate vacancy sites and sulfhydryl groups than Pt and Pd sulfide, which are known as active species for HDN reaction. So potentially Au can be a better HDN catalyst than Pt and Pd.

4.2.2 Preparation of Highly Dispersed Gold Catalysts

The catalytic performance of a Au catalyst depends greatly on the particle size. The particle sizes not only affects the catalyst activity but also the reaction selectivity. It is well accepted that the catalyst activity of supported Au catalysts increases as the mean particle sizes decreases. More interestingly, the reaction selectivity can also be adjusted by controlling of the gold particle size. For example, the main product in the reaction of

propylene oxidation changes from propylene oxide to propane when the mean gold particles size decreases from 2-3 nm to less than 2 nm (Figure 51).¹⁴

The size of Au particles can be tuned by careful control of the preparation conditions. Traditional impregnation method (IMP) and deposition-precipitation (DP) are

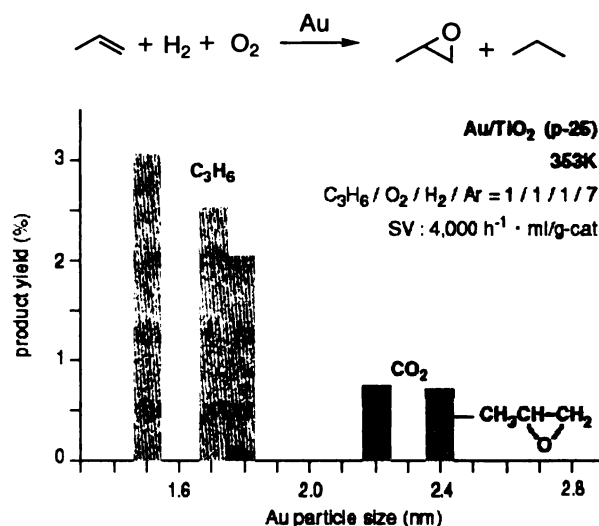


Figure 51. Product distribution of the oxidation of propylene over Au/TiO₂ as a function of Au particle size.

the most frequently applied preparative methods commonly using chloroauric acid (HAuCl₄) as the precursor. In IMP, a metal oxide (support) is immersed in an aqueous solution of HAuCl₄ and then water is evaporated to disperse HAuCl₄ crystallites over the support surface. The dried precursor is then calcined in air above 200 °C and then reduced in a H₂ atmosphere. In this case, the sizes of Au particle are often larger than 30 nm because the interaction of Au metal with the metal oxide support is weak and the remaining chloride on the support surfaces significantly promotes the aggregation of Au particles and results in larger Au particles. To overcome the disadvantages of IMP

method, many new techniques have been developed which can deposit Au nanoparticles on various types of metal oxides: Namely co-precipitation,¹⁵ DP,¹⁶ gas-phase grafting (GG)¹⁷ and the liquid phase grafting (LG).¹⁸ Currently, the most popular one is DP, which was first developed by Haruta and co-workers.¹⁹ In a standard DP procedure, as shown in Figure 52, the pH value of aqueous H₂AuCl₄ solution is adjusted to a fixed point in a range from 6-10 with NaOH. Careful control of the temperature (50 to 90 °C) and concentration of the aqueous H₂AuCl₄ solution (around 10⁻³ M) can lead to a selective deposition of Au(OH)₃ only on the surface of support metal oxides without precipitation in the liquid phase. With this method, it is possible to obtain small metal particles (2-3 nm), but the corresponding Au loading remains rather low (~3%). The DP method was further developed by both Geus and Louis groups.²⁰ Using urea (NH₂CONH₂) as the precipitating base allows the gradual and homogenous generation of gold hydroxide ions throughout the whole solution. Consequently the gold hydroxide concentration is always low because it is consumed almost as soon as it is formed, thus avoiding the precipitation of the metal hydroxide in solution. The other advantage of DP method is that it is easily scalable and can work with almost all supports.²¹ The method of deposition-precipitation with urea (DP urea) can afford small Au particles (2-3 nm) and get Au loading as high as 8% (wt).²⁰ Considering the advantages of the DP method, it was chosen to prepare most of our Au supported catalysts.

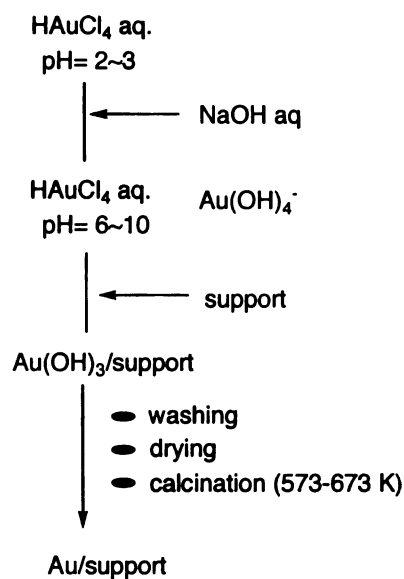


Figure 52. Flow chart of the deposition-precipitation method (DP).

4.2.3. Selection of suitable supports

Another important controlling factor for catalytic activity of Au catalysts is the metal oxide supports. The strong interaction between Au particles and support has been considered as the most important controlling factor to the catalytic performance of Au nanoparticles. For example, the reaction rate of CO oxidation over Au/TiO₂ and Pt/TiO₂ depends on the contact structure. Hemisphere Au particles (strongly bound with support) are more active than spherical Au particles (weakly bound with the support) by four orders of magnitude. The reaction rate (turnover frequencies) of the strongly attached hemispherical Au particles even exceeds that of Pt by one order of magnitude (Figure 53).²² This experiment indicated that the interface might act as active sites for the CO oxidation. This hypothesis was supported by the observation of activity enhancement by calcinations of Au colloids with TiO₂ at higher temperature.²³ Calcination at higher

temperature gives larger Au particles but stronger contact (observed by TEM), leading to higher catalytic activity.¹⁹

The periphery of the particle bound on the support has been the focus of the much of the mechanistic debate. Many investigators proposed that the interface between the small gold particles and the support, along with the availability of defect sites at this interface are probably the reaction zone.²⁴ Different oxidation states of Au (include Au (I) Au (III), Au (0)) have been claimed as the active species.²⁵ It's claimed that the perimeter interfaces contain those oxidic Au (I) and Au (III) species, which may be stabilized and recycled by interaction with metal oxide supports.²⁶

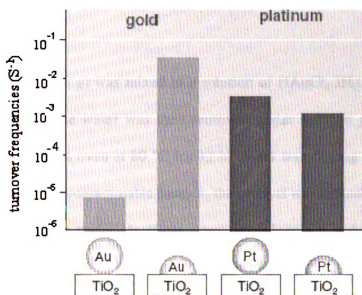


Figure 53. Turnover frequencies for CO oxidation with hemispherical and spherical Au and Pt catalyst supported on TiO₂.

Although the metal support interaction greatly influences the catalytic activity of the final catalysts, the exact mechanism how the different supports influence the activity is still under discussion.²⁷ Different reactions require different supports to gain the highest

activity. For example, Au supported on transition metal oxides such as Fe_2O_3 , TiO_2 , Co_3O_4 is very active for oxidation of CO. Co_3O_4 supported Au catalyst offers the highest yield for the complete oxidation of hydrocarbons. For reactions concerning the nitrogen-containing compounds, ferric oxide and nickel ferrites lead to the highest activity due to their good affinity to nitrogen. Al_2O_3 , MgO and TiO_2 work well as supports for the Au catalyzed conversion of NO to N_2 . With the above considerations, different metal oxide supports were examined in the preparation of our Au-based HDN catalysts.

4.3. Experimental

4.3.1 Catalyst preparation

a. Au-S/C preparation by IMP.

Activated carbon (4.18 g) was mixed in a solution of $\text{HAuCl}_4 \cdot 3\text{H}_2\text{O}$ (1.63 g) and heated at 90 °C for 1 h. The water was then removed under reduced pressure. The resulting solid was dried in an oven at 80 °C for 12 h. After transferring to a quartz U-tube reactor in a temperature programmable furnace, the catalyst was heated from rt to 130 °C (heating rate: 5 °C min^{-1}) under He (flow rate: 100 mL min^{-1}) and heated at this temperature for 1 h. The gas entering the quartz U-tube reactor was switched to $\text{H}_2\text{S}/\text{H}_2$ (10:90) (flow rate: 80 mL min^{-1}) and the temperature increased to 400 °C (heating rate: 5 °C min^{-1}) and held at 400 °C for 2 h. The reactor was subsequently cooled to rt under He (flow rate: 80 mL min^{-1}) and the sulfided catalyst (Au-S/C) stored under Ar. During the presulfiding process, the gas outlet of the quartz U-tube reactor was bubbled through a bleach solution to quench the H_2S in a fume hood.

b. Au/TiO₂ preparation by DP

TiO₂ (6 g) was suspended in a 600 mL solution of HAuCl₄·3H₂O (1 g) and urea (15.12 g). The mixture was heated at 80 °C for 4 h under stirring (final pH = 8) and allowed to cool to rt. The precipitate was centrifuged (15000 g, 10 min), decanted and washed thoroughly with water (600 mL). This water washing, centrifugation, decanting process was repeated 4 times. The washed mixture of HAuCl₄ and TiO₂ was dried under vacuum at 100 °C for 2 h and transferred to a quartz U-tube reactor in a temperature programmable furnace and heated from rt to 100 °C (heating rate: 2 °C min⁻¹) under He (flow rate: 80 mL min⁻¹). The gas was then switched to H₂ (flow rate: 80 mL min⁻¹) and the temperature increased to 300 °C (heating rate: 2 °C min⁻¹) and held at 300 °C for 2 h. The reactor was cooled to rt under He (flow rate: 100 mL min⁻¹) and the reduced catalyst (Au/TiO₂) stored under Ar.

c. Au-S/NiO preparation by DP

The NiO support (6 g, 80 mmol) was added to a 600 mL aqueous solution of HAuCl₄·3H₂O (1 g, 2.52 mmol) and urea (15.12 g, 252 mmol). The suspension was vigorously stirred at 80 °C for 4 h resulting in the solution changing from pH 2 to pH 8. The mixture of HAuCl₄ and NiO was recovered by centrifugation (15000 g for 10 min), resuspended in 600 mL water, and centrifuged again. This water wash followed by centrifugation was repeated 4 times. The washed mixture of HAuCl₄ and NiO was dried under vacuum at 100 °C for 2 h and transferred to a quartz U-tube reactor in a temperature programmable furnace and heated from rt to 100 °C (heating rate: 2 °C min⁻¹) under He

(flow rate: 80 mL min⁻¹). The gas was then switched to H₂S/H₂ (10:90) (flow rate: 80 mL min⁻¹) and the temperature increased to 300 °C (heating rate: 2 °C min⁻¹) and held at 300 °C for 2 h. The reactor was cooled to rt under He (flow rate: 100 mL min⁻¹) and the sulfided catalyst (Au-S/NiO) stored under Ar away from light in a dessicator. During the presulfiding process, the gas outlet of the quartz U-tube reactor was bubbled through a bleach solution to quench the H₂S in a fume hood.

4.3.2. Catalyst characterization by transmission electron microscopy

TEM measurements were performed using a JEOL 2200FS operated at 200 kV. The sample was mounted on a carbon-supported copper grid by placing a few droplets of a suspension of the ground sample in THF on the grid, followed by drying under ambient conditions, all in a N₂ atmosphere. The samples were transferred to the microscope in a sealed plate under Ar. At least 5 representative micrographs were taken for each catalyst.

4.4. Results

4.4.1. Preliminary results

Since TiO₂ is the most thoroughly studied support for Au catalysts and activated carbon gave the highest HDN activity for our presulfided Pt catalysts, HDN of α -amino- ϵ -caprolactam started using Au/TiO₂ and Au/C. For comparison, carbon-supported Au catalysts were prepared using the IMP method while TiO₂-supported Au catalysts were prepared from the DP method. Those catalysts were characterized by transmission electron microscopy (TEM). For regular TEM, the darker the spots are the denser element, in our case, Au. On the contrary, for the bright field TEM, the bright spots are

the Au particles. From the TEM images (Figure 54), the size of Au particle (dark spots) from IMP (20 nm-50 nm) is much larger than that from DP method (about 10 nm), which is consistent with the literature.

Hydrodenitrations of α -amino- ϵ -caprolactam to caprolactam using carbon-supported Au catalyst were examined and the highest caprolactam yield (40%) was observed when Au was presulfided and run under a $\text{H}_2\text{S}/\text{H}_2$ (20/80 psi) atmosphere (Table 38, entry 2). For comparison, HDN of α -amino- ϵ -caprolactam were conducted using Au on TiO_2 . HDN reaction rate was high but unfortunately low caprolactam yields were observed using Au on TiO_2 (Table 38, entries 3 and 4). A 24% caprolactam yield was offered after reaction with Au/ TiO_2 for 2 h and extension of the reaction time resulted in significant reduction of the reaction yield (Table 1, entry 3 vs entry 4). It seems that caprolactam is unstable in the presence of TiO_2 supported Au catalyst. To examine the effect of the support, a control reaction was conducted with only support TiO_2 and no Au (Table 38, entry 1). All starting material was consumed after 8 h to give only 6% desired product. This result confirmed that TiO_2 is not the superior support for HDN of α -amino- ϵ -caprolactam.

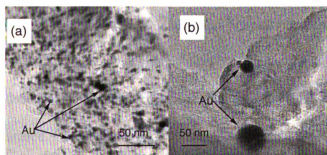
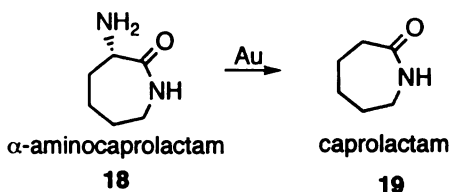


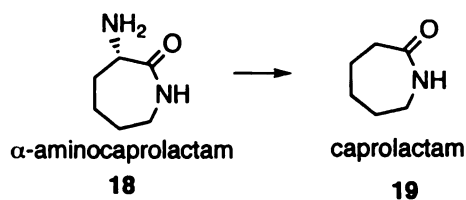
Figure 54. Transmission Electron Microscopy (TEM) images of Au catalyst. (a) Au/ TiO_2 prepared from deposition-precipitation method (DP). (b) Au-S/C prepared from impregnation method. (c) dark spots are the Au particles.

Table 38. Preliminary results of HDN with Au catalyst.

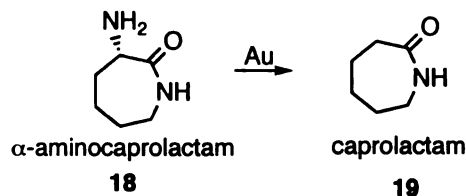
entry	catalyst (8 mol%)	temp (°C)	H ₂ S/H ₂ (psi/psi)	time (h)	yields (% 19/18)
1	Au/C	250	0/100	8	6/0
2	Au-S/C	250	20/80	8	40/0
3	Au/TiO ₂	250	20/80	2	24/25
4	Au/TiO ₂	250	20/80	4	15/0

4.4.2. Screening of supports

Given the importance of the supports for Au catalysts, the effects on HDN activity were examined (Table 2). Those supports effective for nitrogen-containing reactions (decomposition of amines, reduction of NO) or most thoroughly studied are chosen. Control reactions were conducted in our standard reaction conditions (250 °C, H₂S/H₂, 20/80 psi, THF). Among the supports screened (TiO₂, Fe₂O₃, Co₃O₄, NiO, CuO, MgO), NiO, Fe₂O₃ and Co₃O₄ gave higher caprolactam yield, probably due to their high affinity to amines. NiO by itself was capable of catalyzing the HDN and gave a moderate 15% yield with 30% starting material left (Table 39, entry 4). Similar caprolactam yields were obtained with Fe₂O₃ and Co₃O₄ (Table 39, entries 2 and 3). Au catalysts supported on the above three metal oxides were prepared from DP method and HDN of α -amino- ϵ -caprolactam were performed under our standard reaction conditions (250 °C, H₂S/H₂, 20/80 psi, THF) (Table 40). Surprisingly, addition of Au on those metal oxides did not result in noticeable improvement of caprolactam yields (Table 3).

Table 39. Screening of supports

entry	support	temp (°C)	H ₂ S /H ₂ (psi/psi)	reaction (h)	yields (% 19/18)
1	TiO ₂	250	20/80	8	5/0
2	Fe ₂ O ₃	250	20/80	8	18/20
3	Co ₃ O ₄	250	20/80	8	15/5
4	NiO	250	20/80	8	15/30
5	CuO	250	20/80	8	4/3
6	MgO	250	20/80	8	9/13

Table 40. HDN with Au supported on metal oxides.

entry	catalyst (8 mol%)	temp (°C)	H ₂ S/H ₂ (psi/psi)	time (h)	yields (% 19/18)
1	Au/Fe ₂ O ₃	250	20/80	8	17/20
2	Au/Co ₃ O ₄	250	20/80	8	15/30
3	Au/NiO	250	20/80	8	14/40

TEM images of Au catalysts supported on Fe₂O₃, Co₃O₄ and NiO show that Au is well dispersed on those supports but the size of Au particles is up to 10-20 nm (Figure 55). It is well known that Au catalysts are not active until they are small enough (5-10 nm). This may explain why addition of Au failed to improve the HDN activity (Table 40).

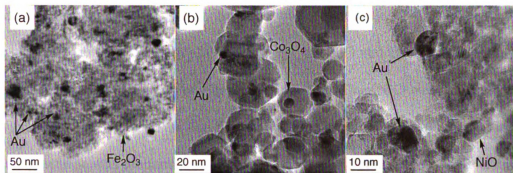


Figure 55. Transmission electron microscopy (TEM) images of Au catalysts. (a) Au/Fe₂O₃-DP. (b) Au/Co₃O₄-DP. (c) Au/NiO-DP.

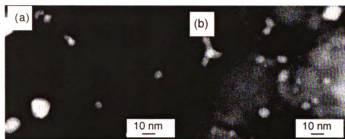


Figure 56. Dark field transmission electron microscopy (TEM) images of Au catalysts. (a) Au/Fe₂O₃-DP. (b) Au/Co₃O₄-DP.

4.4.3. Effect of presulfidation

Our previous experience indicated that presulfidation of transition metals has beneficial effect to the HDN reactions of α -amino- ϵ -caprolactam. A promotion effect of sulfur on Au catalysts has also been observed by Bailie et al.²⁸ In light of this, Au supported on Fe₂O₃, Co₃O₄ and NiO were prepared by a DP method and presulfidated at 300 °C for 2 h in a H₂S/H₂ (10:90) atmosphere and their HDN activities were compared (Table 4). Interestingly, both activity and selectivity had been improved by the presulfidation (except for Fe₂O₃). Co₃O₄-supported Au sulfide gave the highest reaction

rate and caprolactam yield (Table 4, entry 2) while presulfided NiO-supported Au catalyst afforded the best selectivity (Table 4, entry 3). NiO and Co_3O_4 are superior to Fe_2O_3 as supports, and NiO is slightly better than Co_3O_4 . Thus NiO was chosen as the primary support for Au catalyst for further optimization. For comparison, NiO-supported Pt sulfide was prepared and examined in the same conditions (Table 4, entry 4). Presulfided Au actually showed better selectivity than Pt (Table 4, entry 3 vs entry 4). However, low conversion of starting material was encountered for NiO supported Au catalyst. Only 40% of starting material was converted after 8 h reaction at 250 °C (Table 4, entry 3).

Comparison of TEM images shows that the presulfidation significantly decreases the Au particle on all three supports (Figure 6 vs Figure 8). However, the particle size distributions are quite different. Fe_2O_3 gave the largest Au particles (about 10 nm), followed by NiO (5-10 nm) and Co_3O_4 (2-5 nm). The caprolactam yields increased with the decrease of particle size (Table 4 and Figure 8). But the particle size alone can not explain the better selectivity of NiO supported Au sulfide than that of Co_3O_4 . It seems that the electronic structure differences between supports can play a role in the Au catalytic activity. The low conversion was possibly due to the competition adsorption of H_2S on the Au catalyst active sites or the strong interaction between support and α -amino- ϵ -caprolactam, which slow down the turnover frequencies of the reaction.

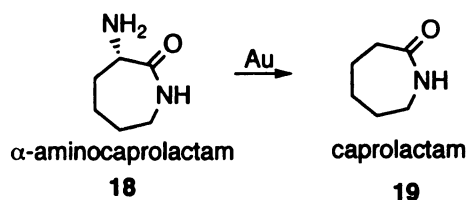
3	Au-S/NiO	250	20/80	8	20/60
4	Pt-S/NiO	250	20/80	8	21/46

4.4.4. Optimization HDN conditions using Au-S/NiO

4.4.4.1 Reaction temperature

To improve the conversion of presulfided Au on NiO (Au-S/NiO), the hydrodenitrogenation temperature was increased while presulfided Au catalyst, reaction time, and the H₂S/H₂ atmosphere were kept constant (Table 5). Caprolactam yield increased from 20% to 54% when the reaction temperature was increased from 250 °C to 300 °C (Table 5). This led to 300 °C (Table 5, entry 6) being used as the routine hydrodenitrogenation reaction temperature for presulfided Au catalyst.

Table 42. Optimization of Temperature



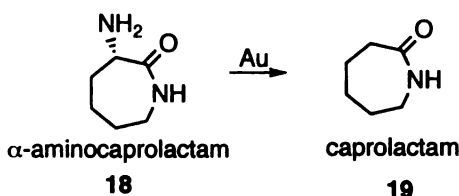
entry	catalyst (8 mol%)	temp (°C)	H ₂ S/H ₂ (psi/psi)	time (h)	caprolactam (% yield)
1	Au-S/NiO	250	20/80	4	20 ^a
2	Au-S/NiO	260	20/80	4	37
3	Au-S/NiO	270	20/80	4	44
4	Au-S/NiO	280	20/80	4	47
5	Au-S/NiO	290	20/80	4	48
6	Au-S/NiO	300	20/80	4	54
7	Au-S/NiO	320	20/80	4	47

(a) 60% α-amino-ε-caprolactam was left.

4.4.4.2 Reaction time

While presulfided Au catalyst, reaction temperature and the H₂S/H₂ atmosphere were kept constant, reaction time was varied. 4 h was confirmed to be the optimal reaction time (Table 6, entry 3). Further extension of reaction time after 4 h led to significant reduction of caprolactam yield (Table 6, entry 4). This indicated that caprolactam is not stable at these prolonged reaction conditions.

Table 43. Optimization of reaction time



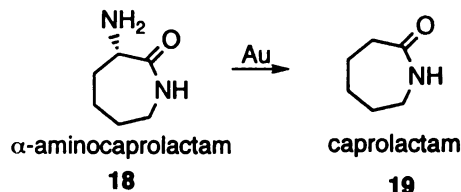
entry	catalyst (8 mol%)	temp (°C)	H ₂ S/H ₂ (psi/psi)	time (h)	caprolactam (% yield)
1	Au-S/NiO	300	20/80	1	25
2	Au-S/NiO	300	20/80	2	40
3	Au-S/NiO	300	20/80	4	54
4	Au-S/NiO	300	20/80	8	37

4.4.4.3 Effect of H₂S/H₂ ratio

As mentioned in the previous chapter, changing the H₂S/H₂ ratio will change the distribution of the vacancy sites and SH groups on the surface of the transition metal sulfides, thus changing the rate of the HDN. Based on this consideration, HDN of α -amino- ϵ -caprolactam using Au-S/NiO catalyst were performed in the different H₂S/H₂ ratios and results were summarized in (Table 44). The caprolactam yield first increased with the increase of the H₂S concentration until it reached the highest yield at 40% H₂S

and then the caprolactam yield started to slowly decrease with further increase of the H₂S concentration.

Table 44. Optimization of H₂S concentration



entry	catalyst (8 mol%)	temp (°C)	H ₂ S/H ₂ (psi/psi)	time (h)	caprolactam (% yield)
1	Au-S/NiO	300	0/100	4	20
2	Au-S/NiO	300	5/95	4	28
3	Au-S/NiO	300	10/90	4	45
4	Au-S/NiO	300	20/80	4	54
5	Au-S/NiO	300	40/60	4	59
6	Au-S/NiO	300	60/40	4	54
7	Au-S/NiO	300	80/20	4	53
8	Au-S/NiO	300	100/0	4	45

4.4.4.4 Effect of presulfidation temperature

Particle size of supported gold catalysts can affect the reaction selectivity. Bailie and coworkers have reported that Au/ZnO are highly selective for the formation of crotyl alcohol through the hydrogenation of crotonaldehyde and the selectivity for crotyl alcohol increased as the Au particle size increased.²⁸ This effect was demonstrated by increasing the calcination temperature of Au/ZnO from 250 to 400 °C and the crotyl alcohol selectivity increased dramatically. To examine the effect of particle sizes for the HDN reaction selectivity, Au catalyst precursors from the same batch were carefully presulfided under different temperatures from 250 to 400°C. HDN reactions were conducted in our standard reaction conditions for Au-S/NiO (Table 45). From the results shown in Table 8, increasing the presulfidation temperature slightly increased the caprolactam yield. TEM

images (Figures 10-12) show that increasing presulfidation temperature increased the number of large particles (5-10 nm) but there are still a large amount of small Au particles (in the range of 2-5 nm). At this stage, because of the coexistence of both large and small Au particles, it is still hard to conclude whether Au particle size will affect the HDN reaction selectivity or not. To elucidate whether large Au particle size or small Au particle size is responsible for the high HDN selectivity, a new preparation method that can give narrow distributions of Au particle sizes is needed.

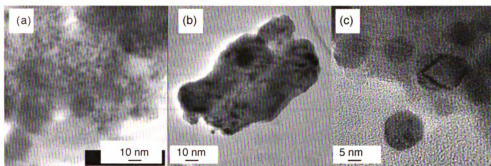


Figure 59. Transmission electron microscopy (TEM) images: (a) unsulfided material; (b) presulfided at 250 °C; (c) presulfided at 250 °C.

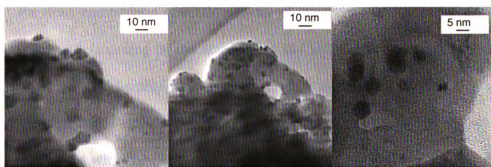


Figure 60. Transmission electron microscopy (TEM) images: presulfided at 300 °C.

good reaction selectivity in many reactions. These studies stimulated our interest in exploring Au as potential new catalysts for HDN of α -amino- ϵ -caprolactam.

HDN reactivity of Au nanoparticles deposited on the most thoroughly studied TiO_2 synthesized from a DP method was compared with Au on carbon obtained by the conventional IMP method. Au-S/C gave a reasonably good caprolactam yield in our standard reaction conditions while a relatively lower yield was observed when Au/ TiO_2 was applied (Table 38). Physical property analysis by transmission electron spectroscopy (TEM) shows that the Au particle size on TiO_2 prepared by the DP method is smaller than that of carbon-supported Au particle size prepared by the IMP method (Figure 54). It is well accepted that the Au catalytic activity increases with the decrease of the Au particle size. The poorer caprolactam yield with smaller Au particle on TiO_2 should not be accounted for only by the particle size. Alternatively, a support effect may better explain the yield difference. Thus, a control reaction of support TiO_2 and α -amino- ϵ -caprolactam was conducted, which demonstrated that α -amino- ϵ -caprolactam is not stable in the presence of TiO_2 (Table 39). Considering the importance of the support for Au catalysts, a series of metal oxides were examined under our standard reaction conditions (Table 39). Fe_2O_3 , Co_3O_4 and NiO stood out for their relative higher HDN activity and were chosen for further exploration. Au catalysts supported on those three supports were prepared and their HDN activities were compared. Surprisingly, deposition of Au on those supports did not result in much improvement of the caprolactam yield (Table 40). TEM images of those Au particles show that those Au particles are too large (10-20 nm) to be catalytically active (Figure 55). These results certainly indicated the HDN activity of Au catalysts depends on the Au particle size. Because the melting point of Au is much lower than Pt

and Pd (Au:1336 K, Pd:1823 K, Pt:2042 K) and the melting point of Au particles with a diameter of 2 nm is lowered to about 573 K due to the quantum-size effect.²⁹ Thus small Au particles tend to aggregate more easily than Pt and Pd at temperature above 573 K during the calcinations procedure.²⁹ This aggregation problem can be alleviated by presulfidation. Presulfidation of the supported Au catalysts inhibited the coagulation of Au particles and significantly decreased the particle size (Figure 57 vs Figure 55). The effect of presulfidation can be explained by the repulsive interaction between Au and sulfur that diminishes the mobility of Au particles, which has been reported in the literature.¹³ As shown in Table 41, presulfidation of the Au catalyst did significantly improve the HDN reaction selectivity. Comparing the HDN activity of presulfided Au supported on Fe₂O₃, Co₃O₄ and NiO shows that Co₃O₄ and NiO are superior to Fe₂O₃ as support, with NiO slightly better than Co₃O₄. Thus NiO was chosen as the primary support for presulfided Au catalyst for the further optimization. Optimization of reaction condition by varying reaction temperatures, reaction time and H₂S/H₂ ratio led to a 59% caprolactam yield (Table 44), which is similar with the highest caprolactam obtained using Pt-S/C.

It has also been demonstrated that the selectivity of Au-catalyzed hydrogenations can be enhanced by increasing the Au particle size as a result of changing the calcination temperature from 250 °C to 400 °C.²⁸ To test the effect of the Au particle size, Au catalyst precursors from the same batch were carefully presulfidated at different temperatures from 250 °C to 400 °C. The effect was less pronounced than expected, only resulting in a slightly higher caprolactam yield. This is consistent with the small difference in Au particle sizes from different presulfidation temperatures according to their TEM images

(Figure 59 to Figure 61). It is probably due to the repulsive interaction between Au and sulfur that keeps the Au particles from aggregating in the range of the temperature examined (250-400 °C). One possible solution to this problem is to first calcinate the catalyst precursors at different temperatures (to eliminate the effect of sulfur) and then followed by presulfidation.

In summary, we have shown that a series of gold catalysts for HDN of α -amino- ϵ -caprolactam can be synthesized via the DP method. A detailed study has been carried out for the presulfided Au/NiO, which shows good HDN activity and reproducibility. This catalyst is also stable upon storage and good stability under optimized reaction conditions. The HDN activity of Au catalysts depends greatly on supports and the Au particle size. Presulfidation of Au catalysts can significantly decrease the particle size of Au catalyst and increase HDN selectivity.

Right now, our Au catalyzed HDN reaction still requires quite high reaction temperature, which may be the major reason for the yield loss. Further decreasing the Au particle size is a possible way to increase the HDN reaction selectivity. With our DP method, it is difficult to obtain very small Au particle while keeping the high Au loading. To improve the HDN reaction selectivity, an efficient method to prepare size-controllable small Au particle (about 2 nm) is highly desirable. Potentially, small Au particles will make it possible to run the reaction at much lower temperature and offers higher HDN selectivity.

References

- 1 Chianelli, R. R.; Berhault, G.; Raybaud, P.; Kasztelan, S.; Hafner, J.; Toulhaot, H. *Appl. Catal. A: Gen.* **2002**, *227*, 83.
- 2 (a) Haruta, M. *CATTECH*, **2002**, *6*, 102. (b) Haruta, M.; Date, M. *Appl. Catal. A: Gen.* **2001**, *222*, 427.
- 3 Haruta, M.; Kobayashi, T.; Sano, H.; Yamada, N. *Chem. Lett.* **1987**, *2*, 405.
- 4 Bond, G. C.; Sermon, P. A.; Webb, G. Buchanan, D. A.; Wells, P. B. *J. Chem. Soc. Chem. Commun.* **1973**, 444.
- 5 (a) Haruta, M. *Nature* **2005**, *437*, 1098. (b) Hutchings, G. J. *Catal. Today* **2005**, *100*, 1647.
- 6 (a) Valden, M.; Lai, X.; Goodman, D. W.; *Science* **1998**, *281*, 1647. (b) Min, B. K.; Wallace, W. T.; Santra, A. K.; Goodman, D. W. *J. Phys. Chem. B.* **2004**, *108*, 16339. (c) (b) Min, B. K.; Wallace, W. T.; Santra, A. K.; Goodman, D. W. *J. Phys. Chem. B.* **2004**, *108*, 14609. (d) Chen, M. S.; Goodman, D. W.; *Science* **2004**, *306*, 252. (e) Haruta, M.; Ueda, A.; Tsubota, S.; Torres Sanchez, R. M. *Catal. Today*, **1996**, *29*, 443. (f) Haruta, M. *Catal. Today* **1997**, *36*, 153. (h) Ito, Y.; Sawamura, M.; Hayashi, T. *J. Chem. Soc.* **1986**, *108*, 6405. (i) Fukuda, Y.; Utimoto, K. *J. Org. Chem.* **1991**, *56*, 3729. (g) Teles, J. H.; Brode, S.; Chabanas, M.; *Angew. Chem. Int. Ed.* **1998**, *37*, 1415.
- 7 (a) Venezia, A. M.; Parola, V. L.; Nicoli, V.; Deganello, G. *J. Catal.* **2002**, *212*, 56. (b) Venezia, A. M.; Parola, V. L.; Deganello, G.; Pawlec, B.; Fierro, J. L. G. *J. Catal.* **2003**, *215*, 317.
- 8 Corma, A.; Serna, P. *Science* **2006**, *313*, 332.
- 9 (a) Wolf, A.; Schuth, F. *Appl. Catal. A* **2002**, *226*, 1. (b) Park, E. D.; Lee, J.S.; *J. Catal.* **1999**, *186*, 1.
- 10 (a) Schubert, M. M.; Hackenberg, S.; Van Veen, A. C.; Muhler, M.; Plzak, V.; Behm, R. J. *J. Catal.* **2001**, *197*, 113. (b) Weiher, N.; Bus, E.; Delannoy, L.; Louis, C.; Ramaker, D. E.; Miller, J. T.; Bokhoven, J. A. *J. Catal.* **2006**, *240*, 100. (c) Comotti, M.; Li, W-C.; Spliethoff, B.; Schuth, F. *J. Am. Chem. Soc.* **2006**, *128*, 917. (d) Overbury, S. H.; Ortiz-Soto, L.; Zhu, H-G.; Lee, B.; Amiridis, M. D; Dai, S. *Catal. Lett.* **2004**, *95*, 99. (e) Olea, M.; Iwasawa, Y. *Appl. Catal. A.* **2004**, *275*, 35.

- 11 (a) Haruta, M. *CATTECH*, **2002**, *6*, 102. (b) Haruta, M.; Date, M. *Appl. Catal. A: Gen.* **2001**, *222*, 427.
- 12 (a) Widrig, C. A.; Alves, C. A.; Porter, M. D.; *J. Am. Chem. Soc.* **1991**, *113*, 2805. (b) Bond, G. C.; Thompson, D. T.; *Catal. Rev.-Sci. Eng.* **1999**, *41*, 319. (c) Johannsson, A.; Stafstrom, S. *Chem. Phys. Lett.* **2000**, *322*, 301.
- 13 (a) Rodriguez, J. A.; Kuhn, M.; Hrbek, J. *Chem. Phys. Lett.* **1996**, *251*, 13. (b) Rodriguez, J. A.; Chaturvedi, S.; Jirsak, T. *Chem. Phys. Lett.* **1998**, *296*, 421. (c) Rodriguez, J. A.; Kuhn, M.; Hrbek, J. *J. Phys. Chem.* **1996**, *100*, 3799.
- 14 Hayashi, T.; Tanaka, K.; Haruta, M. *J. Catal.* **1998**, *178*, 566.
- 15 Haruta, M.; Yamada, N.; Kobayashi, T.; Iijima, S. *J. Catal.* **1989**, *115*, 301.
- 16 Tsubota, S.; Haruta, M.; Kobayashi, T.; Ueda, H.; Nakahara, Y.; *Stud. Surf. Sci. Catal.* **1991**, *63*, 695.
- 17 Okumura, M.; Tsubota, S.; Iwamoto, M.; Haruta, M. *Chem, Lett*, **1998**, 315.
- 18 Okumura, M.; Haruta, M. *Chem, Lett*, **2000**, 396.
- 19 Tsubota, S.; Haruta, M.; Kobayashi, T.; Ueda, A.; Nakahara, Y. *Stud. Surf. Sci. Catal.* **1991**, *63*, 695.
- 20 (a) Hermans, L. A. M.; Genus, J. W. *Stud. Surf. Sci. Catal.* **1979**, *4*, 113. (b) Zanella, R.; Giorgio, S.; Henry, C. R.; Louis, C. *J. Phys. Chem. B.* **2002**, *106*, 7634. (c) Burattin, P.; Che, M.; Louis, C. *J. Phys. Chem. B.* **2000**, *104*, 10482. (d) Burattin, P.; Che, M.; Louis, C. *J. Phys. Chem. B.* **1999**, *103*, 6171. (e) Burattin, P.; Che, M.; Louis, C. *J. Phys. Chem. B.* **1997**, *101*, 7060.
- 21 Khoudiakov, M.; Gupta, M. C.; Deevi, S. *Appl. Catal. A* **2005**, *291*, 151.
- 22 Bamwenda, G. R.; Tsubota, S.; Nakamura, T.; Haruta, M. *Catal, Lett*, **1997**, *44*, 83.
- 23 Tsubota, S.; Nakamura, T.; Tanak, K.; Haruta, M. *Catal, Lett*, **1998**, *56*, 131.

- 24 (a) Davis, R. J. *Science* **2003**, *301*, 926. (b) Chen, M. S.; Goodman, D. W. *Science* **2004**, *306*, 252. (c) Chen, M. S.; Goodman, D. W. *Catal. Today* **2006**, *111*, 22.
- 25 (a) Haruta, M. *Gold Bull.* **2004**, *37*, 27. (b) Sinha, A. K.; Seelan, S.; Tsubota, S.; Haruta, M. *Angew. Chem. Int. Ed.* **2004**, *43*, 1546. (c) Chen, M. S.; Goodman, D. W. *Catal. Today* **2006**, *111*, 22. (d) Daniells, S. T.; Overweg, A. R.; Makkee, M. Moulijin, J. A. *J. Catal.* **2005**, *230*, 52.
- 26 (a) Daniells, S. T.; Overweg, A. R.; Makkee, M.; Moulijin, J. A. *J. Catal.* **2005**, *230*, 52. (b) Hutchings G. J.; Hall, M. S.; Carley, A. F.; Landon, P.; Solsona, B. E.; Kiely, C. J.; Herzing, A.; Makkee, J. Moulijin, J.; Overweg, A.; Carolos Fierro-Gonzalez, J.; Guzman, J.; Gates, B.C.; *J. Catal.* **2006**, *242*, 71.
- 27 Comotti, M.; Li, W-C.; Spliethoff, B.; Schuth, F. *J. Chem. Am. Soc.* **2006**, *128*, 917.
- 28 (a) Beilie, J. E.; Hutchings, G. J. *Chem Commun.* **1999**, 2151. (b) Beilie, J. E.; Abdullah, H. A.; Anderson, J. A.; Rochester, C. H.; Richardson, N. V.; Hodge, N.; Zhang, J-G.; Burrows, A.; Kiely, C. J.; Hutchings, G. J. *Phys. Chem. Chem. Phys.* **2001**, *3*, 4113.
- 29 Buffet, Ph.; Borel, J-P. *Phys. Rev. A*, **1976**, *13*, 2287.

CHAPTER 5

Experimental

General chemistry

All reactions sensitive to air and moisture were carried out in oven and/or flame dried glassware under positive argon pressure. Air or moisture sensitive reagents and solvents were transferred to reaction flasks fitted with rubber septa via syringes. Solvents were removed using either a Büchi rotary evaporator at water aspirator pressure or under high vacuum (0.5 mm Hg).

A LAB-LINE HEET-CAB oven (Model No. 3515) was used for drying catalyst at constant temperature. The quartz U-tube reactor was situated inside of a temperature programmable Barnstead Thermolyne Furnace (Model No F6020C). Hydrodenitrations employed a Parr 4575 high-pressure reactor and a Parr 4842 controller, which controls the temperature and stirring rate. To determine the concentration of pipercolinic acid, α -amino- ϵ -caprolactam and caprolactam, crude residue concentrate was dissolved in D₂O, concentrated to dryness, and then dissolved in 1 mL D₂O containing 10 mM sodium 3-(trimethylsilyl) propionate-2,2,3,3-*d*₄ (TSP, δ 0.0 ppm). Concentrations were determined by comparison of an integrated ¹H NMR resonance corresponding to pipercolinic acid, α -amino- ϵ -caprolactam and caprolactam with the integrated ¹H NMR resonance corresponding to TSP (δ 0.0). A standard calibration curve was individually determined for pipercolinic acid, α -amino- ϵ -caprolactam and caprolactam using solutions of known concentrations prepared from authentic samples of pipercolinic acid, α -amino ϵ -caprolactam and caprolactam. The following resonances were used to

quantify each molecule: pipercolinic acid (δ 2.96, dd, 1 H); α -amino ϵ -caprolactam ((δ 4.29, d, 1 H); caprolactam (δ 2.46, m, 2 H)

Reagents and solvents

Tetrahydrofuran and diethyl ether were distilled under nitrogen from sodium/benzophenone. Methylene chloride, benzene, triethylamine and pyridine were distilled over calcium hydride before use. Organic solutions of products were dried over Na_2SO_4 . Most chemicals were purchased from Aldrich. Sodium salt of 3-(trimethylsilyl) propionic-2,2,3,3- d_4 acid (TSP) was purchased from Lancaster Synthesis Inc. Distilled deionized water was used for all purposes. Charcoal (Darco[®] G-60 ~100 mesh) was used for decolorization at a final concentration of 0.1 g/mL.

General methods

Chromatography

Silica gel 60 (40-63 μm , E. Merck) was used for flash chromatography. Analytical thin-layer chromatography (TLC) utilized precoated plates of silica gel 60 F-254 (0.25 mm, Whatman). TLC plates were visualized by UV or immersing in different stain solution such as phosphomolybdic acid stain (7% phosphomolybdic acid in ethanol) and potassium permanganate stain (1% KMnO_4 , 6.7% K_2CO_3 and 0.08% NaOH in H_2O). Amino acids were visualized by staining with ninhydrin stain prepared by dissolving 15 g of NaOAc in water (40 mL) and adjusting to pH 5-6. Tetramethylene sulfone (40 mL) and ninhydrin (2.0 g) were added followed by hydrindantin (36 mg) after 15 min. The total volume was made up to 100 mL with water.

HPLC chromatography was performed on an Agilent 1100 instrument installed with ChemStation acquisition software (Rev. A.08.03). Column used for all the HPLC purpose was a Zorbax SB-C18 reverse phase column (250 mm x 4.6 mm) and the detector was a VWD UV detector. Solvents were routinely filtered through 0.25- μ m membranes (Pall corporation) prior to use.

Dowex 50 (H⁺) was purchased from Aldrich-Sigma, which was cleaned by treatment with bromine. An aqueous suspension of resin was adjusted to pH 14 by addition of solid KOH. Bromine was added to the solution until the suspension turned a golden yellow color. Additional bromine was added (1-2 mL) to obtain a saturated solution. The mixture was left to stand at room temperature overnight, and the Dowex 50 resin was collected by filtration and washed exhaustively with water followed by 6 N HCl. In an extreme situation that large amount of bromine was used to clean Dowex 50 resin, ethanol was firstly used to remove most of the bromine, followed by H₂O and HCl washing.

AG-1X8 (Cl⁻) was purchased from Bio-Rad, which was converted to the hydroxide form by washing with twenty column volumes of 1 N NaOH. The column was then washed with distilled deionized water until all the chloride was displaced as determined by silver nitrate test.

Spectroscopic measurement

¹H NMR and ¹³C NMR spectra were recorded on either a Varian VX-300 or a Varian VXR-500 FT-NMR spectrometer. Chemical shifts for ¹H NMR spectra are reported (in parts per million) relative to internal tetramethylsilane (Me₄Si, δ = 0.0 ppm) with

CDCl₃, *d*⁶-acetone, *d*⁶-DMSO as solvent and to internal sodium 3-(trimethylsilyl) propionate-2,2,3,3-*d*₄ (TSP, δ 0.0 ppm) with D₂O as solvent. Chemical shifts for ¹³C NMR spectra are reported (in parts per million) relative to internal tetramethylsilane (Me₄Si, δ = 0.0 ppm) with CDCl₃, *d*⁶-acetone, *d*⁶-DMSO as solvent and to internal acetonitrile (CH₃CN, δ 3.69 ppm) with D₂O as solvent. The following abbreviations are used to describe spin multiplicity: s (singlet), d (doublet), t (triplet), q (quartet), m (unresolved multiplet), dd (doublet of doublets), b (broad).

Chapter 2

Cyclization of L-lysine in the presence of Al₂O₃

Conversion of L-lysine 17 to α-amino ε-caprolactam 18: A stirred mixture of lysine·HCl (55 g, 300 mmol), NaOH (12 g, 300 mmol) and Al₂O₃ (275 g, 2700 mmol) in 1.2 L hexanol was heated up to reflux with a Dean-Stark trap used to remove H₂O. The suspension was refluxed for 8 h until all starting material was consumed (determined by ¹H NMR). The suspension was then cooled and filtered to remove byproduct NaCl and Al₂O₃. The filtrate was concentrated to give crude α-amino ε-caprolactam.

Cyclization of L-lysine without Al₂O₃

Conversion of L-lysine 17 to α-amino ε-caprolactam 18: A stirred mixture of lysine·HCl (55 g, 300 mmol) and NaOH (12 g, 300 mmol) in 1.2 L 1,2-propanediol was heated up to reflux. The suspension was refluxed for 8 h until all starting material was consumed (determined by ¹H NMR). The suspension was then cooled and filtered to

remove byproduct NaCl. The filtrate was concentrated and resulting crude α -amino ϵ -caprolactam was dissolved in water. After acidification to pH 6 and partial concentration, crystal formed at rt to afford α -amino ϵ -caprolactam·HCl (37 g) in 75% yield.

Synthesis of 2,7-diaminoheptanoic acid monohydrochloride (homolysine) 25¹

Conversion of phthalic anhydride to 5-bromopentylphthalimide 21 : A mixture of phthalic anhydride (43.0 g, 290 mmol) and 5-aminopentanol (29.9 g, 290 mmol) in 250 ml dry toluene (dried over 4 Å sieves) was heated to reflux (in 120 °C oil bath) with a Dean-Stark trap to remove water. After TLC confirmation of complete of the reaction, phosphorous tribromide (18.2 ml, 190 mmol) in 20 ml dry toluene was added dropwise to the hot reaction mixture. The mixture was stirred for about 1.5 h at 100 °C. After removal of an orange precipitation by filtration through a pad of Celite, the filtrate was concentrated by rotary evaporation. The resulting oil was crystallized from absolute ethanol as white plates (60.1 g, 70%).

Synthesis of Diethyl 2-acetamido-2-(5-phthalimidopentyl) malonate 24: To a suspension of sodium hydride (1.55 g of 60% NaH/oil dispersion washed free of oil with hexane, 38.7 mmol) in 30 ml DMF, diethyl acetamidomalnonate (8.4 g, 38.7 mmol) in 30 ml DMF (dried over 4 Å sieves) was added dropwise over 30 minutes while maintaining the reaction temperature < 10 °C. After the reaction mixture was warmed slowly to rt over 1 hour, a solution of 5-phthalimidopentyl bromide (12.72 g, 42.9 mmol) in 30 ml DMF was added in four portions at rt while keeping the internal temperature < 40 °C. The mixture was stirred for 24 h until completion of reaction confirmed by TLC (product R_f = 0.43, starting material R_f = 0.32, $\text{CHCl}_3/i\text{-PrOH}$ = 20:1). Then pH of the reaction mixture

was adjusted to 6 (with moistened ColorpHast indicator strips, E Merck) with 4 N HCl. The reaction mixture was concentrated by rotary evaporation to give an oil, followed by purification with flash column chromatography (silica gel, CHCl₃ elutant). The desired fractions were concentrated and further purified by crystallization from mixture of ethyl acetate and cyclohexane (1:3) to give **24** (9.0 g, 54%).

Synthesis of 2,7-diaminohepanoic acid monohydrochloride, (DL-homolysine ·HCl)

25: A mixture of diethyl 2-acetamido-2-(5-phthalimidopentyl) malonate **24** (7.32 g, 170 mmol) and 6 N HCl (100 mL) was refluxed for 5 hrs. The reaction mixture was then cooled to precipitate the resulting phthalic acid, which was removed by filtration. The filtrate was concentrated by rotary evaporation, and the resulting residue was redissolved in 200 ml water and concentrated again to remove excess HCl. The residue was precipitated from absolute ethanol/acetone (1:1) as oil. The oil was dissolved in 40 ml water and charged to the top of a strong cation exchange column, AG1-X8. Three column volumes of water was use to wash column followed by elution with an ammonium hydroxide gradient (0-0.5 N). The column effluent was concentrated, neutralize to pH 6 and crystallized from aqueous ethanol to afford the monhydrochloride of DL-homolysine as white solid **25** (4.56 g, 84%).

Deamination of α -amino- ϵ -caprolactam with hydroxylamine-*O*-sulfonic acid

α -Amino ϵ -caprolactam (2.56 g, 20 mmol) was dissolved in 100 mL water and the solution cooled to -5 °C. After addition of KOH (4.48 g, 80 mmol) followed by NH₂OSO₃H (4.52 g, 40 mmol), the reaction was stirred at -5 °C for 1 h. The reaction solution was then heated up to 70-75 °C and stirred at this temperature for 1 h. The solution was stirred again cooled to -5 °C followed by addition of more KOH (4.48 g, 80

mmol) followed by $\text{NH}_2\text{OSO}_3\text{H}$ (4.52 g, 40 mmol). After stirring $-5\text{ }^\circ\text{C}$ for 1 h, the reaction solution was heated to $70\text{-}75\text{ }^\circ\text{C}$ and stirred at this temperature for another 1 h. After concentration, the crude product was purified by sublimation ($90\text{ }^\circ\text{C}$, 0.5 mmHg) to give 1.70 g of colorless, crystalline ϵ -caprolactam in 75% yield.

Deamination of L-lysine in water

L-Lysine hydrochloride (1.83 g, 10 mmol), water (100 mL) and Raney Ni (0.58 g, 10 mmol) were added to the reaction chamber of a Parr high-pressure reactor and the vessel was assembled. The reaction chamber was flushed for 10 min with Ar and then pressurized with H_2 to 100 psi. The reaction chamber outlet valve was then opened to the atmosphere. This process was repeated two additional times. After repressurizing the reaction vessel with 100 psi of H_2 , the temperature of the stirred reaction vessel was increased to $200\text{ }^\circ\text{C}$. The reaction was held at $200\text{ }^\circ\text{C}$ for 8 h. Upon cooling to rt, the pressurized reaction vessel's H_2 was vented in a fume hood. Pipecolinic acid **30** yield was determined by ^1H NMR.

Deamination of α -amino- ϵ -caprolactam in water

α -Amino- ϵ -caprolactam (1.28 g, 10 mmol), water (100 mL) and 5 wt% Ru/C (1.01 g, 0.5 mmol) were added to the reaction chamber of a Parr high-pressure reactor and the vessel was assembled. The reaction chamber was flushed for 10 min with Ar and then pressurized with H_2 to 100 psi. The reaction chamber outlet valve was then opened to the atmosphere. This process was repeated two additional times. After repressurizing the reaction vessel with 100 psi of H_2 , the temperature of the stirred reaction vessel was

increased to 200 °C. The reaction was held at 200 °C for 8 h. Upon cooling to rt, the pressurized reaction vessel's H₂ was vented in a fume hood. Reaction yield was determined by ¹H NMR.

Preparation of 40% Pt/SiO₂²

To a solution of H₂PtCl₆·6H₂O (2.1 g, 5.1 mmol) in distilled, deionized H₂O (60 mL) was added 1.5 g of silica gel (100-200 mesh). The water was removed under reduced pressure and the catalyst mixture was dried in a LAB-LINE HEET-CAB oven (Model No 3515) at 80 °C overnight (about 10 h). The resulting orange powder was ground into fine powder with pestle and mortar, transferred to a quartz reactor in a temperature programmable Barnstead Thermolyne Furnace (Model No F6020C), heated from rt to 130 °C (heating rate = 5 °C min⁻¹) under a flow of He (100 mL min⁻¹) and kept at this temperature for 1 h. The gas was then switched to H₂ (100 mL min⁻¹) with the temperature increased up to 400 °C (heating rate= 5 °C min⁻¹) and held for 2 h. The reactor was cooled down to rt under He. The catalyst was kept under Ar and ready to use for hydrodenitrogenation of α-amino-ε-caprolactam.

Deamination of α-amino-ε-caprolactam of 40% Pt/SiO₂

Hydrodenitrogenation was conducted in a flow apparatus consisting of two U-tubes. α-Amino-ε-caprolactam (1.28 g, 10 mmol) was placed in the first U-tube, which was mixed with reduced 40% Pt/SiO₂ (1.28 g, 2.6 mmol). The second U-tube served as a product chamber and was maintained at -78 °C with dry ice-acetone cooling. Substrate and catalyst U-tubes were heated to 250 °C while H₂ was allowed to flow through the U-

tubes. The resulting product was trapped in the second U-tube. After about 8 hrs, the sand bath heating was removed. The resulting residue was collected and analyzed by ^1H NMR.

Catalytic HDN of α -amino- ϵ -caprolactam with Pt/C and H_2

Under Ar, α -amino- ϵ -caprolactam (1.28 g, 10 mmol), THF (100 mL) and 5 wt% Pt/C (0.4 g, 0.1 mmol) were added to the reaction chamber of a Parr high-pressure reactor and the vessel was assembled. The reaction chamber was flushed for 10 min with Ar and then pressurized with H_2 to 100 psi. The reaction chamber outlet valve was then opened to the atmosphere. This process was repeated two additional times. After repressurizing the reaction vessel with H_2 to 50 psi, the temperature of the stirred reaction vessel was increased to 300 °C, which resulted in a reaction pressure of 1000 psi. The stirred reaction vessel was held at to 300 °C for 4 h. The reaction mixture was cooled to rt. Yields were determined relative to a calibration curve based on the ratios of integrated resonances at δ 2.46 ppm (2 H) corresponding to TSP (δ 0.0 ppm).

Synthesis of β -lysine **29³**

Protection of N-N'-Cbz-protected diazo ketone **27**: The N-N'-Cbz-protected ornithine **26** (7.32 g, 20 mmol) was dissolved in THF (60 mL) under Ar and cooled to -20 °C. After addition of *i*-BuOCOCl (2.88 g, 21 mmol) and N-methylmorpholine (2.3 mL, 21 mmol), the mixture was stirred at -20 °C for 20 min. The resulting white suspension was allowed to warm up to -5 °C, and a solution of CH_2N_2 was added dropwise until the rich yellow color persisted while keeping the internal temperature < 0 °C. The solution

was then stirred at 4 h as the mixture was allowed to warm to rt. Excess CH_2N_2 was destroyed by addition of a few drops of HOAc. The mixture was then diluted with Et_2O and washed with sat. NaHCO_3 solution, 1 N HCl and sat. NaCl solution. The organic phase was dried (by MgSO_4) and evaporated. Purification by flash column afforded the pure diazo ketone **27** as pale yellow solid (4.59 g, 78%).

Homologated carboxylic acid 28: The diazo ketone **27** (4.29 g, 15.6 mmol) was dissolved in aqueous THF (70 mL) containing 10% H_2O and then cooled to 0 °C. All subsequent reactions were run under Ar with the exclusion of light (in the dark room). A solution of silver benzoate (0.86 g, 4.50 mmol) in Et_3N (15 mL) was added while maintaining the internal temperature at 0 °C, the reaction mixture was stirred for 1 h until the second part of silver benzoate solution (0.86 g in 15 mL Et_3N) was introduced. The resulting mixture was allowed to warm from 0 °C to rt in 4-5 h in the dark. The mixture was then concentrated, diluted with sat. aq. NaHCO_3 solution and extracted with Et_2O . The aqueous phase was then carefully adjusted to pH 3 at 0 °C with 1 N HCl and extracted with EtOAc. The organic phase was dried (MgSO_4) and evaporated. Purification with recrystallization (EtOAc /hexane) afforded the pure N-N'-Cbz- β -lysine•HCl **28** (2.22 g, 45%).

Chapter 3

Catalyst preparation⁴

The catalysts were prepared by impregnation of active carbon with H_2PtCl_6 , $\text{RuCl}_3\cdot\text{H}_2\text{O}$, $\text{RhCl}_3\cdot 3\text{H}_2\text{O}$, PdCl_2 , NH_4ReO_4 , or $(\text{NH}_4)_2\text{IrCl}_6$. The loading was 0.83 mmol of metal per gram of catalyst and corresponded to the typical content of Mo in commercial

catalysts. The contents of metals in wt% was: Ru 8.3, Rh 8.5, Pd 8.8, Ir 15.9, Re 15.7 and Pt 16.3. The activated carbon (Norit RX3 Extra, Norit Americas Inc; BET surface area 1370 m²g⁻¹), which is not active under our reaction conditions, was chosen not only to mechanically stabilize the catalyst but also to minimize direct support interaction. The slurry of the support with the solution of catalyst precursor was dried under vacuum in a rotary evaporator. The catalyst mixture was crushed and sieved to 200 mesh. The resulting catalyst precursors were either reduced with H₂ (400 °C, 2 h) to afford carbon-support metal catalysts or presulfided by a H₂S/H₂ (10:90) mixture (400 °C, 2 h) to give carbon-supported metal sulfide catalysts.

Preparation of 16 wt% Pt/C

Activated C (8.37 g, 698 mmol) was mixed with H₂PtCl₆·6H₂O (4.30 g, 8.3 mmol) and water (200 mL) and heated for 1 h at 90 °C. The water was then removed under reduced pressure. The resulting solid was dried in an oven for 12 h at 80 °C. After transferring to a quartz U-tube reactor in a temperature programmable furnace, the catalyst was heated from rt to 130 °C (heating rate: 5 °C min⁻¹) under He (flow rate: 100 mL min⁻¹) and heated at this temperature for 1 h. The gas entering the quartz U-tube reactor was switched to H₂ (flow rate: 100 mL min⁻¹) and the temperature increased to 400 °C (heating rate: 5 °C min⁻¹) and held at 400 °C for 2 h. The reactor was subsequently cooled to rt under He (flow rate: 100 mL min⁻¹) and the reduced catalyst (Pt/C) stored under Ar.

Preparation of 16 wt% Pt-S/C

Activated C (8.37 g, 698 mmol) was mixed with H₂PtCl₆·6H₂O (4.30 g, 8.3 mmol) and water (200 mL) and heated for 1 h at 90 °C. The water was then removed under

reduced pressure. The resulting solid was dried in an oven for 12 h at 80 °C. After transferring to a quartz U-tube reactor in a temperature programmable furnace, the catalyst was heated from rt to 130 °C (heating rate: 5 °C min⁻¹) under He (flow rate: 100 mL min⁻¹) and heated at this temperature for 1 h. The gas entering the quartz U-tube reactor was switched to H₂S/H₂ (10:90) (flow rate: 100 mL min⁻¹) and the temperature increased to 400 °C (heating rate: 5 °C min⁻¹) and held at 400 °C for 2 h. The reactor was subsequently cooled to rt under He (flow rate: 100 mL min⁻¹) and the sulfided catalyst (Pt-S/C) stored under Ar. During the presulfiding process, the gas outlet of the quartz U-tube reactor was bubbled through a bleach solution to quench the H₂S in a fume hood.

Preparation of bimetallic Pt-Re-S/C catalysts⁵

Bimetallic Pt-Re catalysts were prepared either by coimpregnation or by catalytic reduction and then activated by either directly presulfidation or first calcinations and then presulfidation.

Preparation of bimetallic Pt-Re-S/C catalysts by coimpregnation

A given amount of carbon support was immersed in a 0.2 M HCl solution. After addition of Pt and Re precursors (H₂PtCl₆ and NH₄ReO₄), water was evaporated in a reduced pressure. The resulting solid was dried in an oven for 12 h at 80 °C. After transferring to a quartz U-tube reactor in a temperature programmable furnace, the catalyst was heated from rt to 130 °C (heating rate: 5 °C min⁻¹) under He (flow rate: 100 mL min⁻¹) and heated at this temperature for 1 h. The sample was activated either by direct presulfidation (H₂S/H₂ (10:90), 2 h, 400 °C) or was calcined (air, 2 h, 450 °C) and then presulfided ((H₂S/H₂ (10:90), 2 h, 400 °C).

Preparation of bimetallic Pt-Re-S/C catalysts by catalytic reduction

A given amount of the prereduced 'parent' Pt/C catalyst was suspended in a solution of 0.2 M HCl in a vessel. The solution was purged by a N₂ stream in order to eliminate the dissolved O₂ and H₂ was bubbled for 2 h. The solution of NH₄ReO₄ was introduced into another vessel, purged by bubbling N₂ and transferred to the first one and left to react for an hour under H₂ flow. Catalysts were then filtered and washed with water. The resulting solid was dried in an oven for 12 h at 80 °C. After transferring to a quartz U-tube reactor in a temperature programmable furnace, the catalyst was heated from rt to 130 °C (heating rate: 5 °C min⁻¹) under He (flow rate: 100 mL min⁻¹) and heated at this temperature for 1 h. The sample was activated either by direct presulfidation (H₂S/H₂ (10:90), 2 h, 400 °C) or was calcined (air, 2 h, 450 °C) and then presulfided ((H₂S/H₂ (10:90), 2 h, 400 °C).

Preparation of 8 wt% Pt-Cs-S/C catalysts⁶

The Pt-Cs-S/C (Pt:Cs = 1:1) catalyst was prepared as follows: H₂PtCl₆·6H₂O (2.15 g, 4.2 mmol), CsOH (1.25 g, 4.2 mmol) and water (200 mL) were introduced into a 500 mL reactor. After the mixture was stirred for 1 h, activated carbon (8.65 g) was added into the obtained solution, which was stirred for another 2 h. The water was removed under reduced pressure. The resulting solid was dried in an oven for 12 h at 80 °C. After transferring to a quartz U-tube reactor in a temperature programmable furnace, the catalyst was heated from rt to 130 °C (heating rate: 5 °C min⁻¹) under He (flow rate: 100 mL min⁻¹)

and heated at this temperature for 1 h. The gas entering the quartz U-tube reactor was switched to H₂S/H₂ (10:90) (flow rate: 100 mL min⁻¹) and the temperature increased to 400 °C (heating rate: 5 °C min⁻¹) and held at 400 °C for 2 h. The reactor was subsequently cooled to rt under He (flow rate: 100 mL min⁻¹) and the sulfided catalyst (Pt-Cs-S/C) stored under Ar. During the presulfiding process, the gas outlet of the quartz U-tube reactor was bubbled through a bleach solution to quench the H₂S in a fume hood.

Preparation of Pt-S/C-x catalysts with oxidated activated carbon⁷

Activated carbon was oxidized by treating with different concentrations (0.5, 1.0 and 6.0 M) of boiling HNO₃ for 8 h, followed by extensive washing with distilled water, filtered and dried at 80 °C overnight. The resulting supports (denoted as C-0.5, C-1 and C-6) were impregnated with H₂PtCl₆·6H₂O solution. The water was then removed under reduced pressure. The resulting solid was dried in an oven for 12 h at 80 °C. After transferring to a quartz U-tube reactor in a temperature programmable furnace, the catalyst was heated from rt to 130 °C (heating rate: 5 °C min⁻¹) under He (flow rate: 100 mL min⁻¹) and heated at this temperature for 1 h. The gas entering the quartz U-tube reactor was switched to H₂S/H₂ (10:90) (flow rate: 100 mL min⁻¹) and the temperature increased to 400 °C (heating rate: 5 °C min⁻¹) and held at 400 °C for 2 h. The reactor was subsequently cooled to rt under He (flow rate: 100 mL min⁻¹) and the sulfided catalyst (Pt-S/C) stored under Ar. During the presulfiding process, the gas outlet of the quartz U-tube reactor was bubbled through a bleach solution to quench the H₂S in a fume hood.

Catalytic HDN of α -amino- ϵ -caprolactam

General Chemistry: The hydrodenitrogenation of α -amino- ϵ -caprolactam was run in a Parr high-pressure, stainless steel reaction vessel (Model No. 4575) with a working volume of 450 mL. The reactor was heated in a heating mantle. Heating was controlled by a Parr 4842 temperature controller. ^1H NMR spectra were recorded at 300 MHz on a Varian Gemini-300 spectrometer. Chemical shift for ^1H NMR are reported (in part per million) relative to internal sodium 3-(trimethylsilyl) propionate-2,2,3,3- d_4 (TSP, δ 0.0 ppm) with D_2O as solvent. To determine the concentration of caprolactam in the reaction solution, a portion (1 mL) of the solution was concentrated to dryness, concentrated again to dryness from D_2O , and then redissolved in 1 mL D_2O containing 10 mM TSP. Yields were determined relative to a calibration curve based on the ratios of integrated resonances at δ 2.46 ppm (2 H) corresponding to TSP (δ 0.0 ppm).

Catalytic HDN of α -amino- ϵ -caprolactam with Pt/C and H_2

Under Ar, α -amino- ϵ -caprolactam (1.28 g, 10 mmol), THF (100 mL) and 16 wt% Pt/C (0.97g, 0.8 mmol) were added to the reaction chamber of a Parr high-pressure reactor and the vessel was assembled. The reaction chamber was flushed for 10 min with Ar and then pressurized with H_2 to 100 psi. The reaction chamber outlet valve was then opened to the atmosphere. This process was repeated two additional times. After repressurizing the reaction vessel with H_2 to 100 psi, the temperature of the stirred reaction vessel was increased to 250 $^\circ\text{C}$, which resulted in a reaction pressure of 650 psi. The stirred reaction vessel was held at to 250 $^\circ\text{C}$ for 8 h. The reaction mixture was cooled to rt. After filtration, the reaction solution was concentrated, and the residue dissolved in EtOAc. The EtOAc solution was extracted with water followed by stirring the aqueous layer with

activated carbon. Filtration and concentration of the aqueous layer afforded crude caprolactam.

Catalytic HDN of α -amino- ϵ -caprolactam with Pt/C and H₂S

Under Ar, α -amino- ϵ -caprolactam (1.28 g, 10 mmol), THF (100 mL) and 16.3 wt% Pt/C (0.8 mmol) were added to the reaction chamber of a Parr high-pressure reactor and the vessel was assembled. The reaction chamber was flushed for 10 min with Ar and then pressurized with H₂/H₂S (5:1) to 100 psi. The reaction chamber outlet valve was then opened to the atmosphere. This process was repeated two additional times. After repressurizing the reaction vessel with H₂/H₂S (5:1) to 100 psi, the temperature of the stirred reaction vessel was increased to 250 °C, which resulted in a reaction pressure of 650 psi. The stirred reaction vessel was held at to 250 °C for 8 h. Upon cooling to rt, the pressurized reaction vessel's H₂/H₂S atmosphere was vented through a bleach solution in a fume hood. After filtration, the reaction solution was concentrated, and the residue dissolved in EtOAc. The EtOAc solution was extracted with water followed by stirring the aqueous layer with activated carbon. Filtration and concentration of the aqueous layer afforded crude caprolactam.

Catalytic hydrodenitrogenation of α -amino- ϵ -caprolactam with Pt-S/C and H₂

Under Ar, α -amino- ϵ -caprolactam (1.28 g, 10 mmol), THF (100 mL) and 16.3 wt% Pt-S/C (0.97 g, 0.8 mmol) were added to the reaction chamber of a Parr high-pressure reactor and the vessel was assembled. The reaction chamber was flushed for 10 min with Ar and then pressurized with H₂ to 100 psi. The reaction chamber outlet valve was then opened to the atmosphere. This process was repeated two additional times. After

repressurizing the reaction vessel with H₂ to 100 psi, the temperature of the stirred reaction vessel was increased to 250 °C, which resulted in a reaction pressure of 650 psi. The stirred reaction vessel was held at to 250 °C for 8 h. The reaction mixture was cooled to rt. After filtration, the reaction solution was concentrated, and the residue dissolved in EtOAc. The EtOAc solution was extracted with water followed by stirring the aqueous layer with activated carbon. Filtration and concentration of the aqueous layer afforded crude caprolactam.

Catalytic hydrodenitrogenation of α -amino- ϵ -caprolactam with Pt-S/C and H₂S

Under Ar, α -amino- ϵ -caprolactam (1.28 g, 10 mmol), THF (100 mL) and 16.3 wt% Pt/C (0.97 g, 0.8 mmol) were added to the reaction chamber of a Parr high-pressure reactor and the vessel was assembled. The reaction chamber was flushed for 10 min with Ar and then pressurized with H₂S/H₂ (20:80) to 100 psi. The reaction chamber outlet valve was then opened to the atmosphere. This process was repeated two additional times. After repressurizing the reaction vessel with H₂S/H₂ (20:80) to 100 psi, the temperature of the stirred reaction vessel was increased to 250 °C, which resulted in a reaction pressure of 650 psi. The stirred reaction vessel was held at to 250 °C for 8 h. Upon cooling to rt, the pressurized reaction vessel's H₂S/H₂ atmosphere was vented through a bleach solution in a fume hood. After filtration, the reaction solution was concentrated, and the residue dissolved in EtOAc. The EtOAc solution was extracted with water followed by stirring the aqueous layer with activated carbon. Filtration and concentration of the aqueous layer afforded crude caprolactam.

Chapter 4

Preparation of 16 wt% Au-S/C by IMP

Activated carbon (4.18 g) was mixed in a solution of $\text{HAuCl}_4 \cdot 3\text{H}_2\text{O}$ (1.63 g) and heated at 90 °C for 1 h. The water was then removed under reduced pressure. The resulting solid was dried in an oven at 80 °C for 12 h. After transferring to a quartz U-tube reactor in a temperature programmable furnace, the catalyst was heated from rt to 130 °C (heating rate: 5 °C min^{-1}) under He (flow rate: 100 mL min^{-1}) and heated at this temperature for 1 h. The gas entering the quartz U-tube reactor was switched to $\text{H}_2\text{S}/\text{H}_2$ (10:90) (flow rate: 80 mL min^{-1}) and the temperature increased to 400 °C (heating rate: 5 °C min^{-1}) and held at 400 °C for 2 h. The reactor was subsequently cooled to rt under He (flow rate: 80 mL min^{-1}) and the sulfided catalyst (Au-S/C) stored under Ar. During the presulfiding process, the gas outlet of the quartz U-tube reactor was bubbled through a bleach solution to quench the H_2S in a fume hood.

Preparation of 8 wt% Au/ TiO_2 by DP⁸

TiO_2 (6 g) was suspended in a 600 mL solution of $\text{HAuCl}_4 \cdot 3\text{H}_2\text{O}$ (1 g) and urea (15.12 g). The mixture was heated at 80 °C for 4 h under stirring (final pH \approx 8) and allowed to cool to rt. The precipitate was centrifuged (15000 g, 10 min), decanted and washed thoroughly with water (600 mL). This water washing, centrifugation, decanting process was repeated 4 times. The washed mixture of HAuCl_4 and TiO_2 was dried under vacuum at 100 °C for 2 h and transferred to a quartz U-tube reactor in a temperature programmable furnace and heated from rt to 100 °C (heating rate: 2 °C min^{-1}) under He

(flow rate: 80 mL min⁻¹). The gas was then switched to H₂ (flow rate: 80 mL min⁻¹) and the temperature increased to 300 °C (heating rate: 2 °C min⁻¹) and held at 300 °C for 2 h. The reactor was cooled to rt under He (flow rate: 100 mL min⁻¹) and the reduced catalyst (Au/TiO₂) stored under Ar.

Preparation of 8 wt% Au/NiO by DP

The support NiO (6 g, 80 mmol) was added to a 600 mL aqueous solution of HAuCl₄·3H₂O (1 g) and urea (15.12 g, 252 mmol). The suspension was vigorously stirred at 80 °C for 4 h resulting in the solution changing from pH 2 to pH 8. The mixture of HAuCl₄ and NiO was recovered by centrifugation (15000g for 10 min), resuspended in 600 mL water, and centrifuged again. This water wash followed by centrifugation was repeated 4x. The washed mixture of HAuCl₄ and NiO was dried under vacuum at 100 °C for 2 h and transferred to a quartz U-tube reactor in a temperature programmable furnace and heated from rt to 100°C (heating rate: 2°C min⁻¹) under He (flow rate: 80 mL min⁻¹). The gas was then switched to H₂S/H₂ (10:90) (flow rate: 80 mL min⁻¹) and the temperature increased to 300 °C (heating rate: 2°C min⁻¹) and held at 300 °C for 2 h. The reactor was cooled to rt under He (flow rate: 100 mL min⁻¹) and the reduced catalyst (Au/NiO) stored away from light in a desiccator under Ar.

Preparation of 8 wt% Au-S/NiO

The support NiO (6 g, 80 mmol) was added to a 600 mL aqueous solution of HAuCl₄·3H₂O (1 g) and urea (15.12 g, 252 mmol). The suspension was vigorously stirred at 80 °C for 4 h resulting in the solution changing from pH 2 to pH 8. The mixture of HAuCl₄ and NiO was recovered by centrifugation (15000g for 10 min), resuspended in

600 mL water, and centrifuged again. This water wash followed by centrifugation was repeated 4x. The washed mixture of HAuCl_4 and NiO was dried under vacuum at 100 °C for 2 h and transferred to a quartz U-tube reactor in a temperature programmable furnace and heated from rt to 100°C (heating rate: 2°C min⁻¹) under He (flow rate: 80 mL min⁻¹). The gas was then switched to H₂ (flow rate: 80 mL min⁻¹) and the temperature increased to 300 °C (heating rate: 2°C min⁻¹) and held at 300 °C for 2 h. The reactor was cooled to rt under He (flow rate: 100 mL min⁻¹) and the sulfided catalyst (Au-S/NiO) stored away from light in a desiccator under Ar. During the presulfiding process, the gas outlet of the quartz U-tube reactor was bubbled through a bleach solution to quench the H₂S in a fume hood.

Catalyst characterization by transmission electron microscopy (TEM)

TEM measurements were performed using a JEOL 2200FS operated at 200 kV. The sample was mounted on a carbon-supported copper grid by placing a few droplets of a suspension of the ground sample in THF on the grid, followed by drying under ambient conditions, all in a N₂ atmosphere. The samples were transferred to the microscope in a sealed plate under Ar. At least 5 representative micrographs were taken for each catalyst.

Catalytic HDN of α -amino- ϵ -caprolactam with Au-S/NiO and H₂S/H₂

Under Ar, α -amino- ϵ -caprolactam (1.28 g, 10 mmol), THF (100 mL) and 8 wt% Au-S/NiO (2.0 g, 0.8 mmol) were added to the reaction chamber of a Parr high-pressure reactor and the vessel was assembled. The reaction chamber was flushed for 10 min with Ar and then pressurized with H₂S/H₂ (10:90) to 100 psi. The reaction chamber outlet valve was then opened to the atmosphere. This process was repeated two additional times.

After repressurizing the reaction vessel with H₂S/H₂ (10:90) to 50 psi, the temperature of the stirred reaction vessel was increased to 300 °C, which resulted in a reaction pressure of 1000 psi. The stirred reaction vessel was held at to 250 °C for 4 h. Upon cooling to rt, the pressurized reaction vessel's H₂S/H₂ atmosphere was vented through a bleach solution in a fume hood. After filtration, the reaction solution was concentrated, and the residue dissolved in EtOAc. The EtOAc solution was extracted with water followed by stirring the aqueous layer with activated carbon. Filtration and concentration of the aqueous layer afforded crude caprolactam.

Direct conversion of L-lysine to caprolactam.

Under Ar, L-lysine hydrochloride (1.83 g, 10 mmol), NaOH (0.4 g, 10 mmol), EtOH (100 mL) and 16 wt% Pt-S/C (0.12 g, 0.1 mmol) were added to the reaction chamber of a Parr high-pressure reactor and the vessel was assembled. The reaction chamber was flushed for 10 min with Ar and then pressurized with H₂S/H₂ (10:90) to 100 psi. The reaction chamber outlet valve was then opened to the atmosphere. This process was repeated two additional times. After repressurizing the reaction vessel with H₂S/H₂ (10:90) to 150 psi, the temperature of the stirred reaction vessel was increased to 250 °C, which resulted in a reaction pressure of 1050 psi. The stirred reaction vessel was held at to 250 °C for 8 h. Upon cooling to rt, the pressurized reaction vessel's H₂S/H₂ (10:90) atmosphere was vented through a bleach solution in a fume hood. After filtration, the reaction solution was concentrated to afford crude caprolactam.

References

- 1 Payne, L. S.; Boger, J. *Syn. Commun.* **1985**, *15*, 1277.
- 2 Guttieri, M. J.; Maier, W. F., *J. Org. Chem.* **1984**, *49*, 2875.
- 3 Guichard, G.; Avele, S.; Seebach, D. *Helv. Chim. Acta.* **1998**, *81*, 187.
- 4 Vit, Z.; Zdrazil, M. *J. Catal.* **1989**, *119*, 1.
- 5 (a) Pieck, C. L.; Marecot, P.; Barbier, J. *Appl. Catal. A* **1996**, *134*, 319. (b) Pieck, C. L.; Marecot, P.; Barbier, J. *Appl. Catal. A* **1996**, *134*, 287.
- 6 Ishihar, A.; Lee, J.; Dumeignil, F.; Yamaguchi, M.; Hirao, S.; Qian, E. W.; Kabe, T. *J. Catal.* **2004**, *224*, 243.
- 7 Calafat, A.; Laine, J.; Lopez-Agudo, A.; Palacios, J.M. *J. Catal.* **1996**, *162*, 20.
- 8 Zanella, R.; Giorgio, S.; Henry, C. R.; Louis, C. *J. Phys. Chem. B.* **2002**, *106*, 7634.

MICHIGAN STATE UNIVERSITY LIBRARIES



3 1293 03062 4468